Hydrostatic pressure regulates neural crest competence

Delan Ardalan Alasaadi

University College London

2023

This thesis was submitted in requirements for the degree of Doctor of Philosophy in Developmental and Cell Biology

I, Delan Ardalan Alasaadi, confirm that the work presented in my thesis is my own. Where information has been derived from other sources, I confirm that this has been indicated in the thesis.

Acknowledgment

As the last notes of this PhD, a life-changing experience, are being written, it would not have been possible without the support and guidance of many people I had the privilege to meet.

My deepest gratitude and appreciation extended to my supervisor ***Prof. Roberto Mayor*** for the support, encouragement, and continual drive to push further and explore the unknown. I would also like to thank my graduate committee, Dr. ***Yoshiyuki Yamamoto*** and ***Anna Franz***, for their support and advice during my development of this work.

I would like to thank friends and colleagues I have met who positively influenced my journey. Thank you, Christopher Thrasivoulou, Lucas Alvizi, Jonas Hartmann, Namid Stillman, Jorge Diaz, Matyas Bubna-Litic, and Parchiti Moghe. Finally, I would like to thank my family, their undivided support and advice have been unconditional and endless. More importantly, I thank my mother ***Shana Alasaadi*** beyond words, whom I strive to repay and make proud of. Thank you, Mom, my role model and my hero.

أهدي هذا العمل المتواضع الى قدوتي ورفيق حياتي وصديقي في الدنيا والأخرة شنا وسعيد وليلان الأسعدي

Abstract

Since its discovery, embryonic induction has been considered one of the central mechanisms that control the formation of new cell types, tissues, and organ formation. Induction corresponds to the interaction between two tissues (inducing and responding), subsequently leading to a change in the direction of differentiation of the responding tissue. This process is restricted to a precise time and place of tissue differentiation during morphogenesis; however, the mechanisms for this restriction have remained elusive. Despite induction being discovered over a hundred years ago (Nobel Prize to H. Spemann, 1935), only in the last three decades has its molecular basis has been elucidated with the identification of many inducers (e.g., mesodermal, neural, etc.). This process consists of signals produced by the inductive tissue, which has been the focus of many studies in the past years, whereas how the regulation in the responding tissue is controlled is a topic that has been widely neglected.

The ability of one tissue to respond to inductive signals is called competence, a mechanism yet to be fully understood. In this thesis, we aimed to understand the mechanism that controls the competence of responding cells, neural crest cells, a migratory multipotent embryonic cell population. Our key novel finding in this thesis is that mechanical cues regulate *Xenopus* neural crest competence. Specifically, we found that an increase in the hydrostatic pressure of the blastocoel, an embryonic cavity, inhibits neural crest competence at the end of gastrulation when neural crest induction is finished. Furthermore, we identified the molecular mechanism by which hydrostatic pressure regulates neural crest competence. This involves the regulation of the neural crest inductive signal (Wnt) by the mechanotransducer Yes Associated Protein (YAP), showing how mechanical and biochemical cues interplay to control embryonic competence.

These findings challenge the current dominant concept that development is genetically controlled and introduce a new model explaining a pivotal phase of embryonic development in which two independent developmental processes, blastocoel morphogenesis and neural crest induction, are linked via tissue mechanics.

Impact statement

How cells acquire their fate during morphogenesis is a pivotal question in biology, it relates to our understanding of cancer progression and other pathologies. Studying embryonic induction provides insights into building this road map. The process of cells and tissues transitioning from one fate to another is called embryonic induction. J. Gurdon has claimed that embryonic induction "*is probably the single most important mechanism in vertebrate development leading to differences between cells and to the organization of cells into tissues and organs*". During development, embryonic induction occurs in a specific region in the embryos at an exact time that requires the coordination between signals from inducer tissues and the ability to respond to those signals by the induced tissue, called competence. Competence controls the spatial and temporal response of tissues to the inductive signals and is required for patterning tissues and organs during embryogenesis. Several tissues are classified as inducers in the embryo, as has been shown in past studies, yet how timing is regulated in the process of embryonic induction remains unknown. Considerable efforts have been made to understand the molecular basis of embryonic competence without much success. Here we decided to approach the problem from a different angle, asking whether mechanics has a role as a regulator of embryonic competence. We demonstrated for the first time that a purely mechanical cue (hydrostatic pressure) controls neural crest competence during development.

These conclusions have broad implications in areas where embryonic induction and cell differentiation are essential, such as stem cell biology, development, and cancer biology. Additionally, these findings are equally relevant for scientists working in the bioengineering and biophysics fields. In all these fields, the interplay between mechanical forces and biochemical signals remains a central unsolved question, to which our embryological findings contribute an essential cornerstone.

Table of Contents

List of Abbreviations

Table 1 | Acronyms and definitions

A-P axis	Anterior-posterior axis
Activin A	Inhibin subunit beta A
AP	Alkaline phosphatase
ATAC-seq	Assay for Transposase-Accessible Chromatin sequencing
BCIP	5-Bromo-4-chloro-3-indolyl phosphate
BMP	Bone morphogenetic protein
BSA	Bovine serum albumin
ChIP-seq	Chromatin immunoprecipitation
CIP	Contact inhibition of Proliferation
CNS	Cantal nervous system
DEPC	Diethylpyrocarbonate
DFA	Danilchick's Medium for Amy
DIG	Digoxigenin
DKK1	Dickkopf1
DMSO	Dimethyl sulfoxide
E	Embryonic day (embryonic mouse staging)
EMT	Epithelial-to-mesenchymal transition
FA	Focal adhesions
FDX	Fluorescein-dextran
FGF	Fibroblast growth factor
FGFR	Fibroblast growth factor receptor
Foxd3	Forkhead box D3 (neural crest marker)
FRZB	Secreted Fz-related protein family

GFP	Green fluorescent protein
GRN	Gene regulatory Network
GSK3β	Glycogen synthase kinase 3β
hESCs	Human Embryonic stem cells
HH	Hamburger and Hamilton (chick staging)
hiNCCs	Human neural crest cells
HYB	Hybridisation buffer
IGF	Insulin-like growth factor
iPSCs	Induced pluripotent stem cells
ISH	*In situ* hybridisation
Ker	Keratin (epidermal marker)
MEM	Minimum essential medium
MEMFA	Minimum essential medium with formaldehyde 15
MMR	Marc's modified Ringer's
MO	Morpholino oligomer
mRNA	Messenger ribonucleic acid
NBT	4-Nitro blue tetrazolium chloride
NCCs	Neural crest cells
NE	Neural ectoderm
NNE	Non-neural ectoderm
Nodal	Nodal growth differentiation factor
NP	Neural plate
NPB	Neural plate border
NRP1	Neuropilin-1
NT	Neural tube

PBS	Phosphate buffer saline
PBT	Phosphate buffered solution with Triton-X
PCP	Planar cell polarity
PFA	Paraformaldehyde
PKC	Protein kinase C
PNS	Peripheral nervous system
RA	Retinoic acid
RNA-seq	RNA sequencing
Sani2	Snail family zinc finger 2 (neural crest marker)
sFRP2	Secreted Frizzled related protein 2
Sox2	SRY-Box transcription factor 2 (neural plate marker)
Sox9 & 10	SRY-box 9 and 10 (neural crest marker)
Tead2	TEA Domain Family Member 2, Yap binding partner
TGF-β	Transforming growth factor beta
Vg1	growth differentiation factor 1
Wnt8	Wnt family member 8
Wnts	Wingless-related integration proteins
Xbra	Brachyury (mesoderm marker)
XTC	*Xenopus* cultured cells
XTC- MIF	*Xenopus* cultured cells – mesoderm inducing factor
Yap1	Yes-associated protein 1

List of Figures

List of Tables

Chapter 1: Introduction

1.1 Embryonic inductions

1.1.1 Definition and types of Embryonic induction

The idea that tissue fate is influenced by another tissue was proposed by Wilhelm Pfeffer and Curt Herbst as early as 1871 (Oppenheimer 1991). Experiments in the amphibian *Rana* were carried out soon after and suggested that lens formation is controlled by the underlying optic lobe of the brain (Lewis 1904; Spemann 1901). Subsequent work in Hydra showed its ability to regenerate its head after excised, and a graft proxy to the head can induce an ectopic axis (Browne 1909). Using two different pigmented Hydras (brown and green), Browne determined that the ectopic axis is derived from the host, establishing the concept of induction (Browne 1909).

Lewis reported that a graft of dorsal blastopore lip onto an ectopic site could induce a supernumerary structure that resembles a neural plate in amphibians (Lewis 1907). Hans and Mangold aimed to replicate Lewis's findings to understand better and distinguish the contribution of the host from the donor tissues by taking advantage of the existence of newt-pigmented species (*Triturus cristatus*, *T. taeniatus, and T. alpestris*); they showed five different cases of ectopic neural structure driven by the host (Spemann and Mangold 1924). They showed that a graft of the dorsal blastopore lip of unpigmented *Triturus cristatus* onto the ventral blastopore lip of pigmented *T. taeniatus* (or vice-versa) was able to induce a secondary axis that resembles neural plate (Spemann and Mangold 1924). Based on the high volume of studies that examined the process of induction since its proposal, Gurdon defined it as "an interaction between one (inducing) tissue and another (responding) tissue, as result of which the responding tissue undergoes a change in its direction or differentiation" (Gurdon 1987). This definition dictated that a successful induction experiment must distinguish between the host and donor tissues and the change in the outcome of responding tissues (Saxen 1977).

Aiming to understand embryonic induction better, Holtzer classified it as either permissive induction (the outcome is mainly governed by induced tissue) or instructive induction (the outcome is mainly governed by inducing tissue) (Holtzer 1968).

1.1.1.a Permissive induction

Gurdon outlined permissive induction, whereby a responding tissue pre-committed to a specific outcome interacts with a non-specific signal to ensure that outcome (Gurdon 1987). Permissive induction is noted in the differentiation of the pancreas. In mouse embryo (stage 15-somite), the pancreatic mesenchyme induces pancreas differentiation in the responding endoderm (Rutter, Wessells, and Grobstein 1964). However, if the mesenchyme (inducing tissue) is replaced by any other kind of mesenchyme, such as the one taken from organ primordia, the endoderm will still give rise to the pancreas. This suggests that all mesenchyme have a non-specific influence on the responding tissue and that a specific stimulus is generated within the responding tissue to ensure the outcome (Rutter et al. 1964). In addition, this also suggests that by this developmental stage, the endoderm epithelium is already committed to the fate of pancreas differentiation (Wessells and Cohen 1967).

Interestingly in the lens capsule, replacing the inducing tissue with collagen or glycosaminoglycans results in the differentiation of corneal epithelium with an efficiency equivalent to exposure to endogenous inducer tissue (Meier 1975). Meier concluded that the inducer tissue is dispensable in differentiating corneal epithelium (Meier 1975). Although the possible role of interaction between responding tissue and extracellular matrix was suggested, it was not investigated. In addition, no subsequent study proposed the potential aspect of a mechanical stimulus that the inducer tissue provides.

1.1.1.b Instructive induction

Unlike permissive induction, instructive induction is defined as the interaction of an uncommitted (responding) tissue to a specific signal (from inducing tissue) that will dictate the differentiation outcome of the responding tissue (Gurdon 1987). An example of instructive induction has been examined in Chick skin development. Rawles grafted mesoderm of the lower leg area (normally induces scales) onto ectoderm host (normally induces feathers); the grafted mesoderm induces feathers rather than scales (Rawles 1963). This study indicates that the grafted inducer can dictate the fate of responding tissue and subsequently change the outcome of fate. Furthermore, a study showed that xenografting a mouse mesoderm (normally induces hair in the overlaying epidermis) onto Chick corneal epithelium (normally forms cornea) resulted in abnormal feathers rather than cornea (Sengel 1976). These studies shed light on the pivotal role of specific and instructive molecules from inducing tissues that control the fate of the responding tissue, classical examples of which are mesoderm, neural, lens, and neural crest induction.

1.1.2 Mesoderm induction

The earliest study on mesoderm induction in newts by Pieter Nieuwkoop showed that the isolation of explants from animal pole formed ectoderm, and explants from vegetal pole formed endoderm (Sudarwati and Nieuwkoop 1971). Interestingly, a conjugate of vegetal and animal pole cells gave rise to mesoderm in the latter cells. These findings suggest that the inductive signals to induce mesoderm come from the vegetal pole (Boterenbrood and Nieuwkoop 1973; Sudarwati and Nieuwkoop 1971). Furthermore, Dale and Slack showed that this interaction between the vegetal pole and perspective mesoderm happens between the 32-cell stage (where prospective marginal zone does not form mesoderm) and blastula stage (where explants from lateral plate mesoderm form mesoderm), suggesting a temporal facet to this instructive induction (Slack, Dale, and Smith 1984). Markedly, there is a difference between presumptive dorsal

mesoderm, which gives rise to dorsal mesoderm and presumptive ventral mesoderm, which gives rise to ventral mesoderm. This finding strengthens the concept of instructive induction, as it indicates that different signals from dorsal or vegetal cells give rise to different types of mesoderm (Boterenbrood and Nieuwkoop 1973; Slack et al. 1984; Sudarwati and Nieuwkoop 1971).

It is widely accepted that the endoderm and the ectoderm are specified during early development by gene products within the animal and vegetal hemispheres, whereas the mesoderm is specified by inductive signals generated from the vegetal hemispheres (Stern and Downs 2012). This notion was concluded from Nieuwkoop recombinants experiments, where the isolation of animal cap will only form epidermis and vegetal explants will only form endoderm (Nieuwkoop 1969). However, combining animal and vegetal explants will lead to mesoderm induction. Notably, the induced mesoderm type in these experiments depends on the source of the vegetal explants (Dale and Slack 1987). As most vegetal hemisphere only induces ventral mesoderm (i.e. blood), whereas dorso-vegetal explants (also known as Nieuwkoop centre) will form dorsal mesoderm (i.e. notochord). This observation suggests two signals are generated from the vegetal hemisphere to induced mesoderm; one from the Nieuwkoop center and another ventral signal generated by the most vegetal hemisphere (Fig 1.1; left and middle). The outcome of this induction can be observed by mesoderm markers such as *brachyury* (*bra*) which is expressed around the entire marginal zone, as an early response for ventral mesoderm induction and *goosecoid* (*gsc*), a marker for dorsal mesoderm. The organizer generates a third signal, specifying the lateral mesoderm fates (Fig 1.1; right). With these findings, a "three-signal" model was proposed to account for mesoderm induction in *Xenopus* (Slack et al. 1984). Likewise to *Xenopus*, when the epiblast of Chick is treated with activin or conjugated with hypoblast, it generates mesoderm including notochord, primitive streak and/or somite (Perea-Gomez et al. 2002; Stern and Downs 2012). Further studies on mesoderm and primitive streak induction in Chick and

mammals divulged the resemblance to mesoderm induction in *Xenopus* and the involvement of key pathways such as; Vg1, Nodal, Activin, BMPs, and canonical Wnt (Stern and Downs 2012).

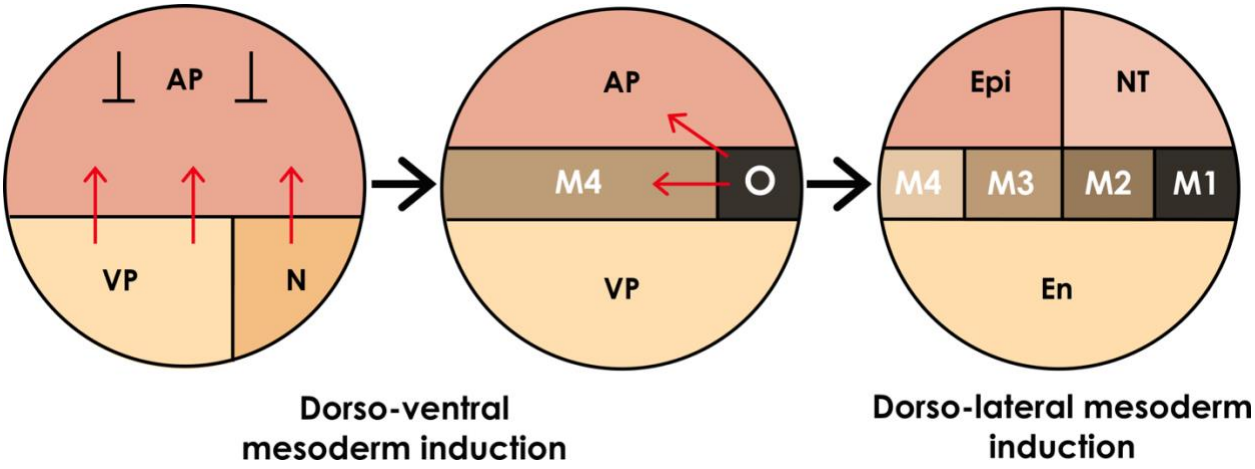

Fig. 1.1 | Mesoderm three-signal induction model.

Mesoderm induction occurs in the marginal zone of the embryo at the blastula stage (left), mediated by three inductive signals. The *first inductive signal* originated from the vegetal pole (VP) side, which induces ventral mesoderm (M4). In addition to the first inductive signal, inhibitory signals from the animal pole (AP) constrain this induction to the marginal zone. The *second inductive signal* originated from a small group of cells in the dorsal side of the embryos (Nieuwkoop center – N) that forms the organizer (O) (middle). The *third inductive signal* originates from the differentiated organizer (M1) that will specify lateral mesodermal fates (M2 and M3) and induce neural tissue (NT) in the dorsal ectoderm. And ventral ectoderm will differentiate into the epidermis.

1.1.2.a Superfamily of TGF-β molecules in mesoderm induction

The first molecule to be associated with mesoderm induction was a component found in *Xenopus* Tissue Culture (XTC) medium, Activin (Smith 1987; Smith et al. 1990). Initially, this medium was identified as a mesoderm-inducing factor (XTC-MIF) (Smith 1987). Further studies linked XTC-MIF to TGF-β superfamily member, activin – A (van den Eijnden-Van Raaij et al. 1990; Thomsen et al. 1990). Studies in *Xenopus* showed the ability of Activin protein to induce dorsal mesodermal tissue in animal pole explants (animal cap assay) (Makoto Asashima et al. 1990; M. Asashima et al. 1990; Smith et al. 1990; Sokol, Wong, and Melton 1990; Thomsen et al. 1990). The soluble protein form of activin exhibited a dose-dependent effect on animal caps; a higher dose of activin induced embryoid-like structures with anteroposterior patterning and head-like structure (Sokol et al. 1990; Thomsen et al. 1990). Moreover, it was shown that a graded dose (1.2X lowest concentration) induced dorsal mesoderm at lower concentrations and ventral mesoderm at higher concentrations, suggesting a morphogen gradient activin-like could induce the observed dorso-ventral patterning of mesoderm *in vivo* (Green and Smith 1990). Further studies in *Xenopus* showed that injecting activin mRNA could also induce dorsal mesoderm (Thomsen et al. 1990), and activin type II receptor was identified as a component of the pathway (Kondo et al. 1991). As injection of the dominant negative form of active type II receptor inhibited mesoderm formation (Hemmati-Brivanlou and Melton 1994), these studies demonstrated the role of an activin-like signal in mesoderm induction and dorso-ventral patterning.

In addition to activin, researchers linked other members of the TGF-β superfamily to mesodermal induction, Vg1 and Nodal (Conlon, Barth, and Robertson 1991; Dale et al. 1989; Melton 1987; Mowry and Melton 1992; Rebagliati et al. 1985; Weeks and Melton 1987). Treatment with a soluble mature form of Vg1 can induce embryoid-like axial organization and head-like structures (Kessler and Melton 1995). Moreover, activin type II receptor inhibition led to mesoderm impairment to induce Vg1 in animal cap (Kessler and Melton 1995; Schulte-

Merker, Smith, and Dale 1994). Similar to activin, Vg1 signals via the Smad2/3 pathway and the expression of Vg1 instead of activin mirrors the mesoderm activity of vegetal cells. Hence, the notion that Vg1 is the inducer of mesoderm induction, acting via activin receptor. On the other hand, Nodal expression was observed in the node of mice, and it plays various roles in development and is considered critical in mesoderm induction (Conlon et al. 1991). Furthermore, investigations in zebrafish showed that Nodal and Vg1 act as heterodimers in mesoderm induction (Montague and Schier 2017). These findings are observed in other species, such as *Xenopus* and Chick (Lohr et al. 1998; Mikawa et al. 2004), suggesting the functionality of Nodal and Vg1 is conserved in vertebrate embryos.

Another critically important component of the superfamily of TGF-β that plays a role in mesoderm induction is BMPs (Dale et al. 1992; Köster et al. 1991). BMPs in *Xenopus* are expressed in animal pole and become enriched ventrally during blastula and gastrulation. And they have been proposed to be inducers of ventral mesoderm (Dale et al. 1992; Graff et al. 1994; Köster et al. 1991). For example, BMP4 expression in the animal cap prevents the dorsalization of the mesoderm (Dale et al. 1992), suggesting that BMP4 plays a role in ventralizing the mesoderm rather than inducing mesoderm like Activin/Vg1/Nodal (Dale et al. 1992; Graff et al. 1994; Suzuki et al. 1994a).

1.1.2.b FGF signaling in mesoderm induction

Fgf proteins, transcripts, and receptors were identified in *Xenopus* embryos (Friesel and Dawid 1991; Gillespie, Paterno, and Slack 1989a; Isaacs, Tannahill, and Slack 1992; Kimelman et al. 1988; Musci, Amaya, and Kirschner 1990). Graft experiments employing beads of Fgf protein exhibited ventro-vegetal-like signals (Slack et al. 1987). Further investigation showed that dominant-negative Fgf recpetor1 (XFC) inhibited mesoderm induction in animal cap explants; however, in whole embryos, dominant-negative resulted in posterior structure and trunk defects with no effect on the anterior side. These findings suggest that FGF signaling is required

for posterior mesoderm development (Amaya, Musci, and Kirschner 1991). In addition, it was found that Fgf signaling via activin is required for mesoderm induction (LaBonne and Whitman 1994).

1.1.3 Neural induction

Uncommitted naïve ectodermal cells acquire neural fate, an instructive induction event in early vertebrate embryogenesis (Sasai et al. 2008; Stern 2005). At this stage, neural inducers are secreted and produced in a specific region, known as the organizer (Crunz 1997; Muñoz-Sanjuán and Brivanlou 2002a; Storey et al. 1992a). Classical graft assays recognized the production of neural inducing signals by grafting the dorsal blastopore lip (later known as Spemann organizer) onto the ventral side, which yielded an embryo with an ectopic neural axis (Spemann and Mangold 1924). Utilizing multi-pigmented newt species confirmed that this secondary axis is derived from the host (Gimlich and Cooke 1983; Spemann 1921; Spemann and Mangold 1924). Despite the determination of the presence of the signaling molecules that orchestrated neural induction, their identity remained elusive till the implementation of molecular biology in the early 90s when Noggin, Follistatin, and Chordin were identified as neural inducers (Hemmati-Brivanlou and Melton 1994; SASAI 1994; Smith and Harland 1991). Indeed, attenuation of these signals secreted by the organizer perturbs neural induction (Khokha et al. 2005). Studies in Chick embryos demonstrated that neural plate arises anteriorly to Henson's node (Hensen 1876), an equivalent to Spemann organizer found in birds and mammals (Beddington 1994; Waddington 1932, 1933, 1936, 1937). Similarly to the Spemann organizer, Henson's node forms during gastrulation and induces neural plate as the epiblast thickens (Stern 2005). These findings of the organizer centers and classification of molecules involved in neural induction instructed a wide range of studies to determine the pathways and the mechanisms by which this induction occurs, such as BMP, FGF and Wnt pathways.

1.1.3.a BMP signaling in neural induction

Animal cap explants taken from the animal pole of *Xenopus* gastrula embryos (equivalent to the post-implantation epiblast of mouse embryos) treated with chordin differentiated to neural cells; otherwise, they would differentiate into the epidermis (Ariizumi, Michiue, and Asashima 2017; Green 1999; Sasai et al. 1995). Subsequent analysis showed that neural inducers secreted from the organizers act as BMP antagonists, binding to BMP extracellularly and preventing the binding of BMP4 into BMP receptors (Hemmati-Brivanlou and Melton 1994; Piccolo et al. 1996; Yu et al. 2018). Consistently, BMP receptor dominant-negative mutant induces neural cells (Suzuki et al. 1994b). These studies suggest the binary nature of ectoderm decision between epidermis or neural cells depending on the existence of BMP signals. Indeed, this postulation gave rise to the "neural default model", which was further supported by merely dissociating animal cap cells, diluting the BMP signal, and leading to neural differentiation of these cells (Muñoz-Sanjuán and Brivanlou 2002b). The neural default model proposes that the normal fate of ectodermal cells is to become neural, a fate which is inhibited by an autocrine BMP signal, whereas the role of the neural inducers secreted by the Spemann organizer is to inhibit this BMP signal by direct binding of chordin, noggin or follistatin to BMP molecules (Figure 1.2). Thus, in the absence of neural inducers, the ectoderm differentiates as epidermis (BMP activation), while neural inducers inhibit (BMP inhibition) this fate and tissue becomes neural. However, analysis in Chick revealed that blocking BMP signals by Noggin or Chordin was insufficient to induce neural plate (Streit et al. 1998). Furthermore, findings in *Xenopus* showed blocking BMP alone is insufficient to induce neural cells and that inhibition of the Fgf signal perturbs neural plate induction (Marchal et al. 2009; Pera et al. 2003). These observations suggest that additional inducing factor(s) are required or involved in neural induction.

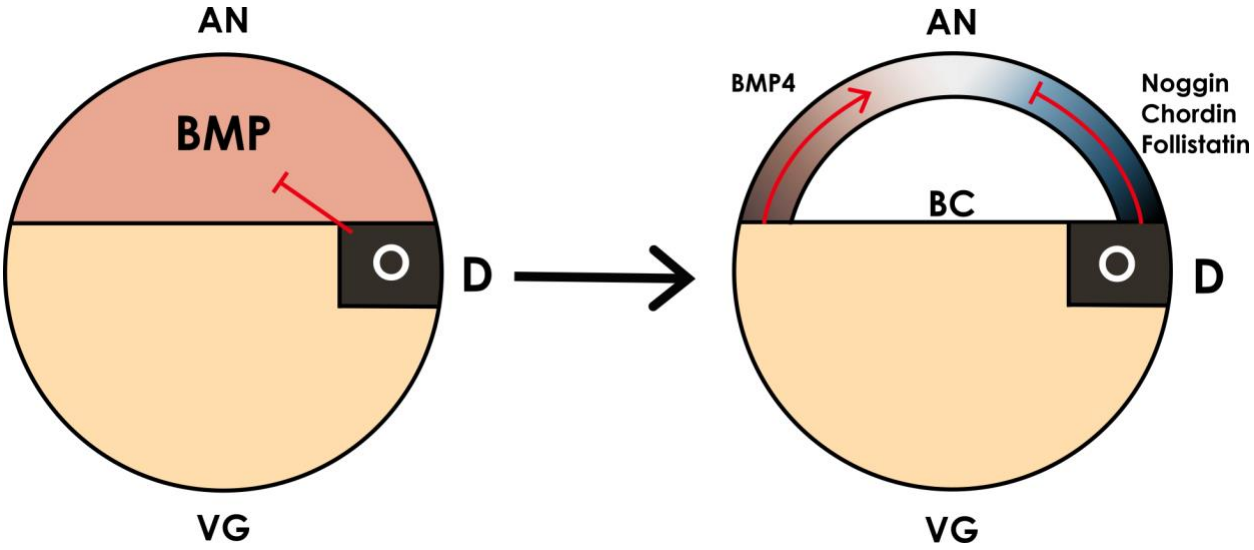

Fig. 1.2|The default model of neural induction.

The ectoderm, by default, will differentiate into neural tissues but is inhibited by the abundant BMP signaling (left). However, BMP antagonists are secreted from the Spemann organizer (left; red arrow). These antagonists, such as Noggin, Chordin, Follistatin, and others will create a gradient by which neural induction is promoted (right) with the aid of other signals (i.e. Fgf - discussed next). AN, animal pole; VG, Vegetal pole; D, Dorsal; BC, Blastocoel cavity; O, Spemann organizer; BMP, Bone morphogenetic protein. Blue is the dorsal side for prospective neural tissue, and brown is the prospective epidermis.

1.1.3.b Fgf signaling in neural induction

Studies in *Xenopus* showed the inhibition of Fgf ligand binding to its receptor (FGFR) in whole embryos (Grunz 1992) or inhibition of Chordin or Noggin in animal caps prevents neural plate induction (Launay et al. 1996; Sasai et al. 1996). Furthermore, Spemann neural induction assay cannot produce neural cells if treated with Fgf inhibitors (Launay et al. 1996). Treatment of *Xenopus* embryos with Fgf inhibitor (SU5402) in a dose-dependent manner showed complete inhibition of neural plate marker *Sox2* (Delaune, Lemaire, and Kodjabachian 2005). Moreover, grafting Fgf beads in the prospective neural plate of Chick led to an ectopic neural axis. This experiment emphasizes the importance of Fgf in neural induction. However, it cannot rule out the possibility of normal host cell recruitment by the bead (Alvarez, Araujo, and Nieto 1998). Further analysis in *area opaca* concluded that Fgf alone is not sufficient to elicit a mature neural plate (Storey et al. 1992b, 1998; Storey, Selleck, and Stern 1995; Streit et al. 2000; Wilson et al. 2000). Hence, the notion that Fgf signaling is required for early steps in neural induction after the BMP inhibition (Stern 2005).

In addition to the early role of Fgf signals in neural induction, it is also linked to the anterior-posterior (A-P) axis patterning. Research in *Xenopus* demonstrated that the inhibition of the Fgf receptor by a dominant negative mutant led to a disorganized neural structure with an absence of posterior markers but not the complete inhibition of neural plate (Amaya et al. 1991; Cox and Hemmati-Brivanlou 1995; Godsave and Durston 1997; Holowacz and Sokol 1999; Kengaku and Okamoto 1993; Kroll and Amaya 1996; Lamb and Harland 1995; Pownall et al. 2003; Ribisi et al. 2000). Furthermore, a study showed that anterior neural plate (prospective forebrain) is caudalized either by the juxtaposition of more posterior neural plate or by exposure to Fgf ligands, which led to the expression of hindbrain markers. Taken together, these findings show the pivotal role of Fgf signaling in the early steps of neural induction and patterning of the A-P axis but not in the maturation of the neural plate (Cox and Hemmati-Brivanlou 1995). This supposition

gives rise to the potential involvement of other signaling pathways, such as Wnt, required for neural induction.

1.1.4 Neural crest induction

Neural crest cells (NCCs) are transient multipotent cells that delaminate and migrate after their induction and differentiate into a wide range of specialized cell types (Hall 2008). NCCs are derived from the dorsal margin of the neural plate (NP); after induction, they delaminate along the anterior-posterior axis of the embryo (Knecht and Bronner-Fraser 2002). In humans, at least 47 different cell types have been identified as derivatives of NCCs, such as glia, smooth muscles, osteoblast, neurons, melanocytes, and chondrocytes. This versatile cell population was first characterized by Wilhelm His over fifteen decades ago (Hall 2008). NCCs significantly contribute to the development of various tissues and organs, and notably, their feature separates vertebrates from other chordate organisms (Hall 2008). In recent years, research on NCCs defects gained vast interest and made impactful progress on several syndromes, such as congenital heart defects and craniofacial aberration (Ji et al. 2019; Knecht and Bronner-Fraser 2002).

Neural crest (NC) induction is an example of instructive embryonic induction. NCCs originate from the neural plate border (NPB), specifically from the ectoderm positioned between the neural plate (NP) – future neurons and the non-neural ectoderm (NNE) – future epidermis and underlined by the paraxial mesoderm (Figure 1.3) (Park et al. 2015; Steventon et al. 2009a). Neural crest cells are induced during gastrulation, where complex interaction between secreted signals occurs, which are derived from the underlying mesoderm, neural plate, and epidermis (Betancur, Bronner-Fraser, and Sauka-Spengler 2010; Ji et al. 2019; Sauka-Spengler and Bronner-Fraser 2008).

Neural crest induction can be divided into two steps, NPB specification and retention of neural crest identity. The first step of NCCs induction is the transformation of the ectoderm into neural plate border (NPB); consequently, the expression of NPB markers is the initial indication of NC induction. A significant number of Xenopus studies implicated several transcription factors for NPB development (Glavic et al. 2004; Hong and Saint-Jeannet 2007; Li et al. 2009a; Monsoro-Burq, Wang, and Harland 2005). Transcription factors that specify NPB, such as *Msx1/2*, *Zic1, Pax3/7, Hairy2, Id3, and Ap2*, are regulated by multiple singling pathways like fibroblast growth factor (Fgf), bone morphogenetic protein (BMP), Wnt singling, retinoic acid (RA), among others (Elkouby et al. 2010; Glavic et al. 2004; Li et al. 2009a). Analysis in Chick showed that Transcription factors such as *Pax7* specify NCCs and are expressed in NPB (Basch, Bronner-Fraser, and García-Castro 2006; Otto, Schmidt, and Patel 2006). Some NPB markers, such as *Msx1, Zic* and *Ap2,* are not restricted to the prospective NCCs, as they are expressed in broader domains suggesting that NPB and neural crest induction are separable events (Khudyakov and Bronner-Fraser 2009). The second step is initiated when NPB cells acquire NCC fate and they can be identified by expression of markers such as, *foxd3, snai1/2, twist,* and *Sox8/9/10* in *Xenopus*, zebrafish, Chick, and human (Aybar and Mayor 2002a; Betters et al. 2010; Honoré, Aybar, and Mayor 2003; Li et al. 2009b; Mancilla and Mayor 1996; Sauka-Spengler and Bronner-Fraser 2008; Simões-Costa and Bronner 2015). Multiple signaling pathways and tissues regulate NC induction. Experiments in *Xenopus* and Chick embryos have shown that the strongest neural crest inducer is the mesoderm adjacent to the prospective neural crest (Fig. 3.1; left). That mesoderm in *Xenopus* corresponds to the dorso-lateral marginal zone (DLMZ), which is the future paraxial mesoderm. It has been shown that DLMZ induces neural crest by secreting Wnt and anti-BMP molecules (Fig. 1.3; pink arrow) and that grafting DLMZ into the ventral region of an embryo induced neural crest in an ectopic location (García-Castro, Marcelle, and Bronner-Fraser 2002; LaBonne and Bronner-Fraser 1998a; Steventon et al. 2009a; Szabó and Mayor 2018). DLMZ is necessary and sufficient

to induce neural crest in naïve animal cap ectoderm *ex vivo* or in ectopic locations *in vivo* (Marchant et al. 1998). In the following sections, we will examine blastocoel morphogenesis and the signaling pathway required in this induction (such as BMP, Hippo, and Wnt) to better understand neural crest induction.

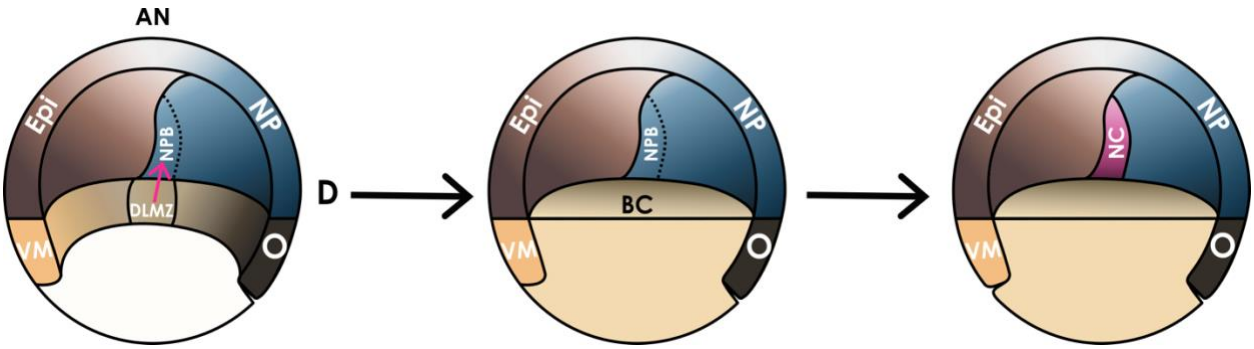

Fig. 1.3|Cascade of neural crest induction.

Neural crest induction is a multistep process regulated by well-characterized inductive molecules. This process commences during gastrulation after the ectoderm has been separated into neural ectoderm (low level of BMP) and non-neural ectoderm (high level of BMP), establishing an intermediate level of BMP in the neural plate border region, which is required for neural crest (left and middle). Then neural plate border cells are induced into neural crest cells by responding to Wnt signals. These Wnts proteins (i.e. *Wnt8, Wnt3a*) are secreted by the dorso-lateral marginal zone and future paraxial mesoderm (left; pink arrow) and initiate the canonical Wnt pathway (right). Epi, epidermis; NPB, neural plate border; NC, neural crest; NP, neural plate; VM, ventral mesoderm; DLMZ, dorso-lateral marginal zone; O, organizer; AN, animal pole; D, dorsal; BC, blastocoel cavity.

1.1.4.a Blastocoel morphogenesis

To better understand the process of neural crest induction, it is crucial to examine the events before this induction commences. The initial cascade of events is the separation of the three germ layers, which happens at early gastrulation (Rebecca F. Spokony et al. 2002). Previous to neural crest induction the three germ layers, endoderm, mesoderm, and ectoderm are specified. Where the endoderm plays a role in the specification of the mesoderm, which in turn will induce the Spemann organizer (Fig. 1.1), thereafter the organizer splits the ectoderm into neural and non-neural ectoderm by producing BMP inhibitors (Fig. 1.2), finally regional secretion of Wnts protein from DLMZ (prospective paraxial mesoderm) plays a pivotal role in the neural crest induction (Fig. 1.3). In addition to the primary cascade of events, a secondary cascade of events is indirectly important for neural crest induction, which is the formation of the first embryonic cavity, the blastocoel (Wolpert and Gustafson 1961). Blastocoel morphogenesis is observed in a wide range of organisms (*Xenopus*, mice, pig, human, cnidarians, echinoderms (sea urchins), Fish (known as *Discoblastula*), Avian, insect, and others); however, in comparison to other cavities during development little much is known of blastocoel initiation, development and early role in embryogenesis (Joshi and Rothman 2005; Schulze and Schierenberg 2011; Wolpert and Gustafson 1961). In *Xenopus*, the anatomical location and morphogenesis have been documented, whereas the function or the role of this cavity during cleavage, blastula, and gastrulation remains poorly investigated (Kalt 1971a, 1971b; Keller 1975a; Winklbauer 2009).

Despite the blastocyst being the first cavity formed during the development of many organisms, their mechanism of formation is different from one organism to another (Chan et al. 2019; Dumortier et al. 2019; Imran Alsous et al. 2021). For example, it has been reported that the blastocoel formation in sea urchin is mediated by "surface plane divisions"(Buske et al. 2012; Wolpert and Gustafson 1961). Indeed, post-fertilization of sea urchin embryos and the subsequent

divisions, the starting point of blastocoel formation is after the 4th division – located in space between the blastomeres (DAN 1952). Wolpert and Gustafson noted that these blastomeres remain "radial" during divisions, suggesting that the low adhesion/compaction between these cells is the main reason for blastocoel formation (Wolpert and Mercer 1963). And it is possible that these embryos are supported in close proximity to each other due to the hyaline layer (a layer that surrounds the entire embryos) (Buske et al. 2012; Itza and Mozingo 2005; Wolpert and Gustafson 1961; Wolpert and Mercer 1963). Although Wolpert and Gustafson model is widely accepted, it requires further experimental investigation to examine the role of the hyaline layer in the blastocoel formation. "it is by no means obvious why successive divisions should give rise to such a hollow sphere rather than compact random clustering of cell" Wolpert adds (Wolpert and Gustafson 1961).

In mice embryos, the blastocoel formation is mediated by "hydraulic fracturing and coarsening" (Maître 2017; Rossant 2016). Mice blastocoel morphogenesis happens during the preimplantation and structurally, an outer epithelial later (trophectoderm) encloses the blastocoel and the inner cell mass (Rossant 2016). Similarly to sea-urchin, mice embryos are surrounded prior to fertilization until implantation by an outer shell composed of glycoproteins, known as zona pellucida (ZP) - common among mammals (Watson, Natale, and Barcroft 2004). Briefly, post-fertilization of mouse zygote, divisions form morula (tightly compacted cells – late 8-cell stage) (Dumortier et al. 2019; Maître et al. 2015a, 2016). Due to the high tension between cell-medium and low tension between cell-cell, apicobasal polarity is established, leading to tight junctions formation at the 2-cell and maturation at the 32-cell stage (Rossant 2016; Watson et al. 2004; Ziomek 1980). The maturation of the tight junction coincides with the initiation of the blastocoel cavity, as it effectively seals the embryo (Rossant 2016). The link between the tight junction and blastocoel formation was established by attenuating the tight junction, which inhibited blastocyst formation (Moriwaki,

Tsukita, and Furuse 2007). Thereafter, hydraulic flux mediated osmotically by ion pumping (Na^+/K^+-pump) into intercellular space leads to the formation of tensed/pressurized micro-sized cavities connected by micro-lumens, creating a transient lumen network (Watson et al. 2004). The high-pressure micro-cavities then coarsen and emptied into larger less pressured cavities (Ostwald ripening process) creating a single cavity. Therefore, blastocoel morphogenesis in mice and presumably in pig, bovine, rabbit, and humans depend on ion pumps and polarized epithelium controlled by two physical properties; osmotic pressure and hydraulic fractioning/coarsening (Dumortier et al. 2019; Maître 2017).

Similar to mice, blastocoel morphogenesis in *Xenopus* is also mediated by osmotic fluid pumping and the physical nature of the yolk (Barua, Parent, and Winklbauer 2017; Frankenberg 2018; Pierre et al. 2016; Slack and Warner 1973a; Winklbauer 2020). *Xenopus* eggs inheritably acquire an acellular outer layer (known as Vitelline membrane) (Byers and Armstrong 1986; Frankenberg 2018), and the apicobasal polarization mediated by the presence of the yolk in the zygote (Byers and Armstrong 1986; Müller and Hausen 1995). Indeed, the yolk is crucial for the polarization of the *Xenopus* zygote (Frankenberg 2018). The yolk granules are concentrated in the vegetal pole (Frankenberg 2018; Pierre et al. 2016). The precursor of the blastocoel cavity is detected as early as the 2-cell stage and will develop thereafter into a mature blastocoel. The accumulation of blastocoel fluid as early as the 2-cell stage is mediated by the formation of tight junctions and adherens junctions that will mature by the 32-cell stage, sealing the embryo from external media (Barua et al. 2017; Fleming et al. 2000; Keller 1975a; Moriwaki et al. 2007). Early studies demonstrated that the expansion of blastocoel after the 32-cell stage is mediated by osmotic forces controlled by ion channels that drive water influx into the newly formed blastocoel precursor (Na^+/K^+-pump) (Slack and Warner 1973a). The role of osmotic-mediated blastocoel expansion was further supported when inhibition of the Na^+/K^+ pump by injection of ouabain inside the cavity, which prevented the blastocoel cavity formation (Slack and Warner

1973a). However, osmotic pressure alone cannot explain the expansion of the blastocoel cavity. Indeed, a single cell taken from the 64-cell stage is able to form an aggregate of cells and have apicobasal polarity and develop to the 8-cell stage like embryos; however, this aggregate does not form a precursor of blastocoel cavity (Müller and Hausen 1995). This suggests that the formation of blastocoel precursor requires the initiation steps at early stages (2-cell stages) (Müller and Hausen 1995). Unlike sea-urchin, blastocoel formation in *Xenopus* is also considered a symmetry breaking point as it is localized in animal pole during early embryonic development (Barua et al. 2017; Frankenberg 2018). These studies highlight the complex steps required to initiate and develop the blastocoel across species and specifically point out the physical and biological elements required for this morphogenesis (Barua et al. 2017; Frankenberg 2018; Pierre et al. 2016). Furthermore, these studies raise far more questions than they address. An in-depth analysis of the formation, expansion, and role of the earliest cavity is essential as these cavities might hold the answer to the most challenging questions; the spatial and temporal regulation of germ layers and to expand our understanding of the earliest and pivotal role of biomechanics in embryogenesis. In this work, we aim to examine the role of the blastocoel of *Xenopus* on the induction of neural crest. Before that, next, we examine cell signalling that is essential for neural crest induction.

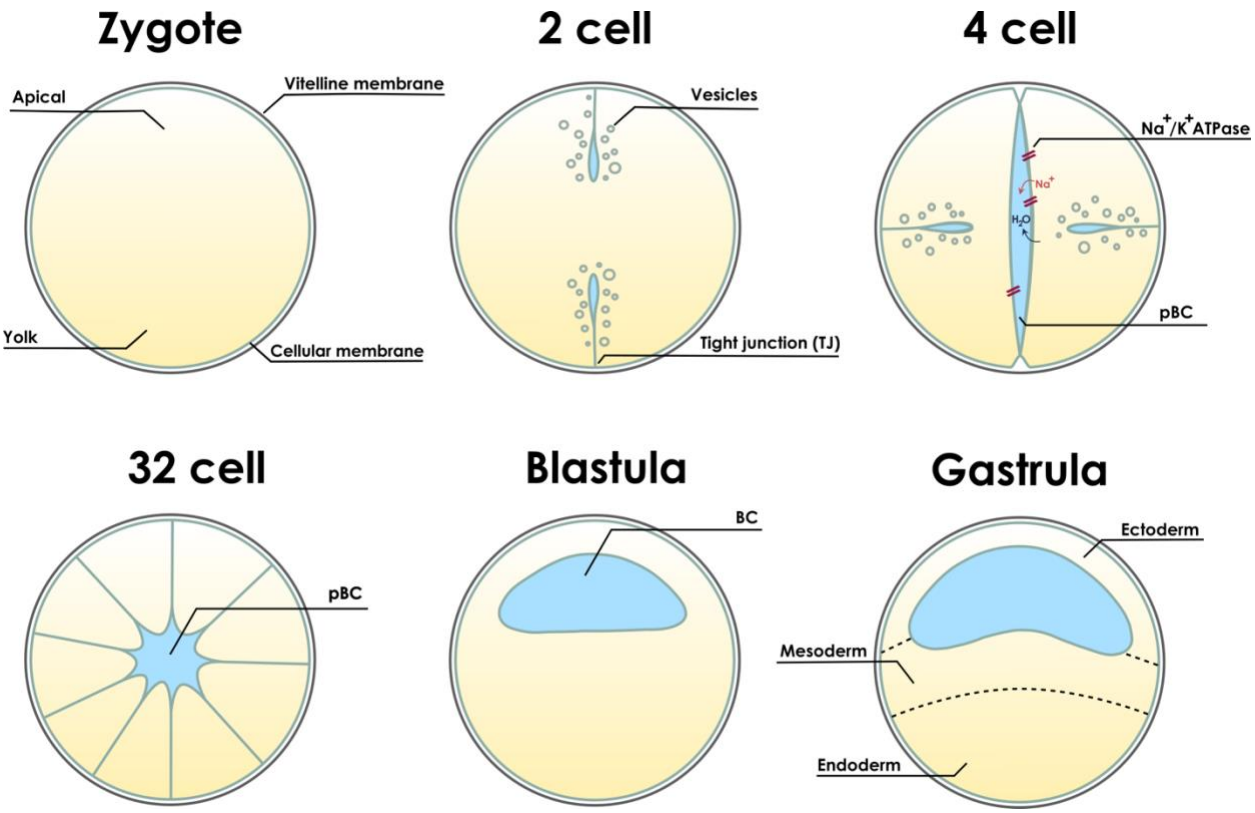

Fig. 1.4 | *Xenopus* blastocoel morphogenesis.

Schematic of blastocoel development prior to fertilization, cleavage, blastula, and early gastrulation. At *zygote*, *Xenopus* eggs have a vitelline membrane (acellular transparent shell) and the apical (white) basal (yellow) polarity has been established due to the presence of yolk. At the *2-cell stage,* the first cleavage has occurred and the earliest formation of tight junctions. At the *32-cell stage*, the tight junction has matured sealing the embryo and with the continuous hydro-flux via ion pumps (red) the interstitial space continually expands (pBC; prospective blastocoel). At *blastula stages*, the blastocoel cavity is localized in the animal hemisphere and expands throughout.

1.1.4.b BMP signaling in neural crest induction

Bone morphogenetic proteins are crucial for multiple steps in the development of CNS of vertebrates (Leung et al. 2016a). For example, at early gastrula stages in *Xenopus*, a gradient of BMP is established and controlled by their antagonists (Noggin, chordin, and others) (Fig. 1.2) (Barth et al. 1999; Conlon et al. 1991; LaBonne and Bronner-Fraser 1998b; Marchant et al. 1998; Tríbulo et al. 2003). Considering that the NCCs are located between the epidermis and the neural plate, it was hypothesized that a level of BMP intermediate to the one required to specify the epidermis and neural plate is crucial for NC induction (Marchant et al. 1998; Tríbulo et al. 2003). This hypothesis was validated in *Xenopus* and zebrafish, and it was found that a BMP gradient is required for the different specifications of the ectoderm; high levels of BMP are required for the epidermis, an intermediate level is required for the development of neural crest, and inhibition of these proteins are necessary for neural plate development (Aybar and Mayor 2002a; Leung et al. 2016a; Marchant et al. 1998; Mizuseki et al. 2003; Ragland and Raible 2004; Steventon et al. 2009a; Tríbulo et al. 2003). This postulation was further supported when the BMP gradient was attenuated, which led to the expansion of neural plate and neural crest cells (Linker et al. 2009; Wawersik, Evola, and Whitman 2005). Indeed, these findings support the notion that ectoderm specification depends on the BMP activity level.

In mice at day (E) 8.0, Noggin (BMP antagonist) is expressed in neural folds and the dorsal side of the embryo after neural tube closure (Anderson et al. 2006). This antagonist plays an essential role in neural crest induction and migration. Moreover, BMP-mediated apoptosis is inhibited by antagonists during migration and differentiation of NCCs. A decrease in BMP antagonists was demonstrated to attenuate PNS derived from NCCs and craniofacial skeletal components. Indeed, Noggin knockout mice exhibited disorganized and fused cranial nerves, except the vagus and glossopharyngeal. In addition, a Chordin and Noggin double-knockout lacked CN and is left with only trigeminal ganglion like-structure

(Anderson et al. 2006). In Chick, BMP activity during the formation of neural crest progenitors is mediated by CKIP/Smurf factors via Smad degradation, yielding an intermediate gradient of BMP levels required for NC induction (Piacentino and Bronner 2018). Additionally, human embryonic stem cells (hESCs) analysis showed BMP inhibition via Noggin during differentiation protocol for 24hrs on different days (0, 1, or 2) led to the inhibition of human NCCs. However, the inhibition was partial if the Noggin was added on the third day, suggesting a temporal window where these cells respond to Noggin (Leung et al. 2016a). This result highlights the role of BMP signaling on neural crest induction.

1.1.4.c Wnt signaling in neural crest induction

1.1.4.c.i β-catenin dependent and independent Wnt pathways

Wnts are secreted glycoproteins that are critically involved in a vast number of cellular processes in development and disease (Nusse and Clevers 2017a). The binding of Wnts proteins to receptors, such as Frizzled (Fzd), low-density protein (LDL), and Lrp5/6, initiate the canonical β-catenin dependent Wnt pathway (Nusse and Clevers 2017a). Activation of the canonical Wnt pathway inhibits β-catenin destruction complex leading to the stabilization of β-catenin in the nucleus and regulates the targeted genes after interacting with TCF/LEF (Fig. 1.4; right side) (V. S. W. Li et al. 2012). In the absence of Wnts glycoprotein, the pathway is inactive due to β-catenin degradation via β-catenin destruction complex (GSK3β) (Fig. 1.4; left side) (Cselenyi et al. 2008; V. S. W. Li et al. 2012; Nusse and Clevers 2017b; Wodarz and Nusse 1998). Wnt/β-catenin pathway activation regulates cellular activities such as cell proliferation, differentiation, and apoptosis (Nusse and Clevers 2017b; Wodarz and Nusse 1998). The non-canonical Wnt pathway which is independent of β-catenin is associated with Planer cell polarity (PCP) found in *Drosophila* and vertebrates in addition to the Wnt/Ca^{2+} pathway, which is found in vertebrates (Humphries and Mlodzik 2018; Kikuchi, Yamamoto, and Sato 2009; Mayor and Theveneau 2014). The latter

pathway results in either an increased cytoplasmic Ca^{2+} after binding of Wnts to Frizzled receptors, production of IP_3 and DAG, or the initiation of Calpain by directed activation of Ror1/2 by Wnts (De 2011; Kühl et al. 2000; Lilienbaum and Israël 2003; Sheldahl et al. 1999). Indeed, β-catenin dependent and independent Wnt pathways have been well-characterized in several cellular processes and steps of embryonic development.

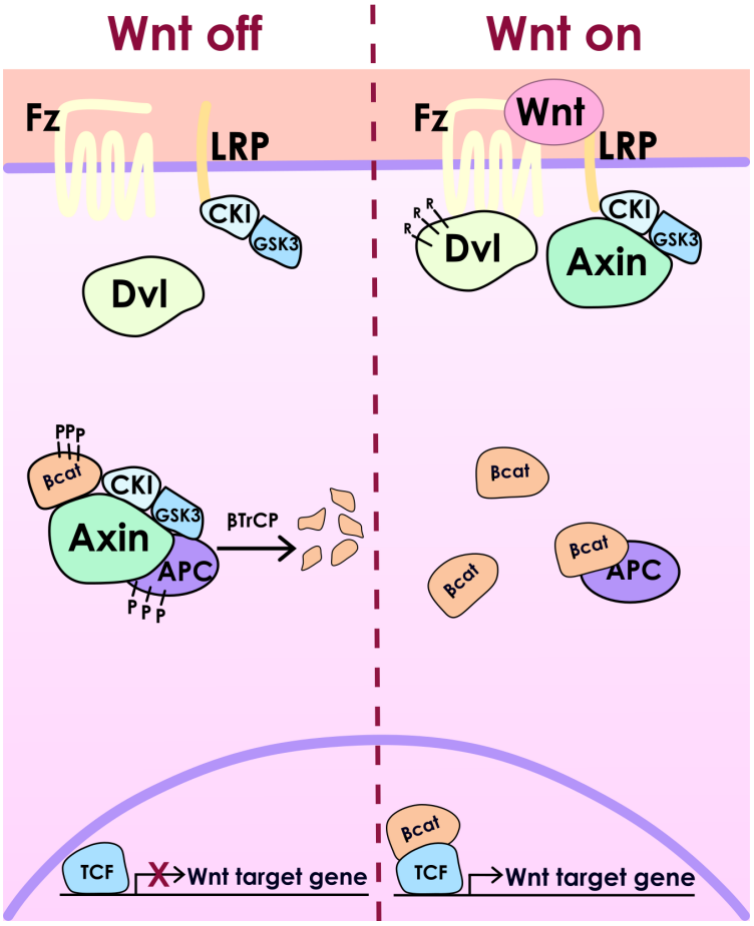

Fig. 1.5 | β-catenin dependent Wnt signaling pathway.

The Wnt pathway is off (left side) when Wnt receptor complexes are not bound by ligand. Where β-catenin is recognized by β-catenin destruction complex and rapidly degraded by the proteasome. The canonical Wnt pathway is activated when the Wnt ligand binds to Frizzled(Fz)/LRP receptor complex (right side). Upon activation β-catenin destruction complex is inhibited, promoting the translocation of β-catenin into the nucleus and binding to TCF to regulate target genes.

1.1.4.c.ii Wnt signaling in neural crest induction and specification

The canonical Wnt pathway is well-characterized and considered a key pathway to modulate neural crest induction. Several components of Wnt proteins, such as *Wnt1, Wnt3a, Wnt7b, Wnt8, Fzd3*, and *Lrp6,* have been linked to NC specification in vertebrates (Borday et al. 2018a; Chang and Hemmati-Brivanlou 1998; Deardorff et al. 2001; LaBonne and Bronner-Fraser 1998a; Saint-Jeannet et al. 1997; Tamai et al. 2000). A study in *Xenopus* showed that Fzd7 (Wnt receptor) is required for the expression of NC markers *Sox9/10, snai1, twist*, and *foxd3*, as the inhibition of this receptor attenuates the expression of these markers, and it can be rescued by β-catenin. This result indicates the role of Fzd7 in the induction of neural crest mediate via the canonical Wnt pathway (Abu-Elmagd, Garcia-Morales, and Wheeler 2006). Further analysis in *Xenopus* suggests that the canonical Wnt pathway is regulated by *RhoV*, which is regulated by *Wnt1* levels (Faure and Fort 2011; Guémar et al. 2007; Weisz Hubsman et al. 2007; Yang et al. 2005). In Chick, it has been shown that Axud1 is downstream of Wnt/β-catenin pathway and required for regulation of NC specifiers (*Sox9, Sox10*, and *Ets1*), but not NPB specifiers (*Pax7*)(Quinlan et al. 2009). In addition, it has been shown that Axud1 interacted with *Msx1* and *Pax7* to form a complex that regulates the expression of *foxd3* (Simões-Costa, Stone, and Bronner 2015). These findings further support the idea that neural crest induction is mediated by canonical Wnt pathway in a β-catenin dependent manner.

In addition to the role of Wnt signaling in the induction of NC, it is also required for A-P axis patterning. It has been proposed that neural crest specification is an indirect effect of the posteriorizing activity modulated by Wnt signalling (Villanueva et al. 2002). As in *Xenopus*, posterior neural tissue is mediated by the Wnt pathway activating Fgf signaling. Thus, Wnt signaling posterization activity can be inhibited by blocking Fgf signaling (Domingos et al. 2001). In contrast, further analysis showed NC markers (*snai2* and *twist*) are expressed after blocking posteriorizing activity, suggesting that the canonical Wnt pathway directly

mediates neural crest induction (Aybar and Mayor 2002a; Wu, Yang, and Klein 2005). These data suggest the elaborate role of Wnt signaling in neural crest development. Together, these studies **strongly demonstrate evidence that the Wnt molecule plays a major role as a neural crest inducer, which is conserved across species.**

1.1.4.d Hippo signaling in neural crest development

The Hippo pathway is one of the crucial signaling pathways from development to adulthood and in pathologies (Aragona et al. 2013; Azzolin et al. 2014a; Jiang et al. 2020; Piccolo et al. 2022). Although detailed information on Hippo signaling has been obtained from *Drosophila* and cell culture, there are significant gaps in our understanding of the Hippo pathway in mammalian systems (Guillermin et al. 2021; Jiang et al. 2020). The Hippo pathway consists of a growing number of components that includes kinases and adaptor proteins that controls the subcellular localization of Yes Associated Protein (Yap), which in turn regulate target genes of this pathway. Once Yap and Taz are translocated into the nucleus, it binds to its TEAD transcription factor regulating a broad number of cellular functions like proliferation, stemness, and growth (Dupont et al. 2011; Guillermin et al. 2021). Whereas cytoplasmic Yap will either lead to its interaction with other signaling pathways like (i.e. canonical and non-canonical Wnt pathway, AMPK, Notch, JNK, mTOR, and Ras/MAP pathways) or are targeted for degradation. The Hippo pathway is activated by extracellular or intracellular signals (Jiang et al. 2020). The nature of the Hippos pathway activator varies from ligands, growth factors, integrin signaling, polarity complexes, cell-cell junction, and a wide range of mechanical inputs. Upon activation of the Hippo pathway (as detailed in Fig. 1.5), it regulates a wide range of specific cellular activity (Franklin et al. 2020; Jiang et al. 2020). A few examples of these are organ size regulation, controlling tissue density by contact inhibition proliferation (Huang et al. 2005), and epithelial-mesenchymal transition (EMT) during embryogenesis (Milewski et al. 2004). Indeed, studies have shown that the downstream co-

transcriptional factor of the Hippo pathway is co-localized with neural progenitor marker *Sox2* in addition to Taz, which stimulates proliferation and its role in promoting EMT (Cao, Pfaff, and Gage 2008; Milewski et al. 2004). The convergence of this pathway with the classical NC genes is still in the early days, and further in-depth analysis is required to fully understand the role of the Hippo pathway in neural crest induction, migration, and differentiation. However, the interaction between *Pax3* (an NC progenitor marker) and Yap/Taz has been investigated (Lei et al. 2008). It has been suggested in mice that Tead2 (TEA Domain Family Member 2, Yap binding partner) is an activator of *Pax3* in prospective NCCs. Indeed, it was found that *Pax3* and Yap are co-localized in the nucleus of NC progenitors in the dorsal neural tube (Milewski et al. 2004). In rodents, it was found that Hippo/Yap/Taz is vital for Schwann cell proliferation and differentiation in a time-dependent manner. Active Yap/Taz complex initiates cell cycle regulators to promote Schwan cell proliferation while controlling differentiation with *Sox10* for myelination (Deng et al. 2017). **Despite these advancements, it is still unclear how the Hippo pathway regulates neural crest induction and whether its activators are biochemical or mechanical signals.**

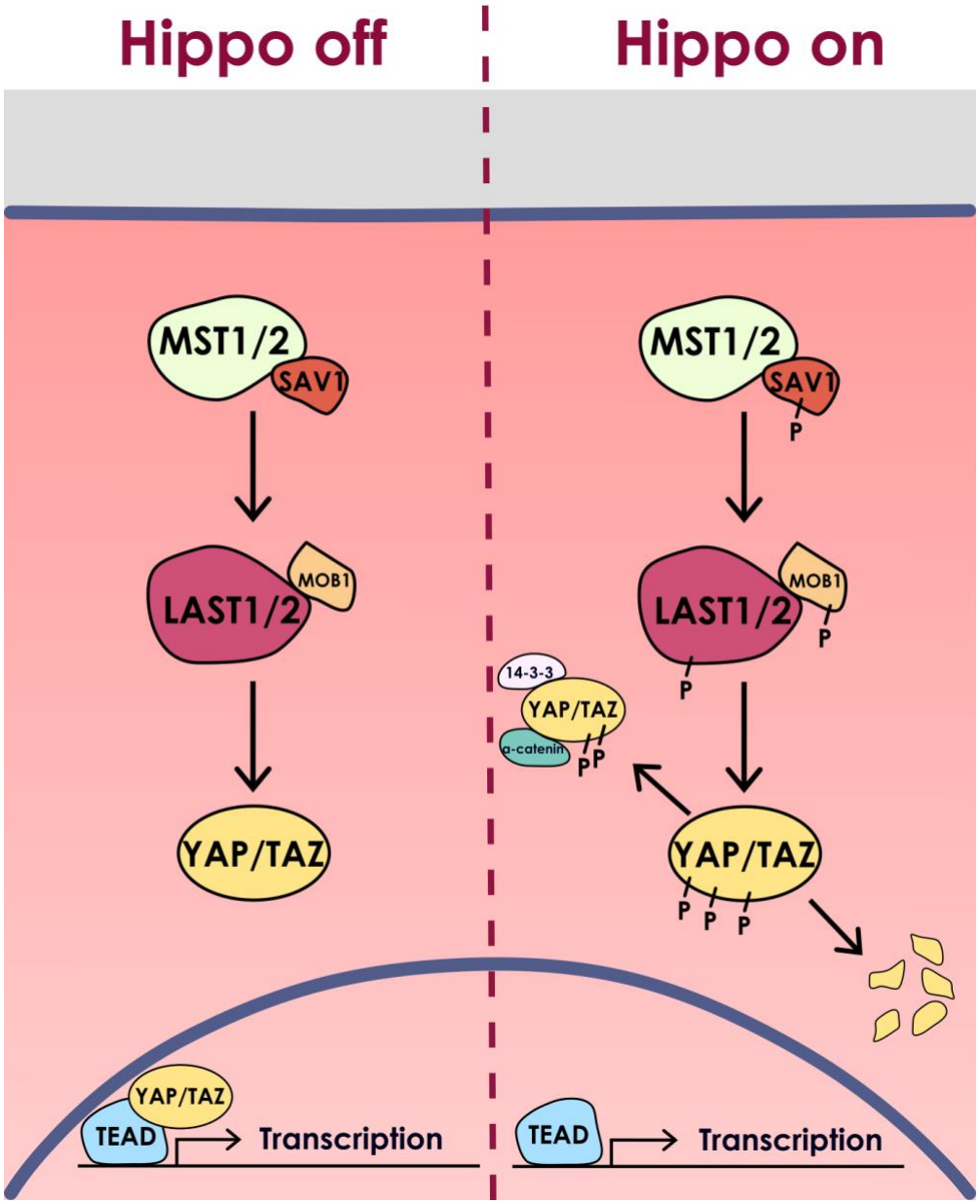

Fig. 1.6 | The Hippo pathway.

Several intra- and extracellular signals modulate the phosphorylation of protein kinases upon Hippo activation. MST1/2 kinases and SAV1 form complexes that activate LATS1/2. Yap and Taz are key downstream proteins of kinases. The phosphorylated LAST1/2 kinases will phosphorylate Yap, leading to its cytoplasmic retention or degradation (right side). Alternatively, the Hippo pathway is off when Yap is not phosphorylated, promoting its translocation into the nucleus and binding to TEAD, regulating targeted genes (right side).

1.2 Competence

1.2.1 Temporal and spatial characteristics of competence

Competence is the change in the direction of fate based upon the ability of receiving tissue to respond to the inductive signals generated by inducing tissue (Pyke 1956; Waddington 1937). However, the ability to respond to instructive signals is restrictive to developmental time. An example of temporal competence was noted when the conjugate of animal pole cells of *Xenopus* and vegetal cells were created at different developmental times. Dale and colleagues showed that the ectoderm (animal pole cells) is not competent to become mesoderm at stage 10, whereas earlier conjugates could induce mesoderm at the expense of the prospective epidermis (Dale, Smith, and Slack 1985). Findings in Chick supported the temporal notion of competence in neural induction by examining the organizer ability to produce the inductive signals and the ability of the epiblast to respond to inductive signals; these studies concluded that epiblast competence to generate neural plate is restricted in time (Dias and Schoenwolf 1990; Gallera 1977; Storey et al. 1992b). Further analysis of ectoderm ability in *Xenopus* to develop lens was done by serial grafting animal cap (stages 10-12) from donor embryos in prospective lens region in host neurula stages, showing animal cap ability to respond was restricted in time (starts stage 11 and lost at 12) (Servetnick and Grainger 1991). The temporal ability of the responding tissue to inductive signals gained interest, and further studies demonstrated that this ability could be extended given the suitable proteins, an example of which is when the ectoderm of *Xenopus* did not lose its competence to induce neural or mesodermal cell when treated with cycloheximide (Grunz H 1970). As short exposure of ectoderm to cycloheximide inhibits protein synthesis, this observation suggests that competence (or at least the signaling interaction required in this case) might be regulated by the synthesis of new protein(s).

Gurdon hypothesized the spatial characteristic of competence is determined by tissue area that can respond to inductive signaling and its proximity to inducing

tissue (Gurdon 1987). Several examples of regional competence have been demonstrated; only 40% of animal pole cells will differentiate into mesoderm if exposed to vegetal cells (Dale et al. 1985), and only the inner layer of the ectoderm can differentiate into the brain (Asashima and Grunz 1982) even though in both cases all of the ectodermal cells are exposed to vegetal inducing signals. These findings suggest that not all the regions in responding tissue are competent. Another study in *Xenopus* demonstrated that dorsal and ventral cells of animal pole treated with the same amount of Fgf would yield different types of mesodermal cells (Sokol and Melton 1991). An alternative explanation is a different orientation during cell division; as cells in responding tissue divide, the apical membrane protein is differentially inherited from the non-competent region (Chalmers, Strauss, and Papalopulu 2003). In conclusion, these studies demonstrate the spatial ability of responding tissue towards inductive signaling; however, the mechanism that governs this phenomenon remains poorly understood.

1.2.2 Molecular regulation of competence

Since the discovery of competence, researchers have aimed to identify or explain this phenomenon in molecular terms. Analysis of mesoderm competence showed that the marginal cells are more susceptible to Fgf signaling than animal pole cells (Godsave and Shiurba 1992), this study used single cell culture to determine the sensitivity of cells to respond to Fgf inductive signaling. Marginal zone (MZ) – prospective mesoderm responded at a lower concentration of Fgf compared to animal pole cells. However, this study associated the higher sensitivity to inductive signals due to higher levels of Fgf transcription factors in MZ than animal pole cells and a high density of Fgf cell surface receptors in MZ cells (Gillespie et al. 1989a). This concludes that since single cells from different regions respond differently to Fgf-like molecules, there is no unbiased test for induction studies of mesoderm (Godsave and Shiurba 1992).

Further investigations claimed to have identified competence "modifiers". An example of which is activin-treated explants at a low dose it generates ventral mesoderm; however, if it is combined with *Wnt8* modifies the tissue response and induces dorsal mesoderm (Christian, Olson, and Moon 1992). On the other hand, when explants are treated with a high dose of activin it generates dorsal mesoderm; however, if it is combined with exogenous retinoic acid (Ruiz i Altaba and Jessell 1991) and BMP4 (Dale et al. 1992) induces ventral mesoderm. Despite these studies that suggest that some of these molecules act as "competence modifiers", their role is unclear, and whether they are direct regulator of competence or simply work as inductive signals remains unclear.

Moreover, researchers aimed to identify whether competence is regulated at the chromatin level. Hence, ATAC-seq/ChIP-qPCR was utilized to reveal that the dorsal genes are not accessible for transcriptional activity due to chromatin condensation after mesodermal induction (loss of competence) (Esmaeili et al. 2020a). Thus, it was hypothesized that loss of competence could be explained at transcriptional levels; however, when neural crest competence cells were analyzed, authors found that when neural crest competence is lost, chromatin accessibility is not reduced. This approach is insufficient to propose an epigenetic mechanism to explain changes in neural crest competence, subsequently, a unifying mechanism to explain competence (Esmaeili et al. 2020a). **In conclusion, these findings cannot provide a mechanism to explain the competence ability of induced tissue to respond to inductive signals and commit to a fate.**

1.3 Impact of the mechanical cues on cell fate

Despite understanding how biochemical signaling directs cell fate which has revolutionized the study of cell biology and embryogenesis over the last century, new insights into how mechanical cues regulate cell fate have gained vast interest over the last two decades (Plusa and Hadjantonakis 2016). Indeed, during embryogenesis, extrinsic mechanical inputs such as fluid flow, sheer stress, hydrostatic pressure, tension, compressive forces, and others, in addition to intrinsic forces such as cell density, shape, and extracellular elasticity and topography, are essential for cell fate, motility, and behavior (Abuwarda and Pathak 2020; Nelson 2022).

The mechanical landscape is highly complex, and extrinsic and intrinsic cues often cannot be decoupled. Mechanical cues are perceived by cells via mechanosensitive elements on the cell surface, such as membrane channels (piezo1/2) (Canales Coutiño and Mayor 2021b, 2021a; Tschumperlin 2011), integrins, focal adhesions (Sun, Guo, and Fässler 2016), or others; this promotes cytoskeleton to respond to counterbalance the force by increasing or decreasing contractility. Tension change in the cytoskeleton mediates downstream transcriptional activity that controls cellular response, such as cell fate (Cho et al. 2019; Swift and Discher 2014). However, this mechanotransduction model is not unidirectional as a direct interaction between the nucleus and cytoskeleton plays a role in how cells perceive these mechanical cues, leading to a feedback loop on transcriptional activity (Mason et al. 2019; Swift and Discher 2014).

An example of how mechanical input influence cell fate can be found in mesenchymal stem cell (MSC) differentiation. Adipogenic or neuronal differentiation from MSC is promoted on soft matrices, whereas stiff matrices induce osteoblast or myocytic differentiation (Dupont et al. 2011; Engler et al. 2006; McBeath et al. 2004). Moreover, if MSCs are cultured in neurogenic stiffness (0.1-1kPa) and after three weeks are incubated with myogenic or osteogenic

media, inductive signals are over-ridden and neurogenic fate is maintained by MSC (Halder, Dupont, and Piccolo 2012). These studies suggest that intrinsic mechanical input (ECM stiffness) is sufficient to drive MSC fate independently; nevertheless, induction media can enhance this response. In addition, these studies strengthen the notion of mechanical input interplay with biochemical signals to prompt cellular fate (Engler et al. 2006; Halder et al. 2012).

Further investigations in embryogenesis have found that several developmental processes can contribute to extrinsic or intrinsic mechanical cues, such as growth, movement, and rearrangement of tissues, among others. These mechanical inputs can be regulated by cell-cell contact as seen in tissue compaction in mice (LI et al. 2009; Maître et al. 2015b), fluid to jamming transition as described for body axis elongation (Bénazéraf et al. 2017; Mongera et al. 2018), or by increasing cell density of the head mesoderm, which is sensed by neural crest cells initiating migration (Barriga et al. 2018). Neural crest cells are one of the cell types with the ability to sense the environment and act accordingly; for example, evidence suggests that neural crest migration (Shellard and Mayor 2021) and differentiation are mediated by mechanical cues (Canales Coutiño and Mayor 2021a). Mechanistically, the mechanosensitivity of neural crest cells can be seen in the increase in cell density of the head mesoderm leading to a rise in mesoderm stiffness from 50 Pa to 150 Pa, which is sensed by neural crest cells via focal adhesions, triggering its migration (Barriga et al. 2018). Moreover, culturing neural crest stem cells (NCSCs) derived from induced pluripotent stem cells (iPSCs) on different hydrogel stiffness will control the fate outcome of these cells between smooth muscle or glial cells (Li et al. 2020; X. Li et al. 2012). Lastly, inhibition of Rho-associated kinases (ROCK) and myosin II lead to the expansion of neural crest markers (*foxd3* and *Sox8*) during induction in *Xenopus* embryos(Kim, Ossipova, and Sokol 2015). The outcome of this study suggests the possible role of mechanical input during neural crest induction and the potential translation of mechanical input via ROCK and myosin II.

Together, these findings shed light on the pivotal role of mechanical input on cell fate and other cellular responses. However, the precise mechanism of the bidirectional mechanotransduction model remains to be investigated.

1.4 Thesis Hypothesis

Embryonic competence is the ability of cells to respond to a particular inductive signal generated from inducer cells, resulting in a different outcome of fate (Martinez Arias and Steventon 2018; Pyke 1956; Spemann and Mangold 1924; WADDINGTON 1934), and it is a vital process during embryogenesis noted as such since it is discovery over one hundred years (Spemann 1901). The spatial and temporal characteristics of competence are pivotal for patterning tissue and organs during embryogenesis (Groves and LaBonne 2014; Gurdon 1987). Although previous studies aimed to explain how competence is regulated via biochemical pathways (Christian et al. 1992; Esmaeili et al. 2020b; Gillespie, Paterno, and Slack 1989b; Groves and LaBonne 2014; Henig, Elias, and Frank 1998; Lim et al. 2013; Pieper et al. 2012; Steinbach, Wolffe, and Rupp 1997; Streit et al. 1997), we still lack a comprehensive understanding of the mechanism that regulates competence during embryonic development. Indeed, since embryonic induction was cornered, vast molecules have been identified that are essential for embryonic induction of mesoderm, neural plate, neural crest, and others (i.e., Fgf, Wnt, BMP, and others) (Groves and LaBonne 2014; Mayor and Theveneau 2014; Stern and Downs 2012). However, these pathways did not provide a clear understanding of how the ability of these cells to respond to signals is controlled during development. In this work, we aimed to understand this embryonic phenomenon using an alternative approach, biomechanical. Indeed, early embryogenesis involves a wide range of cellular movements and tissue rearrangements. Furthermore, there is evidence of how mechanical cues control cell fate (Plusa and Hadjantonakis 2016). An example of this is how mechanical cues control cell fate of neural crest is controlled by stiffness (Li et al. 2020; X. Li et al. 2012), ability to migrate (Barriga, Shellard, and Mayor 2019), and the possibility that mechanical cues could regulate the induction of neural crest (Kim et al. 2015).

Thus, in this thesis, we explored the novel idea that mechanics could regulate embryonic competence. To test this idea, we have analyzed neural crest competence as the biochemical bases of its induction are well characterized (Curchoe et al. 2010; LaBonne and Bronner-Fraser 1998b; Mayor, Morgan, and Sargent 1995; Steventon et al. 2009a). Thus, I propose the hypothesis that "**neural crest competence is controlled by mechanical cues**", which will be addressed by analysing the following aims:

1. Identify the mechanical cues that control the competence of the ectoderm to induce neural crest cells.
2. Investigate how mechanical cues interplay with molecular inductive signals during neural crest competence.

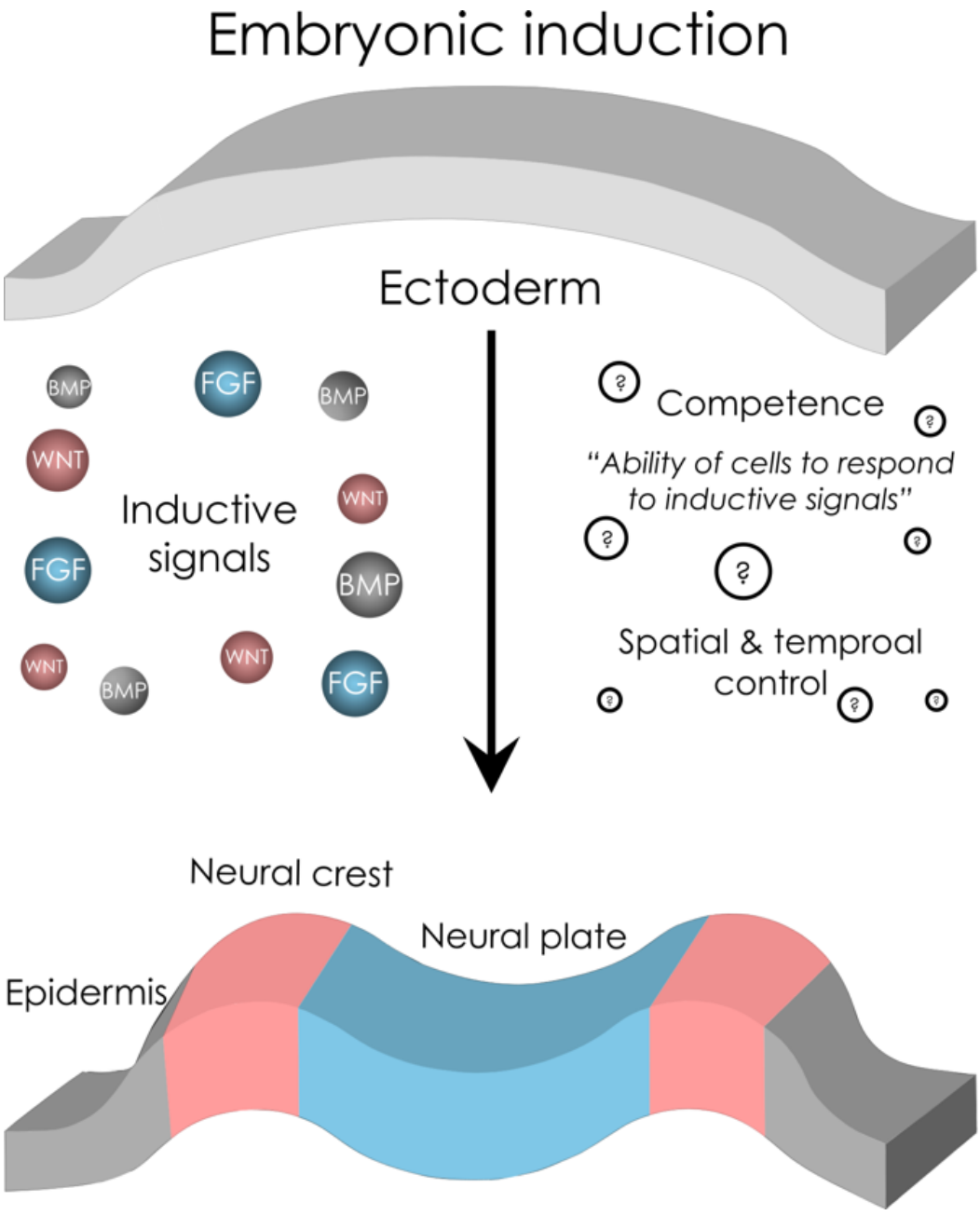

Fig. 1.7 | Graphical introduction.

Embryonic induction controls the formation of new cell types, tissues, and organ formation. Induction corresponds to a change in the direction of differentiation mediated by interaction of inducing and responding tissues. This process is controlled by signaling pathways (left of the arrow), tissue competence, and spatiotemporally restrictive during morphogenesis; however, the mechanisms for this restriction have remained elusive. We aim to examine how neural crest competence is biomechanically controlled during embryogenesis.

Chapter 2: Material and Methods

2.1 *Xenopus laevis* embryos

Adult *Xenopus laevis* (Nasco, and *Xenopus* Resource Centre) were maintained in standard conditions in the animal facilities of University College London. They were used per the Regulations (Scientific Procedures) Act 1986, as described previously (Benjamin et al., 2021). University College London and the UK Home Office approved animal licenses, including establishment, project, and personal licenses.

Xenopus embryos were obtained by *in vitro* fertilization, as previously described (Barriga et al. 2018). Briefly, superovulation of *Xenopus* females was induced by injection of 100 IU pregnant mare serum gonadotrophin hormone, subcutaneously (PMSG; Intervet) 2-5 days before the second injection of 250-300IU of chorionic gonadotrophin hormone (Chorulon; Intervet), which was performed ~12 hours before the planned fertilization. Females who produced eggs 24 hours after the second injection was kept in 0.1X Marc's Modified Ringers (MMR; 5mM HEPES, 0.1mM EDTA, 100mM NaCl, 2mM KCL, 1mM $MgCL_2$, and 2mM $CaCL_2$) at 17C°. Testes were obtained from *Xenopus* males by anesthetization in Tricaine solution for 40 min and then culling by pithing. The testes and stored in Leibovitz L-15 medium (Invitrogen, 11415-064) with added streptomycin (5 μg/mL, Sigma, 85886) at 4C°. Eggs were fertilised *in vitro* in a petri dish (Falcon 734-0006) with 500 μL 0.1MMR, which had a small piece of testes crushed.

After 30 min, 1/10 of Normal Amphibian Media (NAM) was added to the dish. Fertilised eggs were de-jellied no earlier than the 1-cell stage in 2% cysteine solution dH_2O. Then, embryos were incubated at 14.5C° in NAM 1/10 and staged according to the standard table of *Xenopus* development (Nieuwkoop 1967).

2.2 Cell culture Human induced neural crest cells (hiNCCs) and immunostaining

Human induced neural crest cells (hiNCCs) were obtained by Wnt activation and BMP inhibition in induced pluripotency stem cells (iPSCs), as previously reported (Leung et al. 2016b). Briefly, NIBSC8 iPSCs (National Institute for Biological Standards and Control – UK) were plated on Matrigel-coated wells using hiNCC induction media for 5 days. hiNCC induction media was constituted of DMEM/F12 Glutamax (Thermofisher Scientific), 0.5 % BSA (Sigma), 3uM CHIR99021 (Sigma) and 2 % B27 supplement (Thermofisher Scientific). Different iPSC confluences achieved (10% 45%, 100% - confluent, 100+% - dense) were obtained by plating hiNCC with different cell densities. After 5 days, cells were fixed with 4% PFA, permeabilized with PBS 0.1% TritonX and blocked with 5% BSA. Cells were then incubated overnight at 4°C with antibodies for *Sox9* (1:500, Sigma), *Sox10* (1:50, DSHB) and Yap1 (1:200, Proteintech) in a blocking solution. Secondary antibody incubation was performed for 1 hour at room temperature using AlexaFluor 488, AlexaFluor 594 (Thermofisher) and DAPI. Cells were imaged with EVOS 7000, and images were analyzed with ImageJ. This was done with help from Lucas Alvizi.

2.3 Graft assay

Inducing ectopic induction of neural crest requires specific signals from prospective mesoderm known as dorsal lateral marginal zone (DLMZ) (Curchoe et al. 2010; García-Castro et al. 2002; LaBonne and Bronner-Fraser 1998b; Steventon et al. 2009a). The tissue of DLMZ was dissected using a premade hair knife from an early gastrula stage 10 (N&F) donor embryo and grafted into the cavity of the host embryos at different gastrulation stages as previously described to assess the competent ability of the ectoderm to induce NCCs (Mancilla and Mayor 1996). The grafted embryos were incubated in NAM3/8 during the procedure and NAM1/10 up to late neurula stages, then fixed, ectopic induction was analyzed by *in situ* hybridization. As the DLMZ could attach to any side of the ectoderm, we aimed to have the DLMZ attached to the ventral side as much as

possible to have a clear outcome of the assay. As the ventral side of the ectoderm does not induce NCCs, we could potentially rule out the effect of endogenous dorsal signaling. In addition, grafted embryos exhibited an ectopic induction that extended to the dorsal endogenous neural crest induction, which leads to dorsal-lateral ectopic induction rather than ventral ectopic induction, were removed from the analysis, as shown (Fig 3.1).

2.4 Compression assay

Explant compression assay, explants containing the prospective neural crest were obtained by a series of dissections incubated in NAM 3/8 media. The first cut (with a premade hair knife), the ventral tissue was removed (from the dorsal blastopore lip to the animal-ventral side). A second cut was made from the animal pole to the ventral side to open the explants. Then explants were compressed under a coverslip using vacuum grease (Dow Corning GMBH, 0315) to control the compression level. Explants were incubated in NAM1/10 till desired developmental stage, fixed and expression of NC markers were analyzed by *in situ* hybridization. Experimental explants were compressed compared to similarly dissected embryos but not compressed.

2.5 Inflation and Deflation assay

Inflation and deflation of the blastocoel cavity of *Xenopus* embryos were achieved using a microinjector (MicroData Instrument, Inc.). First, a microneedle was prepared to aspirate or increase the fluid in the blastocoel cavity (pulled – Narishige PC-10 and calibrated via microforge – Narishige, MF2) with a 10-20µm tip. To achieve inflated embryos, 100 – 250nL of media was injected inside the blastocoel cavity at a pressure of 23.4Psi for 15 seconds. And for deflation, a microneedle with a 30µm tip was used to aspirate 100 – 175nL of blastocoel liquid from the blastocoel cavity. During inflation, embryos were incubated in 3%FICOL (P7798-500G, Sigma in 1-liter NAM3/8) for 1 hour, then in NAM3/8 till desired

development stage and then fixed for further analysis. In contrast to inflation, deflated embryos were incubated in NAM3/8. Different osmolarity Media were achieved and used in inflation assay: hypotonic (0.1 MMR, of 222 mOsm), hypertonic (3% FICOL, 900 mOsm), isotonic (fluid was taken from the blastocoel cavity from sibling embryos).

2.6 Microinjections and treatments

2.6.1 Calibration

Microneedles for microinjections were prepared using 2 step puller (Narishige, PC-10) and calibrated under a dissecting microscope (LeicaMZ6) for 5nl injections at 23.4Psi every 0.20 seconds. Microinjections of a final volume 5nl were done into two blastomeres (animal pole side) of 8-cell stage embryos using a PM1000 microinjector (MicroData Instrument, Inc.) as described previously (Gee et al. 2011). During microinjections, embryos are continuously incubated in NAM3/8 unless specified otherwise. After calibration and microinjection embryos were incubated at 14.5C till desired developmental stage and then fixed for further analysis.

2.6.2 RNA synthesis and Morpholino

The following constructs were injected into the embryos; a 70ng of Yap morpholino (Gee et al. 2011), obtained from GeneTools, was injected into blastomeres of the 8-cell stage. In addition, the following mRNA were injected as described above: 2ng of YapS127A, 8pg of Xwnt8 (Christian et al. 1991), and 200pg of β-catenin-GR (Carmona-Fontaine et al. 2007; Vleminckx, Kemler, and Hecht 1999). Construct of YapS127A (Addgene plasmid #17790), the original insert was subcloned between these two sites; *Xba1* and *Spe1* sites in pBluescript SK(+) backbone vector, followed by *in vitro* transcription of this construct and other mRNA used in this study (mMessage mMachine kit, Thermo Fisher Scientific, AM1340 for SP6 and AM1334 for T7).

2.6.3 Pharmaceutical treatments

Xenopus embryos were incubated with 70mM of the Na^+K^+-ATPase inhibitor ouabain (Sigma Aldrich, O3125) as previously described (Slack and Warner 1973b) to reduce the volume of blastocoel cavity by inhibition of passive H_2O into the cavity. Ouabain was diluted in DMSO (Sigma Aldrich, D8418) as stock, then diluted in NAM 1/10 or NAM3/8 during treatment. And 25μM of the GSK3 inhibitor BIO (Sigma Aldrich, B1686) as described (Maj et al. 2016). Inhibiting the GSK3 complex and preventing β-catenin degradation leads to the activation of the Wnt pathway. To induce activated β-catenin-GR, stage 10 embryos were treated with 4 mg/mL of dexamethasone (Sigma Aldrich) until stage 17, as previously described (Carmona-Fontaine et al. 2007), and then fixed for further analysis.

2.7 *in situ* hybridization

2.7.1 Antisense probe synthesis

Whole-mount colorimetric *in situ* hybridization for *Xenopus* was performed previously described (Barriga et al. 2019). To generate digoxigenin antisense probes, an *In vitro* Riboprobe system (Promega P1420) was used to synthesize *snai2* (Mayor et al. 1995), *foxd3* (Kelsh et al. 2000), *keratin* (Jonas, Sargent, and Dawid 1985), *Xbra* (Latinkic et al. 1997), and *Wnt8* (Baker, Beddington, and Harland 1999). And a fluorescein antisense probe was synthesized for double colorimetric *in situ* hybridization for *Sox2* (Kishi et al. 2000). The *in vitro* antisense RNA transcription was performed in series of steps. Initially, the full circle construct of DNA was cut at a 5' restriction site with the appropriate endonuclease (depends on the constructs provided by the cited literature; i.e. NotI, Spe1, Xba, and others). Then the linearized DNA and antisense RNA transcription was carried out by adding 1 μg of linearized DNA, 2 μL of 10x DTT, 4 μL of 5x buffer, 2 μL of NTP-Dig, 0.5 μL of ribonuclease inhibitors and 1 μL of RNA polymerase (either T7, SP6, or T3) up to 20 μL solution with RNase free water. The NTP mix contains digoxigenin-

labelled UTP or fluorescein-labelled UTP, yielding an antisense RNA tagged with a dig/fluo label. All reagents were obtained from Promega. The final mixture was incubated at 37C for 4hrs. From this, 1 μL was replaced with 1 μL of DNase to degrade the DNA template and stop the reaction. The total labelled RNA concentration was measured via a Nanodrop spectrophotometer (ND-1000). The working concentration of the probes was made by diluting them into a hybridization buffer. *Snai2/foxd3* was diluted to 700 ng/mL, *Keratin/Xbra* 500 ng/mL, otherwise 1.1ng/mL.

2.7.2 Single whole mount *in situ* hybridization

Xenopus Embryos were fixed overnight in MEMFA (1M MOPS, 10Mm $MgSO_4$, 20Mm EGTA in 100ml) at 4C, dehydrated with a series (100/0%, 75/25%, 50/50%, 25/75%, and 0/100%) of methanol/1XPBS, and bleached (Mayor bleaching solution; 0.25ml Formamide, 0.15ml 20X SSC, 1ml H_2O_2 in 5ml), then overnight incubated with the dig-labeled probe at 65C. Then, embryos were washed with a series (75/25%, 50/50%, 25/75%, 0/100% of 2X SSC, and 0/100% of 0.2X SSC) of Formamide/SSC. The two washes for five minutes of MAB-T, next, blocked in a 2%/MAB blocking reagent (BMBR; Roche, 11096176001) for 2 hours, incubated with anti-digoxigenin-AP antibody (Roche) 1:3000 for 4 hours and then revealed with 4.5μl/mL NBT (Roche, 11585002001) and 3.5μl/mL BCIP (Roche, 11383213001) in 1x Alkaline phosphatase (AP) buffer (1M Tris-HCL, 0.5M $MgCl_2$, and 1M NaCl).

2.7.3 Double whole mount *in situ* hybridization

For double colorimetric whole-mount embryo staining, embryos were treated similarly to the single *in situ* hybridization; however, embryos were incubated with both digoxigenin (2ng/ml) and fluorescein (0.2ng/ml) labeled probes overnight at 65C. Next, embryos were treated similarly, and a digoxigenin probe was revealed, as described above. Then, embryos were de-probed with 1M Glycine pH 2 for 30 min. Finally, embryos were blocked and anti-fluorescein-AP antibody (Roche)

1:3000 and revealed with 3.5µl/mL BCIP in AP buffer only. After single and double *in situ* hybridization, embryos were fixed in 3.7% formaldehyde and imaged with Nikon SMZ800N. Image analysis was done using ImageJ, where a region of interest was selected (ROI) to measure integrated density. Next, the final values were subtracted from the background and normalized to control. In graft analysis, the values of competence (ectopic induction) were further normalized between 0 and 1. All of the values in this work yielded from in situ hybridization are reported in **arbitrary unite (a.u.)** (as it is not quantitative method), unless stated otherwise.

2.8 Readout of Wnt activity

2.8.1 Luciferase assay

As previously described, Wnt activity was measured via Luciferase assay (Veeman et al. 2003). Briefly, *Xenopus* embryos were injected (as described above) into all four animal blastomeres at the 8-cell stage to have a readout of Wnt activity only of ectoderm. First, embryos were either injected with 100pg of super Top-flash M50 or Fop-flash M51 DNA (Addgene plasmid #12456 and #12457, respectively). Next, 3-5 embryos were homogenized in triplicate with 50µl of 50mM Tris HCL (pH 7.5) (total of 9-15 embryos per one biological replicate) and then centrifuged (maximum speed for 5 mins), then a 25µl of Tris was added. Next, the Luciferase assay system (Promega, E4030) was used to lyse the samples with lyse reporter buffer. Finally. 20µl of the final mix was added to 100µl of luciferase substrate assay. After waiting 30 seconds, both samples of Top/Fob-flash activity were measured (Luminometer, Tuaner BioSytem) and normalized to Fop-flash.

2.8.2 Transgenic GFP reporter

To analyze the spatial activity of the Wnt pathway, we used a *Xenopus laevis* transgenic line, as luciferase assay gives only the total activity of Wnt in the ectoderm without any spatial information. The well-characterized transgenic line *Xla.Tg(WntREs:deGFP)*^{1Vlemx} was used as previously described (Tran and Vleminckx

2014). Briefly, transgenic testes were obtained and used for *in vitro* fertilization, as described above. Then embryos were incubated till early gastrula stage 10, where embryos were either inflated or deflated, as explained above. Next, embryos were incubated in NAM3/8 till stage 12 to ensure signal turnover. Images were then taken using a fluorescent microscope (Nikon SMZ25), and for quantification, a selection of ROI in ImageJ was made to measure integrated density. Finally, integrated intensity values were normalized to the control values and plotted.

2.9 High-resolution micro-Computed Tomography (µCT) scan

After reaching the desired developmental stage, *Xenopus* embryos were fixed with 4F1G fixative (1% glutaraldehyde and 3.7% formaldehyde in 0.2 M phosphate buffer) overnight at 4C while on the rocker. Next, embryos were washed a few times with dH_2O and stained with 10% IKI (iodine potassium iodide) overnight, as described previously (Metscher 2009). Finally, embryos were prepared to be scanned by mounting them in a fixed position either in a 2µl tip or placed at the bottom of a 50ml falcon. Scan of the embryos run (XT H 225, Nikon) at 60-80kV, 8W and an exposure time of 0.5 seconds with an optional 0.250mm copper filter. Reconstruction (X-inspect, Nikon) of the images of the scan was done at a cubic voxel size of 12µm after 2 x 2 binning. Analysis of the volumes of the blastocoel cavity and the whole embryos were obtained by using gmsh (GNU General Public License, version 4.8.4), a 3D finite element mesh generator for volume analysis. For visual representation images, ImageJ was used to reconstruct the volume in 3D using the built-in plugin, volume viewer. Automated volume quantification was done by a python code provided by Namid Stillman.

2.10 RT-qPCR

Total RNA was extracted from a pool of embryos (20 per sample) using the RNeasy Micro Kit (Qiagen, Valencia CA). Embryos were homogenized To extract RNA. To synthesize cDNA from RNA VILO cDNA Synthesis Kit (Invitrogen, Grand Island, NY)

was used. RT-qPCR was performed on an Eco Real-Time PCR System (Illumina, San Diego CA). These are the primers used in this study: *snai2* (Bae, Hong, and Saint-Jeannet 2018); Fw: CATGGGAATAAGTGCAACCA, Rev: AGGCACGTGAAGGGTAGAGA and *foxd3* (Watanabe et al. 2015); Fw: TCTCTGGGGCAATCACACTC, Rev: GTACATTTGTTGATAAAGGG. Power SYBR Green PCR Master Mix (Invitrogen) was used. The reaction mixture contained the following, Power SYBR Green PCR Master Mix, 250 nM primers, and 4 ml cDNA in a final volume of 20 µl. The PCR cycles were done as such: 95C (10min, 40 cycles), at 95C (10 seconds) and at 60C (30 seconds). *odc1*(Bae et al. 2018) was used for in-house normalization.

2.11 Hydrostatic pressure measurement

The hydrostatic pressure of the blastocoel cavity during gastrula stages was measured directly using the SYS-900A micropressure system (World Precision Instruments, CA), a well-established technique with a resolution of 13Pa, was used a previously described (Petrie, Koo, and Yamada 2014). In brief, pre-pulled and calibrated microneedles were obtained with 0.5-1µm tip size (World Precision Instruments, TIP05TW1F and TIP1TW1, respectively). The needles were filled with 1M KCl solution, attached to the microelectrode holder to avoid bubbles (World Precision Instruments, MEH6SF), and then connected to the SYS-900A system. The microelectrode was calibrated using a calibration chamber (World Precision Instruments, CAL900A). After a successful calibration (reaching a baseline of 0 kPa), the microelectrode was positioned onto a micromanipulator, and the reference electrode was fixed in position inside the NAM3/8 media under the dissecting microscope (LeicaMZ6). *Xenopus* embryos were secured in place using plasticine to ensure embryos do not move during pressure measurement. The microelectrode was inserted into the blastocyst at a depth above the ectoderm thickness of 100µm, around 300µm, strictly measured using a micromanipulator to ensure the tip of the needle was not obstructed by tissues and in contact with the blastocoel cavity. After a successful puncture of the microelectrode, it was

maintained in place for ~10 seconds. The hydrostatic pressure was calculated as the mean pressure of the whole 10 seconds. Data points were excluded from analysis if a decrease in pressure within 10 seconds of probe insertion was noted, which indicates a failed stabilization. This was achieved by collaborating with Takashi Hiiragi lab and with the help of Parchiti Moghe.

2.12 Immunostaining and Cryosection

Xenopus embryos were fixed in 4% paraformaldehyde/1X-PBS for 30 mins at room temperature (RT), then treated with 0.03% Triton (100-X, Sigma Aldrich) for 12 mins on a rocker at RT, blocked in 20%NGS/1X-PBS for 2 hours on a rocker at RT. Then incubated with Yap1 antibody 1:200 (Proteintech, 13584-1-AP) overnight in 20%NGS/1X-PBS. After multiple washes, an appropriate secondary antibody was added, for example, AlexaFluro488 1:360 (Thermo Fisher Scientific) and DAPI 1:1000 (Sigma Aldrich, D9542). Next, embryos were washed with 1X-PBT and then fixed with 1% paraformaldehyde and then dehydrated overnight with 30% sucrose/1X-PBS for cryosection. After dehydration of the embryos, they were embedded in with 30%O.C.T/sucrose/1X-PBS and sectioned using a cryostat OTF5000 (Bright Instrument, UK) with slices of 30µm thickness. Finally, the sections were submerged with 70% glycerol and covered with a coverslip and imaged using a confocal microscope (TCS SP8; Leica microsystems). For immunofluorescence analysis, the intensity of Yap staining was measured by ImageJ by obtaining the integrated density. Then the N/C ratio was calculated using a mask based on DAPI staining to identify the nucleus. Then the intensities of the nucleus were obtained and subtracted from the total cell intensity to get the cytoplasmic value. For cell packing of the ectodermal cells was obtained as previously described (Hannezo and Heisenberg 2022): $\text{Packing index} = \frac{n_{cells} \times \bar{X}_{cell\ area}}{Total\ area}$, which is also done using ImageJ. Packing index for random of range of spheres (in our case cells) is expressed by the ratio of the sphere volume (in our case area of cell defined by membrane of cells) to the total volume

occupied space (in our case ROI of the ectoderm) (Rogers, Dijkstra, and Smalley 1994).

2.13 Statistics

Data points were first tested for normality using the d'Agostino-Pearson and/or Shapiro-Wilk test via Prism 9 (GraphPad). In two group comparisons, significances were computed with Student's t-test (two-tailed, unpaired) when data points passed the normality test or Mann-Whitney (two-tailed, unpaired) for data that did not pass the normality test. In more than two group comparisons, significance was computed with one-way analysis (ANOVA) with Dunnett's test correction for data points that passed the normality test and Dunn's test for data sets that did not pass the normality test. No statistical methods were computed to determine the sample size required; it was based on previous studies in the field. Each experiment in this study was repeated at least three times on different days and with different batches of *Xenopus* females, subsequently, different embryos (three biological replicates), unless stated otherwise. Finally, during the experiment, the authors were not blinded, as embryos were selected based on viability. After exclusion criteria were met, analysis was done at random.

2.14 Solution

Table 2| Solution constitution

4FIG (10ml)	1 ml of (1X PBS), 1 ml of (37% Formaldehyde), and 0.8 ml of glutaraldehyde.
Anti-digoxigenin-alkaline phosphatase (AP) buffer	100 mM NaCl, 50 mM $MgCl_2$, 100 mM Tris-HCl, pH 9.8, 0.1% Tween-20.
Bleaching buffer	20% H_2O_2, 2.5% 20X SSC, 5% formamide.

Clearing mix	Two volumes of benzyl alcohol and 1 volume of benzyl benzoate (Sigma-Aldrich).
Cysteine solution	2% L-cysteine (Sigma, C7352) in H_2O with 50 mM NaOH.
Danilchick's medium for Amy (DFA)	53 mM NaCl, 5 mM Na_2CO_3, 4.5 mM K-Gluconate, 32 mM Na-Gluconate, 1 mM $MgSO_4$, 1 mM $CaCl_2$, 0.1% Bovine calf serum albumin (BSA; Sigma, A4503), pH 8.3 adjusted with bicine.
Diethylpyrocarbonate water (DEPC)	0.1% diethylpyrocarbonate.
Ficoll solution	3% polysucrose (Ficoll, Sigma) in NAM 3/8.
Hybridization buffer	50% formamide, 5X SSC, 1X Denhardt's solution, 1 mg/mL ribonucleic acid, 100 μg/mL heparin, 0.1% CHAPS, 1tenmM EDTA, 0.1% Tween-20, pH 5.5.
In situ hybridization washing solutions	• Washing buffer 1: 50% formamide, 10% 20X SSC. • Washing buffer 2: 25% formamide, 10% 20X SSC. • Washing buffer 3: 12.5% formamide, 10% 20X SSC. • Washing buffer 4: 10% 20X SSC, 0.1% Tween-20. • Washing buffer 5: 1% 20X SSC, 0.1% Tween-20.
Maleic acid buffer (MAB)	100 mM maleic acid, 100 mM NaCl, 0.1% Tween-20, pH 7.6.
Marc's modified ringer's (MMR)	100 mM NaCl, 22 mM KClone, 1 mM $MgSO_4$, 2 mM $CaCl_2$, 5 mM HEPES, 0.1 mM EDTA, pH 7.6.
MEMFA	100 mM MOPS, 1 mM $MgSO_4$, 2 mM EGTA, 3.7% formaldehyde.
Normal Amphibian Media (NAM A)	1.1M NaCl (64.28g), 20mM KCl (1.49g),10mM Ca(N03)2 (2.36g), 10mM MgSO4 (1.2g), and 1mM Disodium EDTA (0.37g)
Normal Amphibian Media (NAM B)	20mM Sodium phosphate NaH2PO4 (7.16g) and adjust pH to 7.5.

Normal Amphibian Media (NAM C)	100mM NaHCO3 (0.84g).
O.C.T/Sucrose	50ml of 30%Sucrose with 50ml 100% O.C.T.
PBS with Tween (PBT)	1X PBS with 0.1% Tween-20.
Phosphate buffer saline (PBS)	137 mM NaCl, 2.7 mM KCl, 4.3 mM Na_2PO_4, 1.4 mM H_2PO_4, pH 7.3.
Sucrose/PBS(1X) 30%	30g of sucrose in 100ml of PBS.
Tricaine solution	20 mM tricaine methanesulfonate (Tricaine, or MS-222).
Tris-HCL (9.5) 1M	Dissolve 60.55g of tris in 400 dH_2O. Adjust pH by adding concentrated HCL pH 9.5 (approx. 3 ml). Adjust volume to 500ml, then autoclave.
Agarose gel 1%	1g in 100ml 1X TAE. Mix, then heat up in microwave. Add 10ul ethidium bromide after it cools down.
PFA 8%	300 ml 1x PBS to 60C,40g PFA, clear the mixture by adding 1N NaOH, cool then filter, adjust the volume up to 500 ml by adding 1X PBS, balance pH up to 6.9 by adding HCL.
BMBR 10%	10% MAB-BMBR (10 g of BR + 100 ml of MAB 1X). 10g of Blocking Reagent Roche powder (cupboard) Adjust to 100ml with MAB.
Normal Amphibian Media (1/10)	10 ml of NAM (A), 10 ml of NAM (B), 1 ml of NAM (C), and 1 ml streptomycin (250mg 50 ml dH_2O) (5mg/ml) rest of H_2O.
Normal Amphibian medium (NAM 1/10)	11 mM NaCl, 0.2 mM KCl, 0.1 mM $Ca(NO_3)_2$, 0.1 mM $MgSO_4$, 10 mM EDTA, 0.2 mM NaH_2PO_4, 0.1 mM $NaHCO_3$, pH 7.5, 50 μm/mL streptomycin.

Normal Amphibian Media (3/8)	40.7 mM NaCl , 0.74 KCl, 0.37 mM $Ca(NO_3)_2$, 0.37 mM $MgSO_4$, 37 μM EDTA, 0.37 mM NaH_2PO_4, 0.1 mM $NaHPO_4$, pH 7.5, 50 μm/mL streptomycin.
$MgCl_2$ 0.5M	Dissolve 50.82g in 500 ml dH_2O, then autoclave.
NaCl 1M	Dissolve 29.22g in 500 ml dH_2O, then autoclave.
Glycine – HCL 1M (pH 2)	30ml dH_2O, 0.3g Glycine, adjust the pH to 2 by adding HCL up to a volume of 32.
Streptomycin Stock at 5mg/ml	250mg of streptomycin powder in 50 mL.
Saline-sodium citrate buffer (20X - SSC)	3 M NaCl, 0.3 M tri-sodium citrate, pH 7.0.

Chapter 3: Loss of neural crest correlates with increased hydrostatic pressure

3.1 Introduction

Neural crest cells are induced during gastrulation by inductive signals generated by a specific type of prospective mesodermal cells found in the dorso-lateral marginal zone (DLMZ)(LaBonne and Bronner-Fraser 1998b; Mayor et al. 1995; Steventon et al. 2009a) of early gastrula embryos. One of the inductive signals that DLMZ produce is Wnt, a well-characterized neural crest inductive signal (Curchoe et al. 2010; García-Castro et al. 2002; LaBonne and Bronner-Fraser 1998b; Steventon et al. 2009a), as described in chapter 1.1.4 and Fig 1.3. It has previously been shown that explants of DLMZ taken from early gastrula stages (Stg10 N&F)(Nieuwkoop 1967) can induce ectopic neural crest when grafted into competent ectoderm (Mancilla and Mayor 1996; Mayor et al. 1995; Steventon et al. 2009a). Furthermore, Steventon and colleagues showed that conjugate of DLMZ and ectodermal cells or grafting them into whole-mount embryos is sufficient to induce neural crest cells (Steventon et al. 2009a). These results demonstrate the ability of DLMZ to induce ectopic neural crest cells. The DLMZ can be grafted onto tissue to determine the effect of the signaling of one tissue onto another and the ability of the tissue to respond to inductive signals and assess competence. As neural crest induction occurs during gastrulation, we aimed to graft the tissue inside the blastocoel cavity (as illustrated in Fig 1.3). In addition, the blastocoel cavity provides an ideal location for DLMZ graft as it is in contact with all ectodermal cells (Keller 1975a), providing a suitable option to assess the competence of the ectoderm.

3.2 Results

3.2.1 Temporal loss of neural crest competence

To assess the temporal loss of neural crest competence to be induced in the ectoderm, we grafted DLMZ explants into the blastocoel cavity, as illustrated (Fig. 3.1a). The grafted DLMZ was randomly located into the blastocoel cavity; if the graft ended up next to the host neural crest, it induced expansion of the endogenous neural crest domain (Fig 3.1b), whereas when the grafted was located in a ventral position, it induced ectopic neural crest (Fig 3.1b, c); only ectopic neural crest induction was subsequently analyzed in this study. Temporal analysis was done by grafting DLMZ tissues into the blastocoel cavity of consecutively older embryos of embryos at stages 10, 11, and 12 (Fig. 3.2a; stages 10, 11, 12), then cultured until mid-neurula, followed by expression analysis of *snai2* (Mayor et al. 1995) and *foxd3* (Kelsh et al. 2000) as neural crest markers. Our results indicate that the ectopic induction of neural crest cells is strongest at early gastrulation (stage 10), decreases at stage 11 and is lost at stage 12 (Fig. 3.2b, c, d); these results are consistent with previous reports (Mancilla and Mayor 1996).

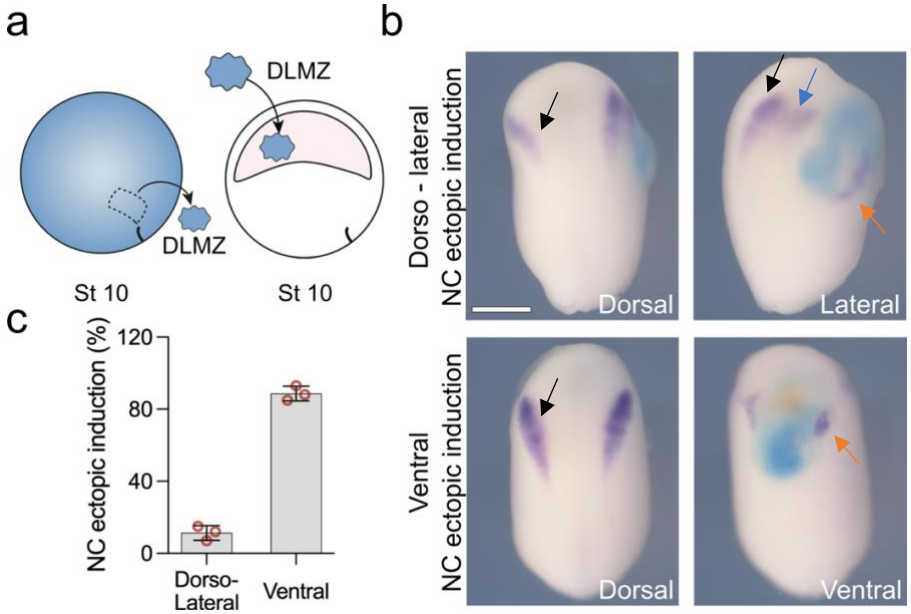

Fig. 3.1 | Analysis of neural crest competence to DLMZ.

a, Illustration of competence graft assay that shows the dorsal lateral marginal zone (DLMZ) explant dissected from stage 10 donor embryo, which is injected with FLDX as a lineage tracer (cyan) in two blastomeres at the 2-cell stage and then grafted into host's blastocoel cavity at stage 10. **b**, *In situ* hybridization at stage 16 showing *snai2* (purple) and DLMZ (cyan). Endogenous neural crest induction is indicated with a black arrow and is induced on the dorsal side. The competence graft assay gives two kinds of ectopic induction. The first ectopic induction is dorso-lateral (two upper panels), and the second is ventral (two lower panels) ectopic induction. Lateral induction is indicated with a blue arrow. Since this induction fuses with endogenous expression, it is difficult to distinguish where it ends and when the ectopic induction starts. Moreover, it will be hard to quantify the strength of the induction. Thus, embryos exhibiting dorso-lateral induction were removed from further analysis and only ectopic ventral induction, indicated with an orange arrow, of NCCs was considered in the competence of NCCs to DLMZ. **c**, Spread of data points indicating the percentage of embryos exhibiting either ventral or dorso-lateral ectopic induction. Histograms represent the mean, and error bars are s.d. Scale bar 450 µm (**b**). Data represent mean, error bars are s.d Statistical analysis was performed using Dunnett's test; ****$P \leq 0.0001$.

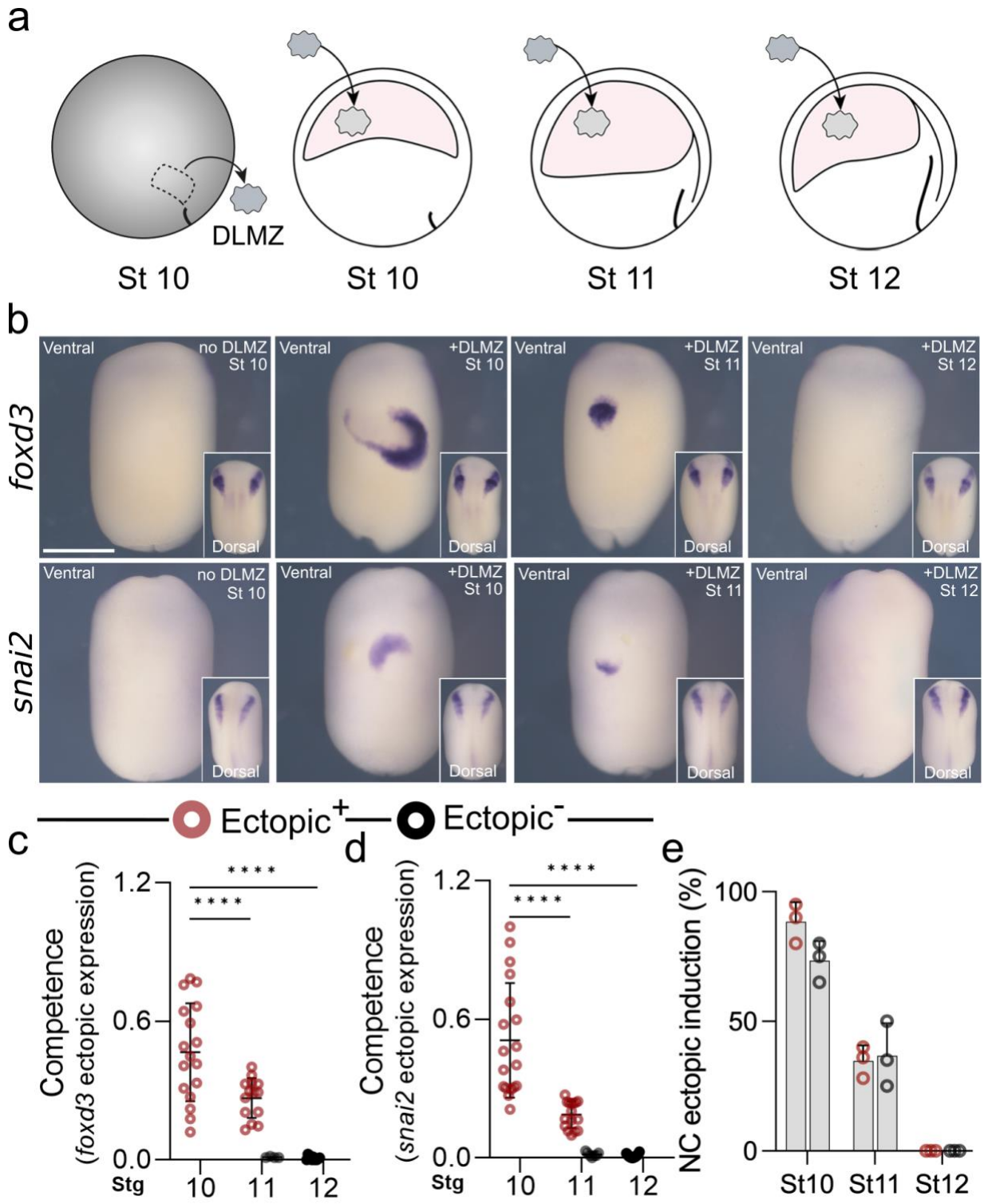

Fig. 3.2|Temporal loss of neural crest competence at mid-gastrulation.

a, Illustration of neural crest graft assay using DLMZ as the inducer (grey), which is dissected at stage 10 and grafted into host blastocoel cavity (red) at different stages 10, 11, and 12. **b**, Analysis of *snai2* at stage 18 and *foxd3* at stage 17 via *in situ* hybridization

seen in ventral view, and the inset shows the dorsal view of embryos. The first panel is control embryos with no DLMZ and the following panels include DLMZ graft at stage 10 and fixed at the indicated stage. **C** and **d**, Quantification of competence of neural crest at stages; 10 (n_{snai2} = 18, n_{foxd3} = 15 embryos), 11 (n_{snai2} = 16, n_{foxd3} = 12 embryos), and 12 (n_{snai2} = 18, n_{foxd3} = 12 embryos) normalized to control ($n_{snai2+foxd3}$ = 15 embryos) with no DLMZ graft. Red circles (Ectopic^{+}) indicate embryos with ectopic induction of NC markers whereas black circles (Ectopic^{-}) indicate embryos with no ectopic induction. At stage 11 both markers exhibited embryos with ectopic and no ectopic induction. Embryos with no ectopic induction were measured by selecting random ventral location and subtracted to the background. **e**, Data points indicate the percentage of ectopic induction; each point represents one biological replica. Scale bars, 450 μm for ventral and 200 μm for dorsal. Statistical analysis was performed using one-way ANOVA (**c** and **d**); $^{**}P \leq 0.01$, $^{****}P \leq 0.0001$. (**c** and **d**) show mean and error bars indicating s.d.

3.2.2 Change in blastocoel cavity volume during gastrulation

As we are interested in linking the loss of neural crest competence to a change in a mechanical cue, we noticed that the blastocoel cavity size changed during gastrulation (Keller 1975b); thus, we decided to explore this further. Initially, we aimed to precisely measure the change in blastocoel volume; we utilized the micro-CT technique to scan whole-mount embryos at different stages of gastrulation (Fig. 3.3a). We noted an increase in blastocoel volume while observing no change in whole embryos volume. (Fig. 3.3c-d). These results imply that a physical change might be related to the loss of neural crest competence to the DLMZ signals. However, it is improbable that cells sense the volume change of the adjacent cavity directly. Thus, we investigated potential physical cues dependent on blastocoel fluid. We concluded that hydrostatic pressure is a promising candidate, as it can travel long distances. We used micro-pressure probes, a well-established method previously used in mice embryos and cells, to measure hydrostatic pressure directly. The micro-pressure probe involves poking the ectoderm to reach the blastocoel cavity precisely via a microelectrode (Fig. 3.4a, b) (Chan and Hiiragi 2020a). We observed a marked increase in the hydrostatic pressure between stages 10 and 12 (Fig. 3.4c) when the ectoderm loses its competence to generate neural crest in response to a DLMZ graft, showing an inverse correlation between competence and hydrostatic pressure (Fig. 3.4d). These results suggest that the change in the physical volume of the blastocoel cavity modulates hydrostatic pressure, and this change could be a potential mechanical stimulus that regulates ectoderm commencement.

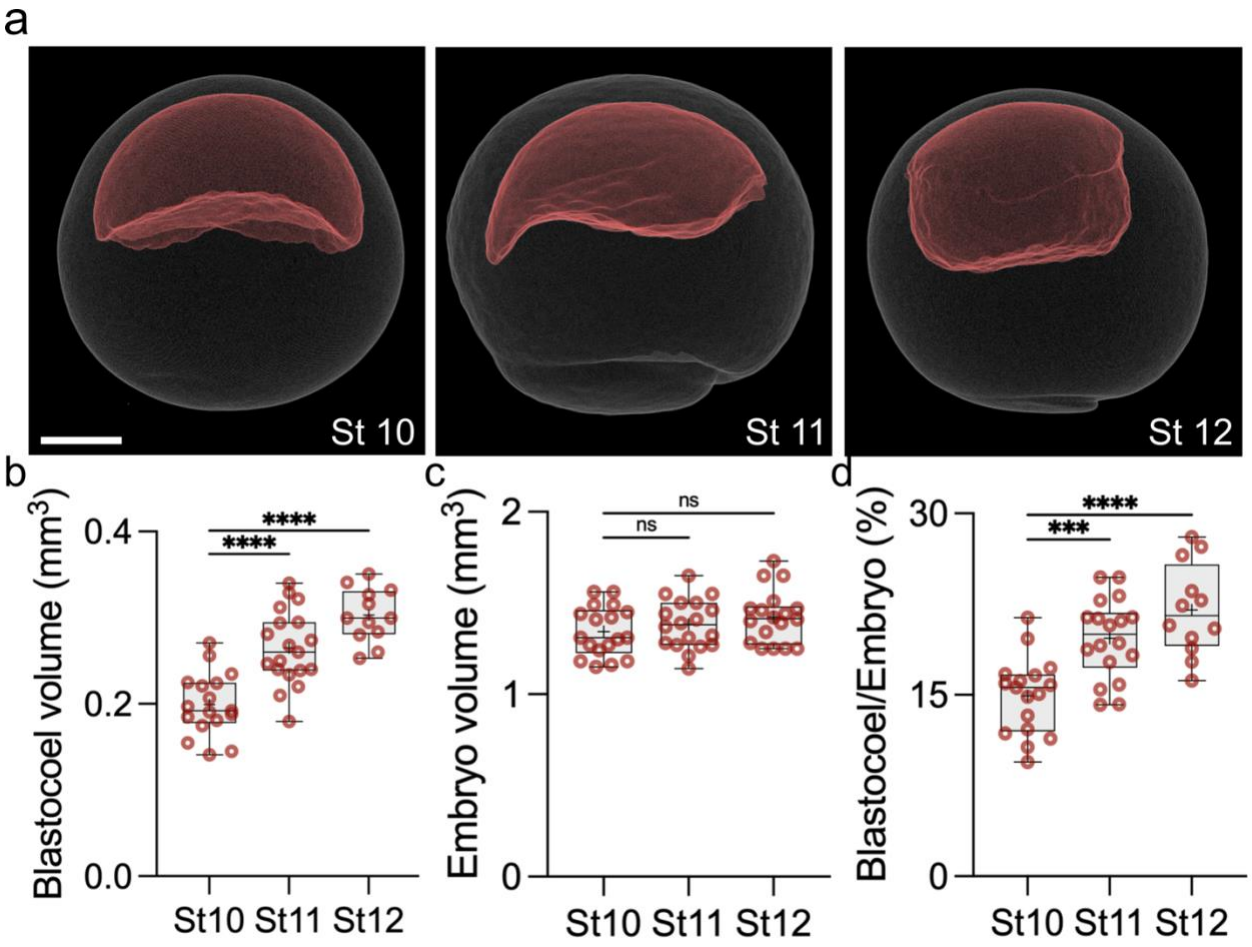

Fig. 3.3 | Loss of competence coincides with loss in blastocoel volume.

a, micro-CT of a whole mount *Xenopus* embryo (grey) at stages 10, 11, and 12 with blastocoel cavity (red). **b**, Spread of data points indicating blastocoel volume at gastrulation stages 10 (*n* = 17 embryos), 11 (*n* = 19), and 12 (*n* = 12). **c**, Quantification of embryo volume at stage 10 (*n* = 18 embryos), 11 (*n* = 18 embryos), and 12 (*n* = 18 embryos). **d**, Percentage of the ratio of blastocoel volume to whole embryo volume at stage 10 (*n* = 17), 11 (*n* = 18), and 12 (*n* = 12). Scale bar 300 µm (**a**). Statistical analysis was performed using Dunnett's test; NS, $P>0.05$, ***$P \leq 0.001$, ****$P \leq 0.0001$. Box plots (**a** and **b**) show median, 25th and 75th percentiles, and whiskers extend to the minimum and maximum values.

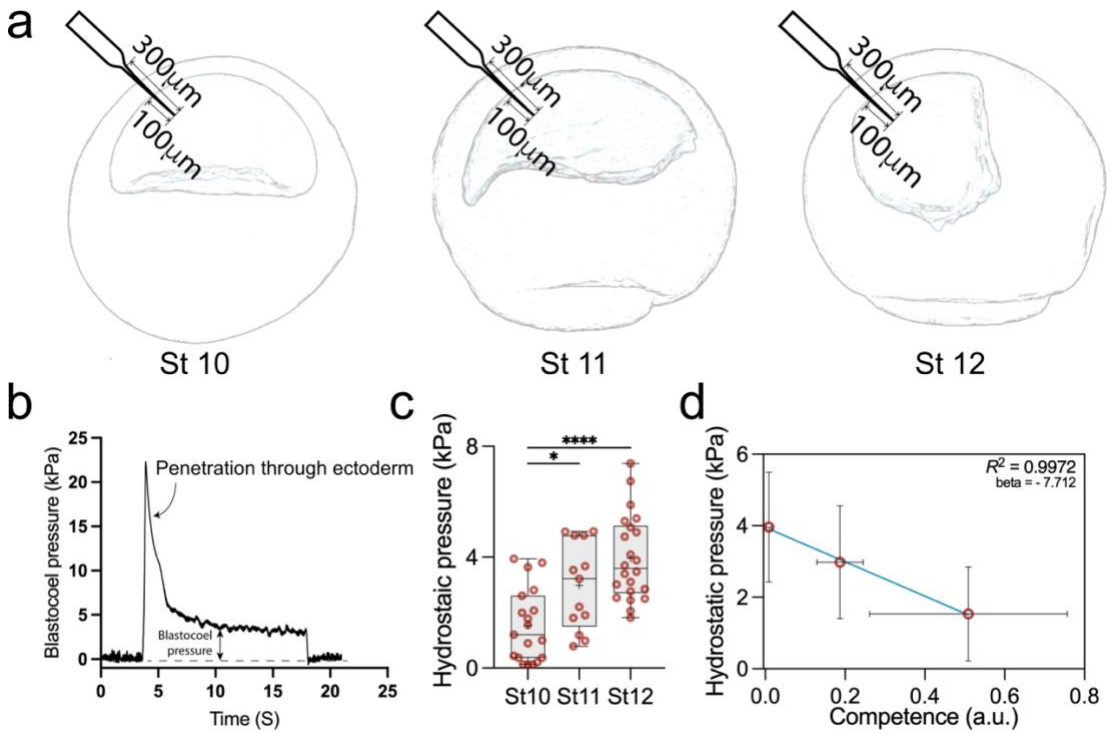

Fig. 3.4 | Loss of competence coincides with an increase in blastocoel hydrostatic pressure.

a, Illustration of embryos at different stages indicating the process of microelectrode penetration (0.5-1 µm tip) through ectoderm required to measure hydrostatic pressure. **b**, Profile of successful hydrostatic pressure measurement of blastocoel cavity. Pressure is close to zero after calibration and maintained at zero whilst the microelectrode is not in contact with the embryo prior to and post-measurement. A transient spike is notable during penetration of the microelectrode through the ectoderm as the tip of the needle is blocked by cells. A stable phase between five to ten seconds is achieved after the transient spike, indicating the actual blastocoel pressure and a successful stabilization of the micropressure system. **c**, Quantification of blastocoel hydrostatic pressure at stages 10 (*n* = 19 embryos), 11 (*n* = 13), and 12 (*n* = 22). **d**, Correlation between competence and hydrostatic and competence. "R^2 =0.99 and beta = -7.7, to account for the variability in estimation neural crest competence and the hydrostatic pressure values within the blastocoel cavity, the correlation was calculated via orthogonal distance regression (ODR). Statistical analysis was performed using Dunnett's tests (**c**); $*P \leq 0.1$, $****P \leq 0.0001$. Box plots (**c**) show median, 25th and 75th percentiles, and whiskers extend to the minimum and maximum values.

3.3 Discussion

The capacity of tissues to respond to inductive signals was defined as competence (WADDINGTON 1934). Since identifying the term "competence" many studies aimed to understand how this mechanism is controlled, how some tissues gain and loss this ability during early development. The focus of these studies has been the molecular approach; however, the question remains unanswered (Christian et al. 1992; Esmaeili et al. 2020b; Gillespie et al. 1989b; Henig et al. 1998; Lim et al. 2013; Steinbach et al. 1997; Streit et al. 1997). Alternative to molecular approach, we asked whether biomechanics might regulate neural crest competence to the DLMZ. To address this question we first chose the process neural crest induction as it is well-characterized (Chapter 1.1.4) (Aybar and Mayor 2002a; Mancilla and Mayor 1996; Mayor et al. 1995; Mayor and Theveneau 2014). In addition, we chose *Xenopus* embryos as a model since they are emendable to mechanical assays. To address the first question, when neural crest competence is lost, we performed a graft assay whereby we grafted the tissue that provides the required inductive signals for neural crest induction (DLMZ) onto the blastocoel cavity (Steventon et al. 2009b). Our findings show that neural crest competence is lost mid-gastrulation. Thereafter, we investigated a change that occur during gastrulation that possibly modulates mechanical cue leading to loss of competence. We noted that the blastocoel is a suitable candidate as it changes its volume during development. We aimed to measure the volume of the cavity and the hydrostatic pressure as it is filled with fluids. Our results show an increased hydrostatic pressure and volume of blastocoel cavity of *Xenopus* embryos. These results indicate the possibility that the neural crest competence could be regulated by the increase in the volume of the blastocoel cavity and the hydrostatic pressure. In the next chapter, we aim to address this hypothesis by manipulating the hydrostatic pressure and assessing the competence of neural crest induction.

Chapter 4: Neural crest competence is extended by lowering hydrostatic pressure

4.1 Introduction

As our results (in Chapter 3) suggest the possible role of change in hydrostatic pressure of blastocoel cavity on neural competence, it is pivotal to consider the possibility of the inorganic (Ions; source of osmotic pressure) and organic (RNA or proteins; possibly could act as inhibitors or promotors) mediated by the cavity on the ectoderm. In *Xenopus,* blastocoel formation is dependent on the activity of the Na+/K+ ATPase (Slack and Warner 1973b), and it starts at the early segmentation stages and continues gradually until gastrulation (Keller 1975a). The blastocoel expands with a continuous fluid influx after the first division (2-cell stage). This exchange of ions and fluids as early as the 2-cell stage can generate osmotic pressure. Indeed, like in many systems, a change in osmotic pressure is proposed as the mechanism that leads to cell specifications (Chan and Hiiragi 2020b). Furthermore, recent studies investigated the organic blastocysts composition of mice embryos and found various proteins that promote a wide range of cellular functions, like cell differentiation, division, apoptosis, and others (Banliat et al. 2022; Jensen et al. 2014). Thus, whilst investigating the mechanical cues generated from the blastocoel volume change, it is important to experimentality distinguish between hydrostatic pressure, osmotic pressure, and blastocoel composition.

Furthermore, as noted in the introduction, gastrulation is a highly dynamic process that involves tissue migration (i.e. mesoderm), epiboly (the process of blastopore closure), induction of the mesoderm (chapter 1), and tissue rearrangements (Asashima and Grunz 1982; Steventon et al. 2009a, 2021). Thus, it is pivotal to examine the effect of mechanical cues in the early steps before neural crest induction. In this chapter, we examine the source of mechanical cues that regulate neural crest competence.

4.2 Results

4.2.1 Changes in blastocoel volume lead to changes in hydrostatic pressure

To investigate the causal link between neural crest induction and hydrostatic pressure, we developed assays to directly alter the hydrostatic pressure of the blastocoel cavity either by increasing (inflation) or decreasing (deflation) volume of the cavity (Fig. 4.1a). Inflation assay was achieved by injecting the normal culture medium of *Xenopus* embryos into the blastocoel cavity, which subsequently led to an increase in its volume (Fig. 4.1b, st. 10) and hydrostatic pressure (Fig. 4.1c, st. 10); in contrast, deflation assay was achieved by aspirating preexisting fluid from the blastocoel cavity, subsequently led to embryos with reduced cavity volume (Fig. 4.1b, st. 12) and hydrostatic pressure (Fig. 4.1c, st. 12). Furthermore, we deflated and inflated *Xenopus* embryos at early gastrulation (stage 10) and preformed temporal analysis of blastocoel volume (Fig 4.2). We note that after deflation there is no further expansion of cavity and it remains relatively the same volume, unlike the inflated embryos. We have developed a unique method to manipulate hydrostatic pressure that will be used in subsequent experiments.

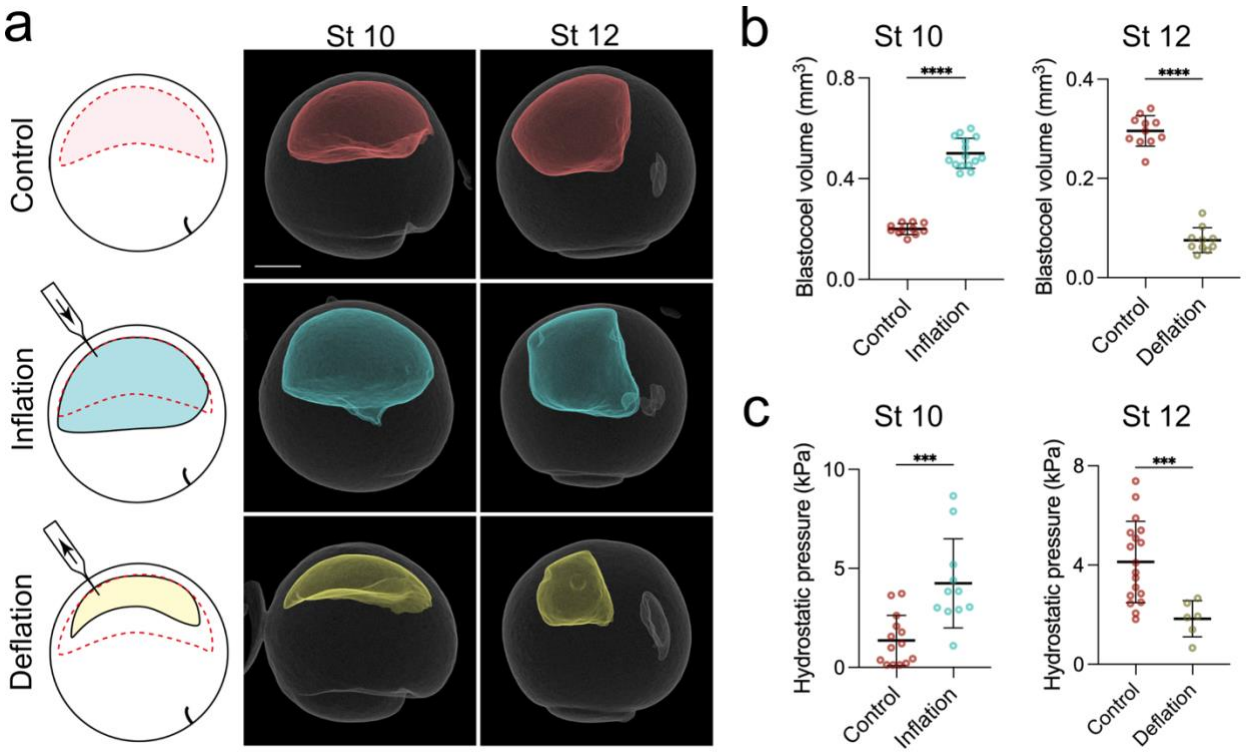

Fig. 4.1 | Blastocoel volume controls hydrostatic pressure.

a, Left panels indicate an illustration of the inflation and deflation assays. Middle to right panels are micro-CT scans of whole-mount *Xenopus* embryos in control (red blastocoel cavity), inflation (cyan blastocoel cavity), and deflation (yellow blastocoel cavity) embryos. **b**, Spread of data points indicating blastocoel volume at the indicated stages between control and treatment. **c**, Spread of data points indicating hydrostatic pressure in the blastocoel cavity at the indicated stages between control and treatment. The experimental embryos were mechanically treated at stage 10, and parameters were measured at the indicated stages (**b** and **c**). Scale bars 300 µm (**a**). Data points represent mean, and error bars are s.d. Statistical analysis was performed using unpaired two-tailed *t*-tests (**b** and **c**); ***$P \leq 0.001$, ****$P \leq 0.0001$. n_{st10} = $11_{control}$, $15_{inflation}$ and n_{st12} = $11_{control}$, $10_{deflation}$ embryos (**b**), n_{st10} = $14_{control}$, $11_{inflation}$ and n_{st12} = $18_{control}$, $16_{deflation}$ embryos (**c**).

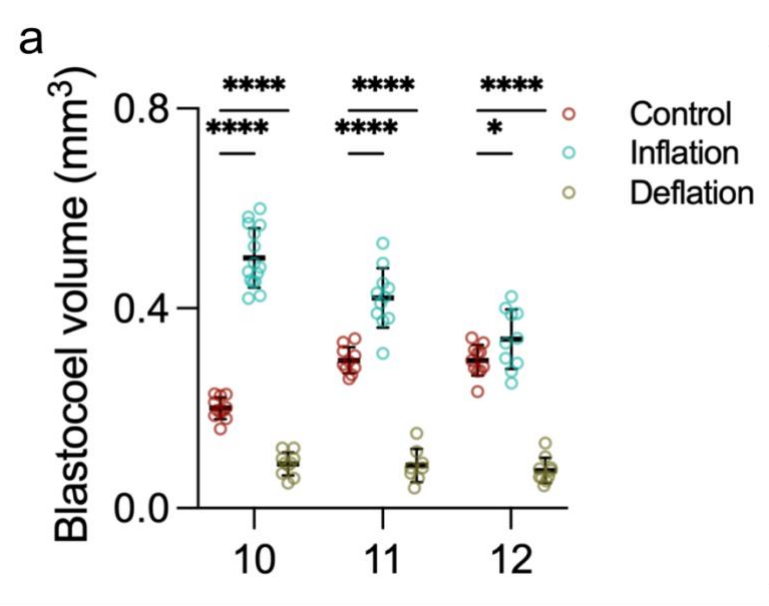

Fig. 4.2|temporal analysis of blastocoel volume.

a, Quantification indicating the change in blastocoel volume between control, inflation, and deflation at stage 10 (*n* = 11, 15, 10 embryos, respectively), 11 (*n* =10, 11, 8 embryos, respectively), and 12 (*n* = 11, 10, 10 embryos, respectively). Mechanical assays were done at early stage 10, and embryos were analyzed at the indicated stages. Data represent mean, error bars are s.d. Statistical analysis was performed using Dunnett's test; *$P \leq 0.01$, ****$P \leq 0.0001$.

4.2.2 Hydrostatic pressure modulates neural crest induction

We hypothesize that hydrostatic pressure controls neural crest induction. More precisely, we theorize that neural crest induction requires a low level of hydrostatic pressure. To address our hypothesis, we analyzed the effect of altering hydrostatic pressure (inflation or deflation) on neural crest markers. We found that Inflating blastocoel cavity leads to inhibition of both neural crest markers *snai2* and *foxd3* as analyzed via *in situ* hybridization (Fig. 4.2a, b) and RT-qPCR (Fig. 4.2c); in contrast, deflation showed an expansion of those markers. These data align with our notion that neural crest induction is regulated by hydrostatic pressure. These observations suggest that mechanics could regulate neural crest competence.

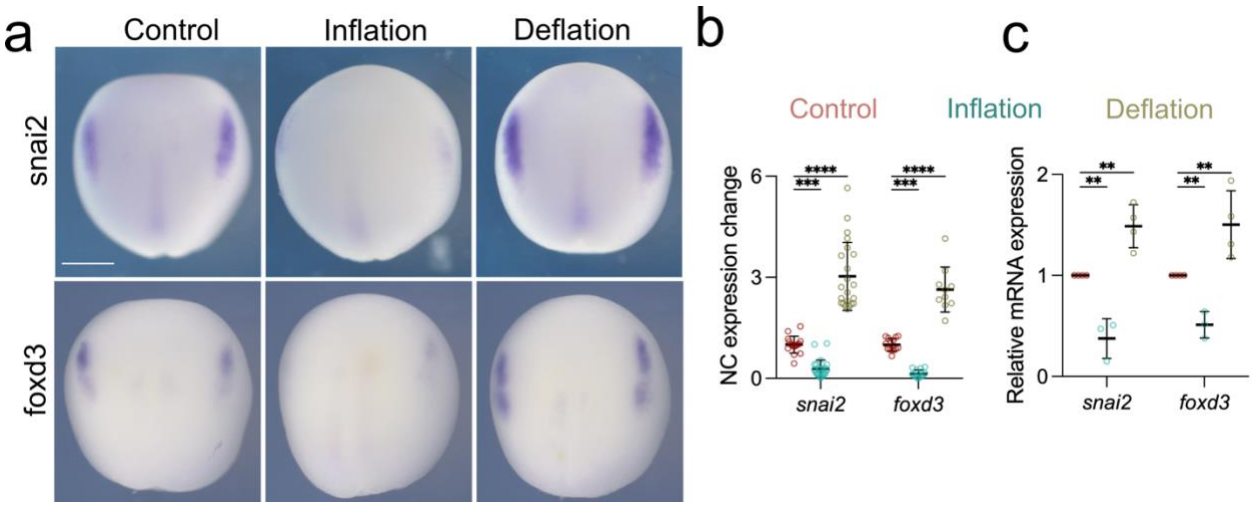

Fig. 4.3 | Hydrostatic pressure regulates neural crest induction.

a, Analysis via *in situ* hybridization (ISH) of neural crest markers *snai2* and *foxd3* at stage 15 after the indicated mechanical treatments. **b**, Spread of data showing the expression of the neural crest markers *snai2* and *foxd3* by ISH after inflation and deflation normalized to control embryos. **c**, Spread of data indicating relative expression via RT-qPCR of *snai2* and *foxd3* normalized to *odc1*. Scale bar 400 µm (**a**). Data points represent mean, and error bars are s.d. Statistical analysis was performed using Dunnett's tests (**b** and **c**); $^{**}P \leq 0.01$, $^{***}P \leq 0.001$, $^{****}P \leq 0.0001$. n_{snai2} = 22 $_{control}$, 25$_{inflation}$, 22$_{deflation}$, n_{foxd3} = 22$_{control}$, 14$_{inflation}$, 10$_{deflation}$ embryos (**b**), at least three independent experiments (**c**).

As the mechanical manipulation of blastocoel volume could affect other cellular activities different to hydrostatic pressure, we performed a series of controls that we will describe in the following paragraphs and sections. First, a similar perforation of the embryo with an equivalent needle but without inflation or deflation did not affect neural crest induction (Fig. 4.3a-c), indicating that inserting a needle in the ectoderm does not affect induction. Second, to further support the notion that blastocoel volume controls neural crest induction, we referred to an alternative method to change blastocoel volume. It has been demonstrated that the volume of the *Xenopus* blastocoel cavity is controlled by the activity of the Na^+K^+-ATPase (Slack and Warner 1973b), whose activity, as early as the 2-cell stage, aids in the expansion of the blastocoel cavity by passively allowing H_2O molecule to get into the cavity for every Na^{+2} molecule. Na^+K^+-

ATPase can be pharmaceutically inhibited via ouabain, leading to a decrease in blastocoel volume (Slack and Warner 1973b). Analysis of embryos via *in situ* hybridization treated with ouabain shows an expansion of the neural crest domain (Fig. 4.4a, b), a similar phenotype to the one produced when we deflate *Xenopus* embryos (Fig. 4.2a-c). These results suggest that treating embryos either with mechanical (deflation) or pharmaceutically (ouabain) manipulations, it would elicit neural crest expansion, suggesting specificity in our treatment.

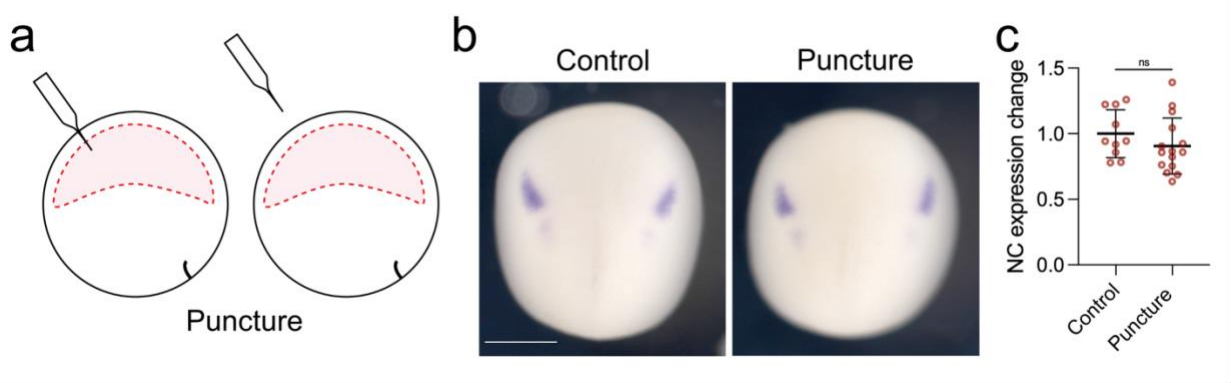

Fig. 4.4 | Puncture of the ectoderm by microneedle.

a, Illustration indicating the puncture procedure of blastocoel mechanical assay (inflation and deflation). Embryos were punctured in a similar manner with a microneedle to the one used for the inflation and deflation experiments; however, the total volume of the cavity was maintained. **b**, Embryos analyzed via *in situ* hybridization with NC marker *snai2* at stage 15. **c**, Spread of data points showing the change in expression of neural crest in control embryo (*n* = 10 embryos) and punctured embryo (*n* = 15 embryos). Scale bar 450 µm (**b**). Data points represent the mean, and error bars are s.d. Statistical analysis was performed using an unpaired student *t*-test; NS, *P*>0.05.

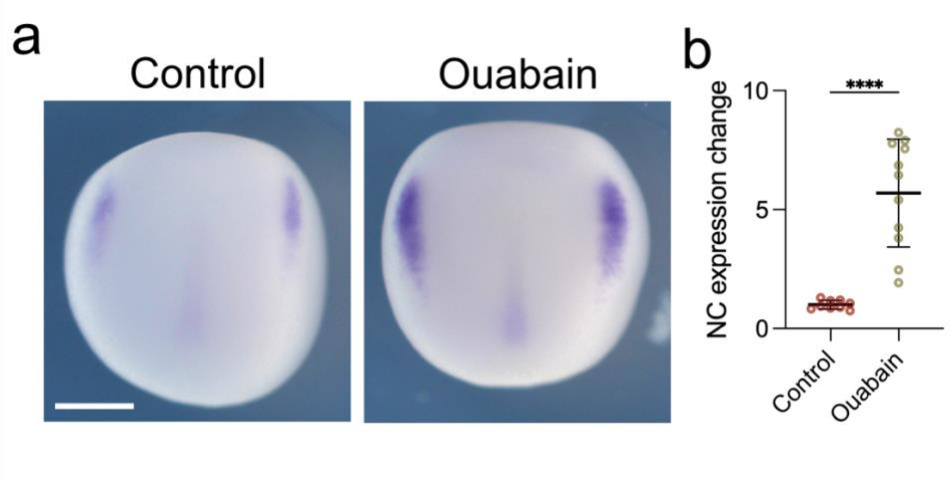

Fig. 4.5 | Inhibition of blastocoel expansion.

a, Analysis of snai2 marker via in situ hybridization between control and ouabain-treated embryos, analyzed at stage 14. **b**, Spread of data points indicating the change in neural crest expression levels between the control (*n* = 9 embryos) and treated group (*n* = 11 embryos). Scale bar 450 µm (**a**). Data points represent the mean, and error bars are s.d. Statistical analysis was performed using an unpaired student *t*-test; ****$P \leq 0.0001$.

4.2.3 Investigating alternative stimuli which modulate neural crest competence.

Our data indicate that the increase in blastocoel volume increases the hydrostatic pressure (Fig. 4.2), which regulates the competence of neural crest induction. However, an alternative potential mechanical cue is osmotic pressure. To investigate the possible role of osmolarity change which potentially could result from injecting fluid into the cavity, hence, influencing neural crest induction, we inflated embryos by injecting hypotonic and hypertonic solutions (Fig. 4.5a, b), which produced similar inhibition of the neural crest marker *snai2* (Fig. 4.5d). Moreover, injecting the "endogenous" content of a blastocoel cavity taken from a control embryo, yielding embryos of an equivalent isotonic solution (Fig. 4.5c), we again noted a reduction in the territory expressing the neural marker *snai2* (Fig. 4.5d). These results suggest that changes in blastocoel osmolarity are not the central factor in regulating the process of neural crest induction.

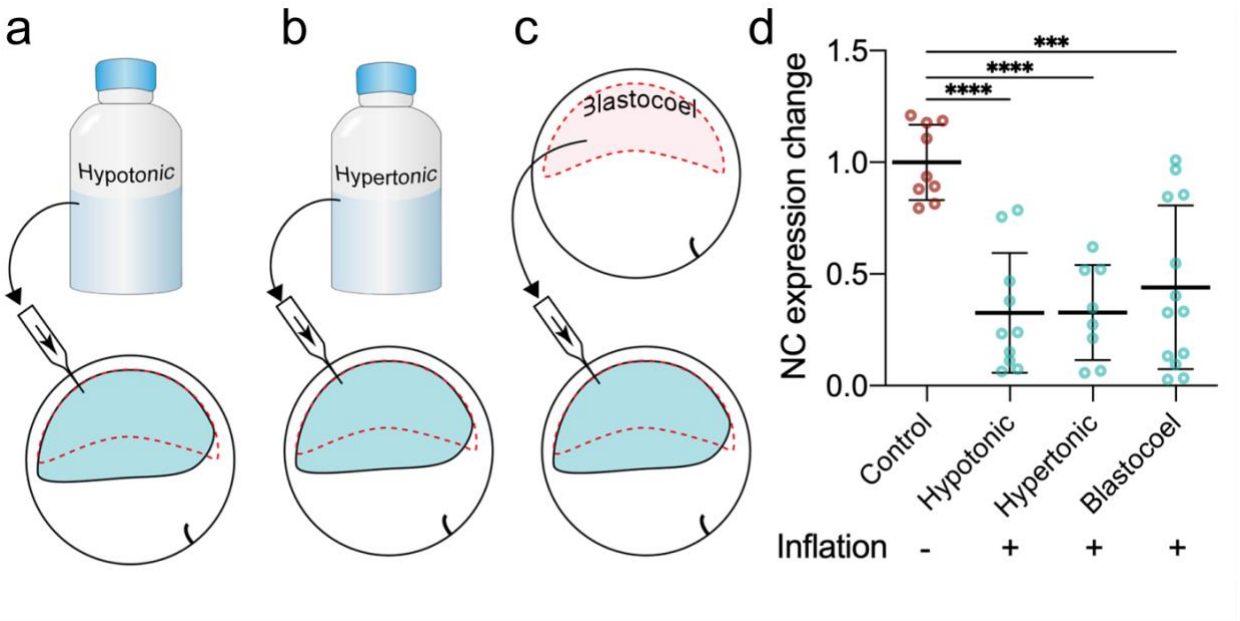

Fig. 4.6 | Investigate the osmolarity effect on neural crest induction.

a-c, Illustration of inflating embryos with solutions of different osmolarity; hypotonic, hypertonic, and blastocoel fluid (isotonic), respectively, described in detail in methods. **d**, Spread of data points comparing the change in the expression level of neural crest marker *snai2* at stage 14 between control (*n* = 9 embryos), hypotonic (*n* = 10 embryos), hypertonic (*n* = 8 embryos), and Blastocoel (*n* = 13 embryos). Data points represent mean, and error bars are s.d. Statistical analysis was performed using Dunnett's test; ***$P \leq 0.001$, ****$P \leq 0.0001$.

Another possibility is biochemical factors; it is possible that removing pre-existing blastocoel fluid during deflation leads to the depletion of an inhibitor of neural crest induction present in the blastocoel cavity, leading to neural crest expansion not related to hydrostatic pressure. To test this idea, we deflated embryos and then reinflated the blastocoel cavity with a saline media until it returned to its starting volume (Fig. 4.6a). Post blastocoel reinflation, the expression level of *snai2* was restored to normal levels (Fig. 4.6b). The results eliminate the possibility of the presence of a neural crest inhibitor in the blastocoel cavity. This experiment yielded an embryo with a chemically and osmotically altered blastocoel cavity but with a normal-sized blastocoel cavity. Despite these changes to the

blastocoel constitution (Fig. 4.6), we noted normal induction of neural crest cells, which further supports the notion that osmolarity does not affect neural crest induction, as concluded from the previous experiment (Fig. 4.5).

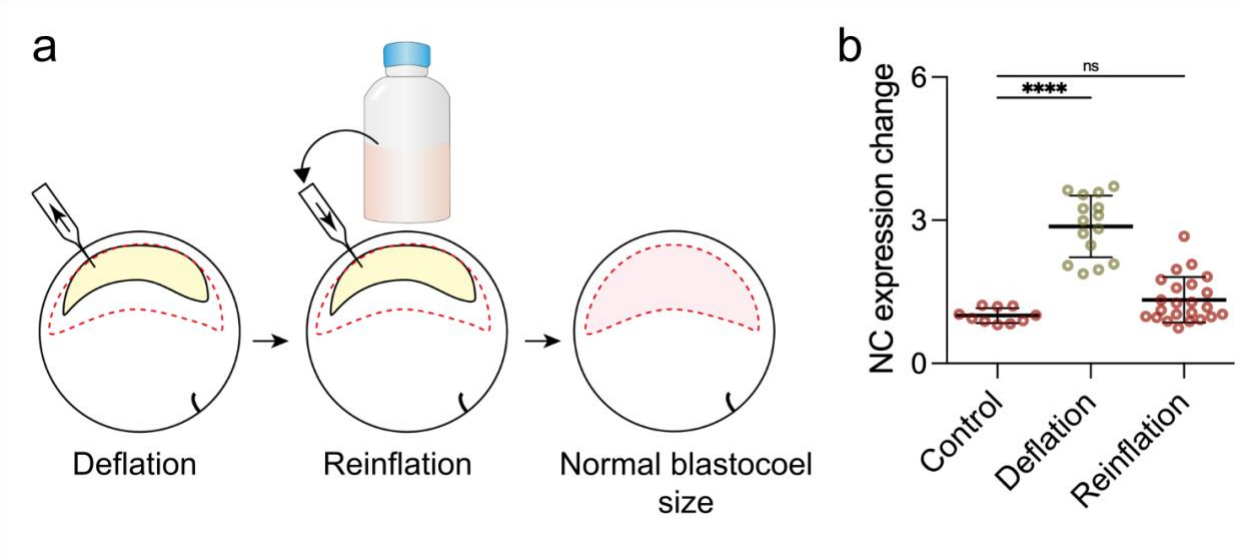

Fig. 4.7 | Biochemical effect on neural crest induction.

a, Illustration of reinflation assay, where an embryo restored to normal blastocoel size after deflation with a saline solution. **b**, Spread of data points comparing the change in expression levels of neural crest via *in situ* hybridization at stage 14 between control (*n* = 10 embryos), deflated (*n* = 15 embryos), and reinflated embryos (*n* = 23 embryos). Data points represent mean, and error bars are s.d. Statistical analysis was performed using Dunn's test; NS, $P>0.05$, ****$P \leq 0.0001$.

4.2.4 Change of hydrostatic pressure effect on gastrulation

Our data indicate that osmolarity and biochemical composition are not involved in neural crest induction, in contrast to hydrostatic pressure. Nevertheless, an alternative is that our observed phenotype is an indirect consequence of affecting the inducer tissue. The mesoderm plays a pivotal role in neural crest induction, as it expresses Wnts protein (*Wnt8)*, which activates the main signaling pathways in neural crest induction (Curchoe et al. 2010; García-Castro et al. 2002; LaBonne and Bronner-Fraser 1998b; Steventon et al. 2009a). To address this point, we analyzed via *in situ* hybridization the expression of the pan-mesodermal

marker *Xbra* and neural crest inducer *Wnt8* at different stages of development after inflation and deflation (Fig. 4.7a, b, c), and no change was noted comparing control to inflated and deflated embryos. These data suggest that mesoderm at early gastrulation is not affected. Moreover, no difference was noted in the notochord length between control and deflated and inflated embryos (Fig. 4.7d, e) nor the position or levels of *Wnt8* at stage 15 (Fig. 4.7f, g). These observations indicate that mesoderm migration during gastrulation and its ability to produce *Wnt8* is not affected. Lastly, the blastopore closure showed no difference between control and treated embryos (Fig. 4.7h, i), indicating that gastrulation had not been disrupted. These observations suggest a specific effect of hydrostatic pressure on the process of neural crest cells induced from the ectoderm.

Next, we hypothesized that the hydrostatic pressure regulates cell fate of the ectoderm. This implies that the neural crest domain can be controlled by hydrostatic pressure, and the expansion of this domain would occur at the expense of either the adjacent neural plate or non-neural ectoderm cells. To address this, we analyzed other ectodermal markers (*Keratin*, non-neural and *Sox2*, neural plate marker). We observed that the expansion of neural crest domain that is caused by deflation occurs at the expense of the epidermis but not neural plate (Fig. 4.8). Taken together, all these experiments and controls show that neural crest induction and presumably its competence is controlled by blastocoel hydrostatic pressure.

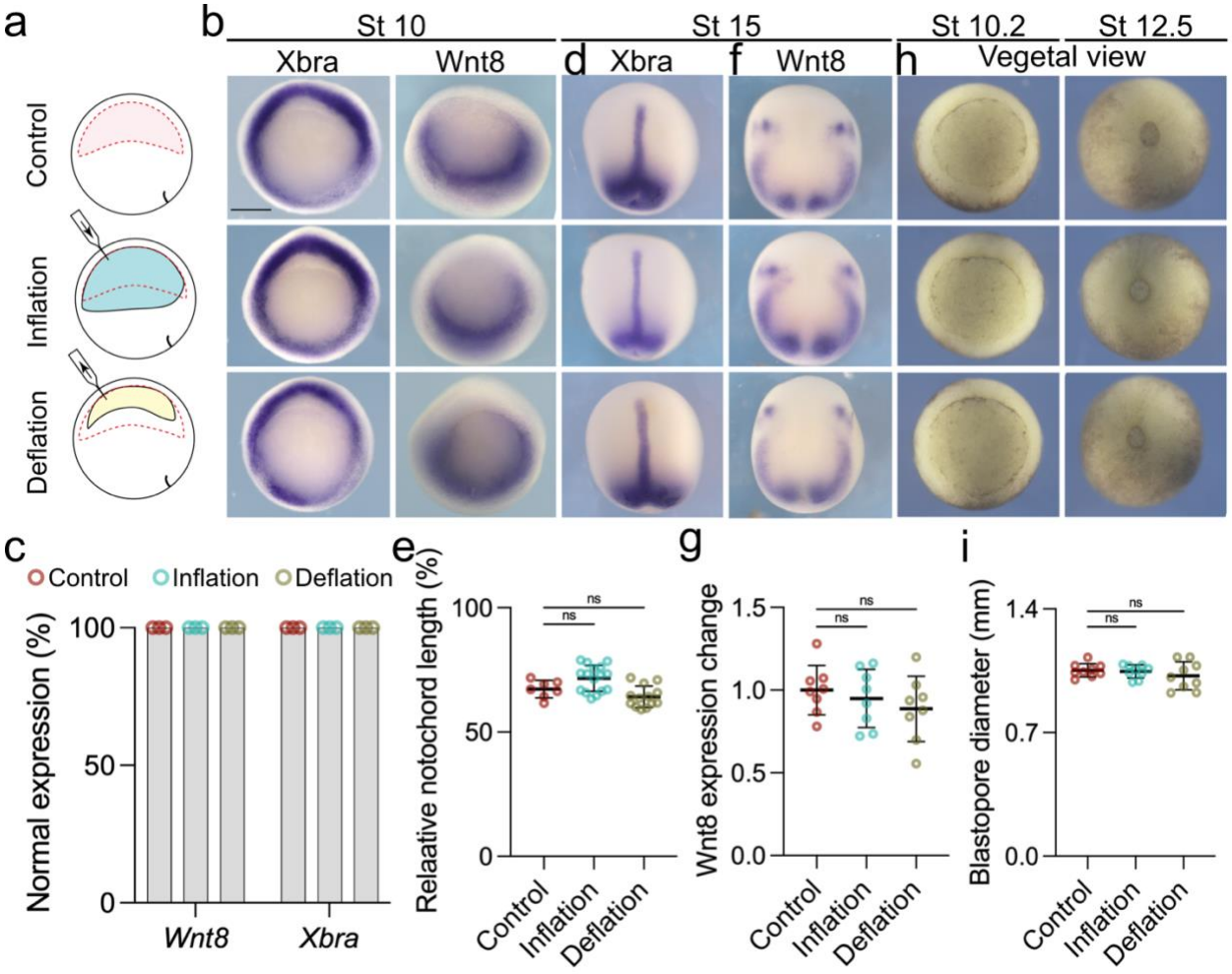

Fig. 4.8 | Changes in hydrostatic pressure do not affect the process of gastrulation.

a, Illustration of mechanical assays to change blastocoel volume. **b**, Embryos analyzed via *In situ* hybridization at stage 10 the neural crest inducer gene *Wnt8* and the pan-mesodermal marker *Xbra*. **c**, Spread of data points indicating the percentage of embryos expressing *Wnt8* or *Xbra* markers comparing control to deflated and inflated embryos. **d**, Embryos analyzed via *In situ* hybridization at stage 15 showing the expression of the pan-mesodermal marker *Xbra* and neural crest marker gene *Wnt8*. **e**, Spread of data points showing the change in length of the notochord, which is normalized to total length in control (*n* = 7 embryos), inflation (*n* = 16 embryos), and deflation (*n* = 13 embryos) embryos. **f**, Embryos analyzed via *in situ* hybridization showing the effect of inflation and deflation on mesoderm via *Wnt8*. **g**, Spread of data points comparing change in *Wnt8* expression in control (*n* = 8 embryos), deflation (*n* = 8 embryos), and inflation (*n* = 8 embryos). **h**, Live pictures showing blastopore formation and closure after

mechanical treatment compared to control embryos. **i**, Data points showing the diameter of blastopore closure in control (*n* = 9 embryos), inflation (*n* = 8 embryos), and deflation (*n* = 9 embryos) embryos. Scale bar 350 µm (**b**). Data (**e, g, i**) represent mean, and error bars are s.d. Statistical analysis was performed using Dunnett's test; NS, *P*>0.05.

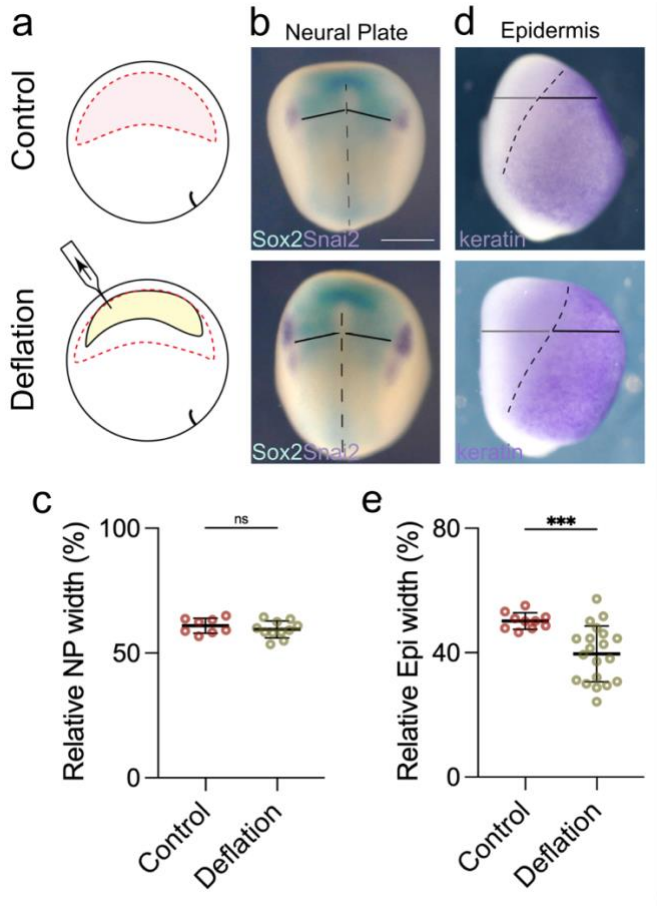

Fig. 4.9 | Deflated embryos expand neural crest domain at the expense of epidermis.

a, Illustration mechanical assay to reduce blastocoel volume; deflation. **b**, Embryos analyzed via double *in situ* hybridization at stage 14 showing neural plate marker (*Sox2*, cyan) and neural crest marker (*snai2,* purple). **c**, Data points comparing the relative width of neural plate (indicated by a continuous line) originating from the midline (indicated by a dashed line) to the outer limit of the neural plate in control (*n* = 8 embryos) and deflated (*n* = 11 embryos) embryos. **d**, Embryos analyzed via *In situ* hybridization at stage 14 showing epidermis marker (*keratin*, purple). **e**, Data points indicating the relative width of the epidermis to the total width of the embryo (indicated by continuous lines). Epidermis border was determined based on the expression (indicated by a dashed line) of *keratin* in control (*n* = 10 embryos) and deflated (*n* = 20 embryos) embryos. Data

represent mean, and error bars are s.d (**c, e**). Statistical analysis was performed using an unpaired student *t*-test; NS, $P>0.05$, $^{***}P \leq 0.001$.

4.2.5 Neural crest responds to pressure

Our findings show that the neural crest can respond with specificity to hydrostatic pressure and raise the possibility that these cells are responding to pressure mediated by hydrostatic pressure. To test this possibility, we applied direct mechanical pressure to open-faced explants with the prospective neural crest and the DLMZ (further details in the method chapter). Explants analysis via *in situ* hybridization showed inhibition of neural crest markers in compressed explants in contrast to uncompressed control explants (Fig. 4.9). This result indicates that the induction process of prospective neural crest into neural crest cells is mediated by pressure (hydrostatic or mechanical), as an increase in pressure inhibits neural crest induction.

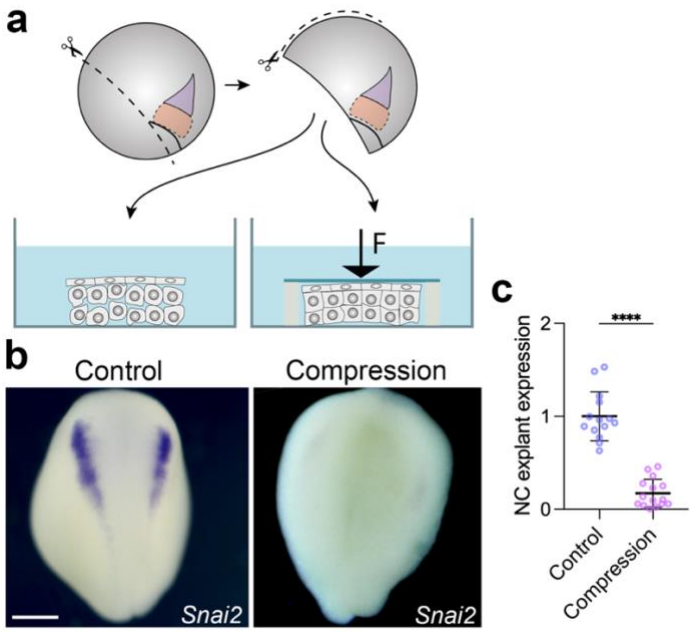

Fig. 4.10 | Inhibition of neural crest by mechanical pressure.

a, Illustration of *in vitro* compression assay of prospective neural crest explants; explants with prospective neural crest and DLMZ were obtained by dissection from dorsal blastopore lip to ventral side to remove ventral side. Then, a dissection from the animal

pole to the ventral side opens the explants. Next, explants were compressed under a coverslip and cultured until stage 18, and the expression level of *snai2* was analyzed via *in situ* hybridization. **b**, Explants show *snai2* expression of control (uncompressed) and experimental (compressed). **c**, Data points comparing the *snai2* expression levels in control (n = 11 explants) and compressed (n = 11 explants) explants. Scale bar 400 µm (**b**). Data represent mean, and error bars are s.d. Statistical analysis was performed using an unpaired student *t*-test; ****$P \leq 0.0001$.

4.2.6 Ectoderm requires low hydrostatic pressure to be competent for NCCs

Our data imply that neural crest induction is regulated by hydrostatic pressure. Mechanistically, an increase in hydrostatic pressure inhibits neural crest induction (Fig. 4.1 and 4.2). These findings gave rise to the notion that the loss of competence is possible due to increased hydrostatic pressure of the blastocoel cavity during early gastrulation. To address this hypothesis, we performed competence graft assay in conjunction with mechanical manipulation. Stage 12 embryos were grafted with DLMZ after deflation (a reduction in hydrostatic pressure) at stage 10 (Fig. 4.11a; illustration). Stage 12 is when the ectoderm lost its competence to induce neural crest in response to DLMZ graft, as described in Figure 3.2. Analyzing the outcome of this assay, we noted that control embryos (With DLMZ and no deflation) failed to induce neural crest ectopic induction, whereas deflated embryos did induce ectopic induction (Fig. 4.11a, b). To support the notion that during normal development, ectoderm competence to induce NCCs is mediated by hydrostatic pressure, we took competent stage 10 embryos and grafted them with DLMZ after inflation (an increase in hydrostatic pressure) at stage 10 (Fig. 4.11c; illustration). We noted that control embryos (DLMZ with no inflation) exhibited ventral neural crest ectopic induction, in contrast to experimental embryos (DLMZ and inflated) where they exhibited no ectopic neural crest (Fig. 4.11c, d). These findings show that simple mechanical manipulation of hydrostatic pressure can modify the ectoderm competence for

neural crest response to DLMZ signals. **In conclusion, neural crest competence is lost during gastrulation due to an increase in the hydrostatic pressure of the blastocoel cavity.**

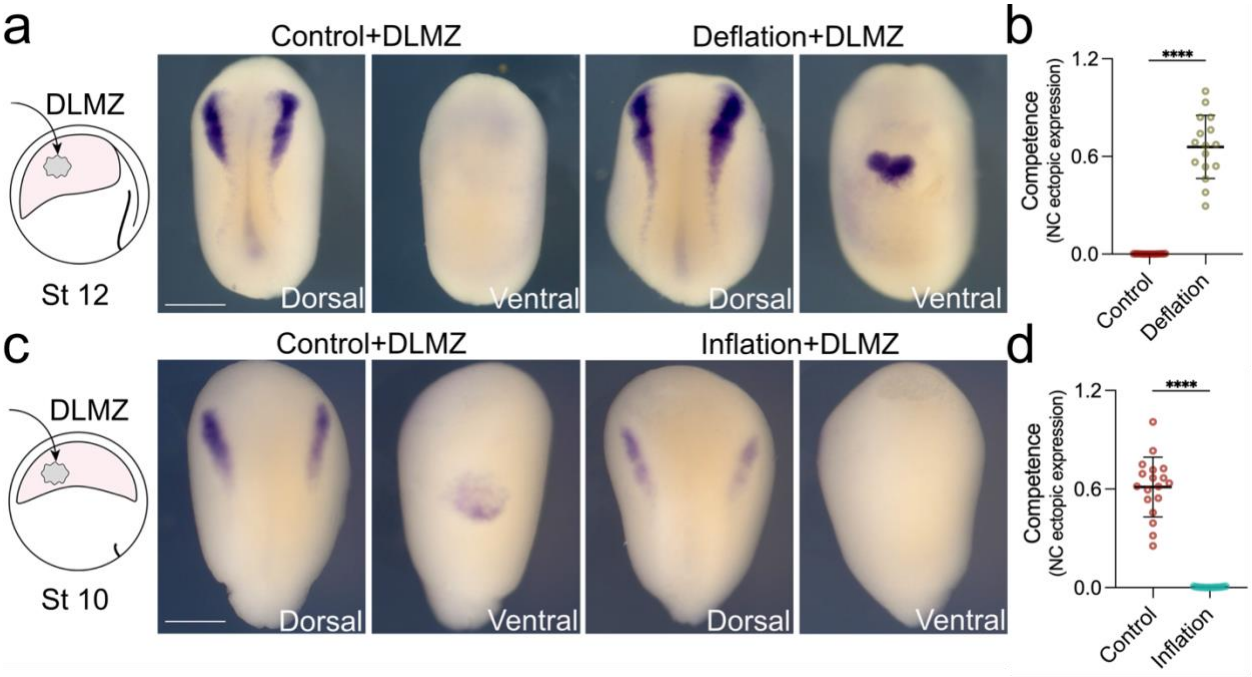

Fig. 4.11 | Hydrostatic pressure mediates ectodermal competence to induce NCCs.

a, Illustration of competence assay in conjunction with a reduction of hydrostatic pressure (deflation) and embryos showing *snai2* analyzed via *in situ* hybridization at stage 18 comparing embryos with DLMZ grafted at stage 12 and embryos that are deflated at stage 10 and then grafted with DLMZ at stage 12. **b**, Spread of data points indicating neural crest competence at stages 12. **c**, Illustration of competence assay in conjunction with an increase of hydrostatic pressure (inflation) and embryos showing *snai2* analyzed via *in situ* hybridization at stage 16 comparing embryos with DLMZ grafted at stage 10 and embryos that are inflated at stage 10 and then grafted with DLMZ at stage 10^{+}. Scale bars 450 µm (**a, c**). Data represent mean, and error bars are s.d. Statistical analysis was performed using unpaired two-tailed *t*-tests (**b**, **d**);$^{****}P \leq 0.0001$. $n_{competence} = 16_{control\ and\ deflation}$ embryos (**b**), $n_{competence} = 18_{control\ and\ inflation}$ embryos (**d**).

4.3 Discussion

We demonstrate (Chapter 3) that the change in blastocoel volume and hydrostatic pressure correlate with the loss of neural crest competence. These results provide a possible explanation of how competence is lost during gastrulation. To investigate this, we increased and decreased the hydrostatic pressure, which led to the alteration of neural crest induction. However, this manipulation of hydrostatic pressure also might change the osmotic pressure, the composition of blastocoel (presence of competence inhibitors), or the observed phenotypes could be the indirect result of affecting a crucial step, the neural crest induction. We ruled out the effect of the osmotic pressure by inflating with different solutions (hypotonic, isotonic, and hypertonic) and the impact of inhibitor by reinflating a deflated embryo. These results suggest that the loss of neural crest competence is mediated by the hydrostatic pressure increase as a mechanical cue. Moreover, we investigated the role of hydrostatic pressure on mesodermal induction (which provides inductive signaling, chapter 1) and the progression of gastrulation by examining mesoderm migration and epiboly (the closure of blastopore). Importantly, this change in hydrostatic pressure during morphogenesis and artificial mechanical assays does not affect the inducer tissue, the mesoderm, or its ability to produce the key inductive signals to induce neural crest cell, *Wnt8*. In addition, we show other processes during gastrulation, such as blastopore closure, are unaffected. The observations suggest the specificity effect that hydrostatic pressure elicits during gastrulation. In addition, we note that the increase in blastocoel volume is not accompanied by an increase in the total volume of the embryos during gastrulation. These results suggest competence loss is due to compressive forces caused by the blastocoel volume and pressure increase. We confirmed this idea by directly compressing the ectoderm. As hypothesized, we extended ectoderm competence by decreasing the hydrostatic pressure. In conclusion, these results strongly show the role of hydrostatic pressure on the loss of neural crest competence.

Chapter 5: Hydrostatic pressure regulates Wnt signalling in a Yap-dependent manner

5.1 Introduction

The process of neural crest induction commences during gastrulation at the border of the neural plate by multiple signalling steps, mainly Wnt signalling. Wnt proteins are secreted from DLMZ (Aybar and Mayor 2002b; Mancilla and Mayor 1996; Mayor and Theveneau 2014), activating canonical Wnt pathway (chapter 1.1.4b and Fig. 1.4). We demonstrate that the induction of these cells is modulated by mechanical cues *in vivo* and *in vitro*. Moreover, the generation of the Wnt proteins is not affected by this mechanical cue (hydrostatic pressure). These findings suggest that hydrostatic pressure (increase) during gastrulation controls the loss of neural crest competence and that ectodermal cells sense this pressure change. Thus, in this chapter, we aim to investigate the mechanotransduction mechanism of hydrostatic pressure onto biochemical signaling. Since the canonical Wnt pathway is the primary signaling pathway in the induction of neural crest, we propose that the hydrostatic pressure regulates Wnt activity. However, this idea does not address how these ectodermal cells sense mechanical cues. Since the Hippo pathway (chapter 1.1.4c and Fig. 1.5) has been proposed to have a role in neural crest induction (Yap) (Gee et al. 2011), yet still poorly understood, we propose that hydrostatic pressure regulates Wnt activity via controlling the localization of Yap. The challenge in examining how Yap interacts with Wnt signaling is due to the wide range of reports on this interaction occur. Indeed, Yap interacts at different levels of the Wnt pathway such as Dvl (Sun et al. 2017), β-catenin destruction complex (Azzolin et al. 2014a), stabilization of β-catenin into the nucleus (Pan et al. 2018), among others interaction (Oudhoff et al. 2016a; Quinn et al. 2021; Yang et al. 2017). Thus, we aim to understand how Yap interacts and regulates Wnt activity as a possible mechanotransduction mechanism on how hydrostatic pressure regulates competence of neural crest induction.

5.2 Results

5.2.1 Hydrostatic pressure regulates canonical Wnt activity

We show that hydrostatic pressure can regulate neural crest response to DLMZ (Aybar and Mayor 2002a; Mancilla and Mayor 1996; Steventon et al. 2009a). Next, we asked whether hydrostatic pressure could modulate Wnt activity. To test this notion, we used TOP flash luciferase assay to directly measure Wnt activity *in vivo*. We expressed the Wnt sensor super TOP-flash (Veeman et al. 2003) in the ectoderm of *Xenopus* embryos. To confirm the functionality of this assay, we activated the Wnt pathway (Fig. 1.4) with a GSK3 inhibitor (BIO) (Maj et al. 2016). Inhibition of the GSK3 complex will prevent degradation of β-catenin, leading to its localization and regulating target genes (Maj et al. 2016). Our result shows an increase in Wnt activity while treated with BIO compared to non-treated embryos, suggesting the successful measurement of Wnt activity in the ectoderm of *Xenopus* embryos (Fig. 5.1a). Next, we deflated or inflated the blastocoel cavity at the early gastrula stage and measured luciferase activity at stage 12.5 (Veeman et al. 2003). Our data show that a reduction in hydrostatic pressure by deflation leads to an increase in Wnt activity, whereas an increase in hydrostatic pressure by inflation inhibits it (Fig. 5.1b). These observations suggest the possibility that hydrostatic pressure regulates Wnt activity.

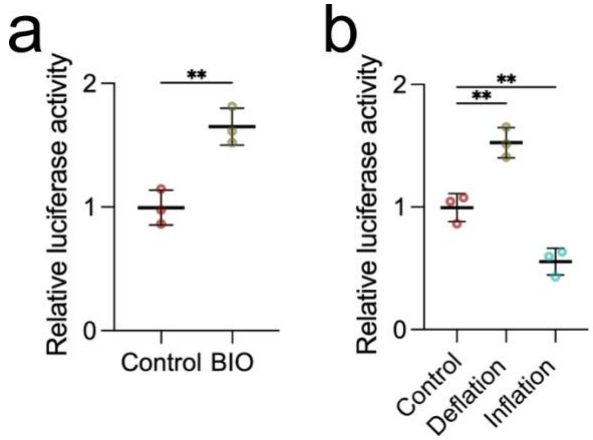

Fig. 5.1 | Wnt activity readout by a change in hydrostatic pressure of blastocoel cavity.

a, Data points indicate relative readout Wnt activity measured by super TOP-flash assay in control and BIO-treated embryos treated. BIO is an inhibitor of the GSK3 complex,

which would lead to an increase in Wnt activity by stabilizing β-catenin into the nucleus and regulating target genes. **b**, Spread of points indicating relative luciferase activity of super Top flash after inflation and deflation. Each data point represents three replicates (3-5 embryos homogenized per replicate), and each treatment represents three independent experiments. Data represent mean, and error bars are s.d. Statistical analysis was performed using student *t*-test (**a**) and unpaired Dunnett's tests (**b**); $^{**}P \leq 0.01$.

5.2.2 Regional Wnt activity regulated by hydrostatic pressure

Despite that Wnt luciferase assay is well-established and a good indicator of Wnt readout, it requires homogenization of the embryo; hence, its unclear whether changes in Wnt activity mediated by change in hydrostatic pressure in the ectoderm were regionalized in the prospective neural crest domain. To spatially determine Wnt activity *in vivo,* we used an *X. laevis* transgenic embryo that would express GFP under the control of the TCF/LEF, β-catenin binding partner to regulate Wnt target genes (Tran and Vleminckx 2014). As previously reported (Borday et al. 2018b), we noted an evident GFP fluorescence in the neural fold domain that contains the prospective neural crest cells (Fig. 5.2a; control). Following our blastocoel mechanical treatments as hypothesized, we observe that a reduction in hydrostatic pressure elicits a substantial increase in GFP intensity (Fig. 5.2a; deflation), unlike an increase in hydrostatic pressure, which prompts an inhibition of GFP fluorescence in the embryos in the neural fold region (Fig. 5.2a; inflation). These data are consistent with the luciferase assay, indicating that hydrostatic pressure generated in the blastocoel cavity can regulate Wnt activity in the prospective neural fold domain and consistent with **the role of blastocoel pressure as a mediator of Wnt response and neural crest competence**.

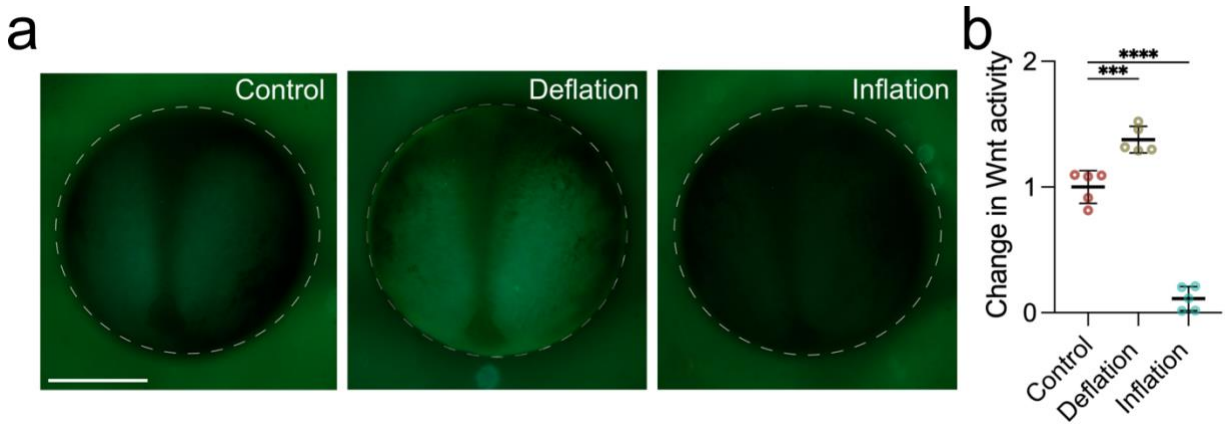

Fig. 5.2 | Regional Wnt activation mediated by change in hydrostatic pressure.

a, *Xenopus* transgenic embryos *Tg(pbin7Lef-dGFP)* were used to detect Wnt activity at stage 12.5 after the indicated inflation and deflation at stage 10. **b**, Spread of data points exhibiting levels of GFP intensity normalized to control embryos. Scale bar and 450 μm (**a**). Data represent mean, and error bars are s.d. Statistical analysis was performed using unpaired Dunnett's tests (**b**); ***$P \leq 0.001$, ****$P \leq 0.0001$.

5.2.3 Yap1 is required for neural crest induction.

Next, we hypothesized the possibility by which neural crest cells sense the change in mechanical input and subsequently regulate the Wnt pathway. We found that Yes Associated Protein (Yap1) is a possible mechanosensitive element that could modulate NCCs sensitivity to mechanics as Yap has been characterized as a mechanosensor factor of the Hippo pathway and also interacts with the canonical Wnt signalling signaling (Azzolin et al. 2014b; Barry et al. 2013; Guillermin et al. 2021; Marshall et al. 2023; Oudhoff et al. 2016b; Park et al. 2015; Tsutsumi et al. 2013), making Yap a good mechanosensitive candidate in our model. To establish the link of Yap as an element downstream of hydrostatic pressure, we first aimed to investigate if Yap is required for neural crest induction. Consistent with our notion, we found that morpholino-mediated inhibition of Yap (Gee et al. 2011) impairs neural crest formation (Fig. 5.3). These data suggest an adequate formation of neural crest requires activation of canonical Wnt pathway and Yap.

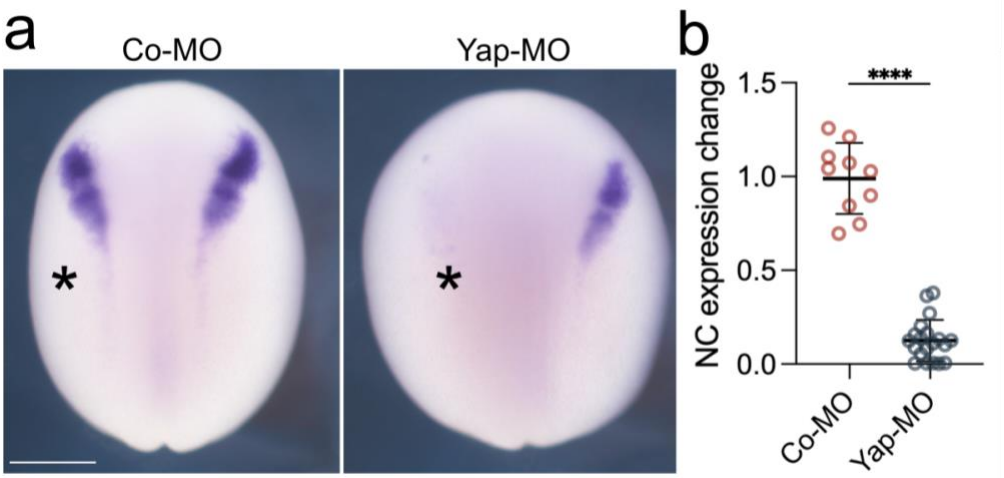

Fig. 5.3 | Inhibition of Yap impairs the neural crest formation.

Xenopus embryos were injected at the 8-cell stage with control-MO or Yap-MO on the left side (asterisk) and analyzed via *in situ* hybridization at stage 16 for *snai2* marker. **b**, Data spread shows the NC marker expression change between embryos injected with control-MO (*n* = 10 embryos), shows normal expression and Yap-MO (*n* = 15 embryos) shows inhibition of neural crest. Scale bar 450 µm (**a**). Data represent mean, and error bars are s.d. Statistical analysis was performed using Mann-Whitney *U*-test; ****$P \leq 0.001$.

5.2.4 Yap1 as a potential regulator of NCCs competence.

As we identified that Yap is required for neural crest induction; next we aimed to further examine the possible crosstalk between the Wnt pathway and Yap during neural crest induction. To address this aim, we also investigated whether activation of the Wnt pathway could rescue neural crest formation in Yap-depleted embryos (Yap-MO). Overexpression of Xwnt8, which leads to expansion of the NC domain (Chang and Hemmati-Brivanlou 1998), failed to rescue NCCs in Yap-depleted embryos (Fig. 5.4a, b), nor activation of Wnt pathway using the GSK3 inhibitor (BIO)(Fig. 5.4c, d). These data suggest that Yap is unlikely to regulate Wnt activity at the extracellular Wnt, Wnt receptor level, or through degradation of β-catenin by GSK3 phosphorylation, meaning it acts downstream. Finally, overexpression of an activated form of β-catenin (Carmona-Fontaine et al. 2007) can rescue neural crest induction in Yap-inhibited embryos (Fig. 5.4e, f),

suggesting that during neural crest induction Yap regulates Wnt activity at the level of β-catenin.

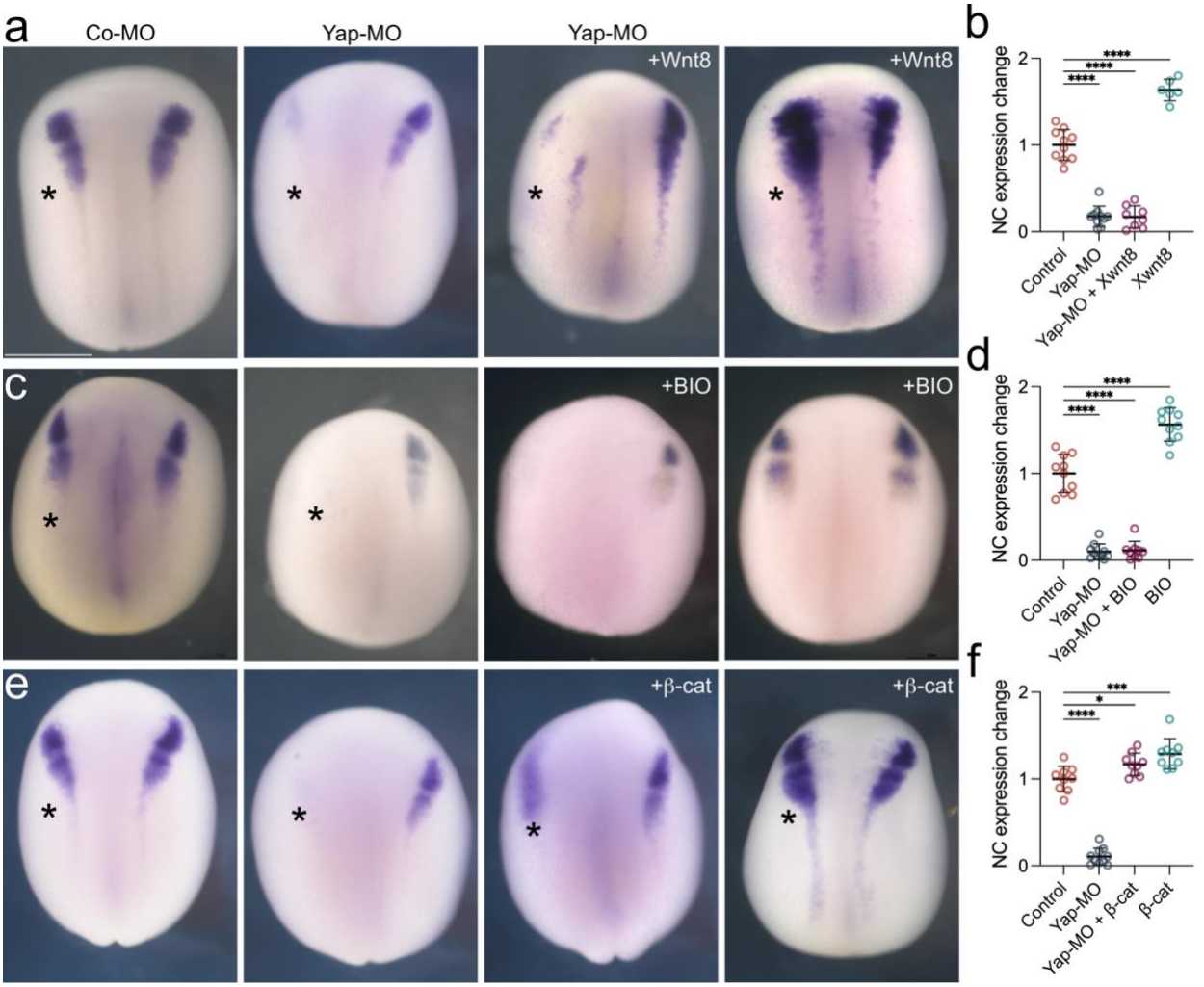

Fig. 5.4 | Crosstalk of Wnt pathway with Yap.

a, **c**, and **e**, Embryos analyzed via *in situ* hybridization of *snai2* neural crest marker at stages 16, 15, and 17, respectively, after the indicated injections at the 8-cell stage (**a**, **e**) or BIO treatment at stage 10 (**c**). Asterisks indicate injected side. β-cat in (**e**) indicates an activated form of β-catenin induced by treatment with dexamethasone at stage 10. **b**, **d**, and **f**, Spread of data points indicating the expression level of *snai2* with respect to indicated treatments. Scale bar and 450 μm (**a**). Data represent mean, and error bars are s.d. Statistical analysis was performed using unpaired Dunnett's tests (**b**, **d**, and **f**); $^{*}P \leq 0.1$, $^{***}P \leq 0.001$, $^{****}P \leq 0.0001$. $n = 10_{control}$, $10_{Yap\text{-}MO}$, $8_{Yap\text{-}MO + Xwnt8}$, 6_{Xwnt8} embryos (**b**). *n*

= $10_{control}$, $10_{Yap\text{-}MO}$, $9_{Yap\text{-}MO + BIO}$, 10_{BIO} embryos (**d**). *n* = $9_{control}$, $10_{Yap\text{-}MO}$, $9_{Yap\text{-}MO + \beta\text{-}cat}$, $9_{\beta\text{-}cat}$ embryos (**f**).

5.2.5 Hydrostatic pressure controls Yap localization

Having demonstrated that hydrostatic pressure and Yap independently control Wnt activity, we hypothesized that Yap activity is controlled by hydrostatic pressure to modulate neural crest competence by regulating the activity of Wnt signaling, consistent with previous observations (Kemppainen et al. 2016; Nardone et al. 2017; Panciera et al. 2017). To address this hypothesis, we performed immunofluorescence against Yap and studied its subcellular localization at different stages, as nuclear Yap can be used as a proxy for Yap activity (Cao et al. 2008; Dupont et al. 2011; Franklin et al. 2020; Lavado et al. 2013). We noted that competent stage 10 ectoderm shows nuclear localization of Yap, in contrast to non-competent stage 12 ectoderm, where a reduction of nuclear Yap is observed (Fig. 5.5a). Consistently, increasing hydrostatic pressure of the blastocoel cavity by inflation decreases nuclear localization of Yap (Fig. 5.5b). On the other hand, a reduction in hydrostatic pressure of the blastocoel cavity by deflation increases the amount of nuclear localization of Yap (Fig. 5.5c).

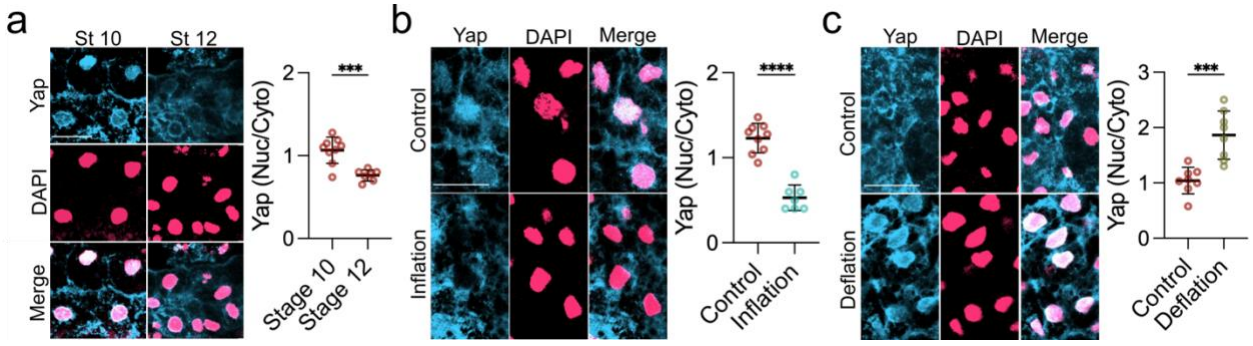

Fig. 5.5 | Yap activity mediated by change in hydrostatic pressure of blastocoel cavity.

a-c, Immunofluorescence analysis of ectoderm showing staining against Yap (blue) and DAPI (pink) taken at different developmental times and mechanical treatments; graphs indicate quantification of Yap nuclear to cytoplasmic ratio at different developmental times and mechanical treatments. Scale bar 20 μm (**a, b, c**). Data represent mean, and error bars are s.d. Statistical analysis was performed using unpaired *t*-test; ***$P \leq 0.001$,

****$P \leq 0.0001$. $n = 9_{st10}$, 6_{st12} embryos (**a**). $n = 9_{control}$, $7_{inflation}$ embryos (**b**). $n = 8_{control}$, $8_{deflation}$ embryos (**c**).

Furthermore, during gastrulation when competence is lost (Fig. 3.1), we observed an increase in cell density of the ectoderm alongside a decrease in intercellular space (Fig. 5.6a-d). In addition, we note cell aspect ratio is maintained (Fig. 5.6e). These findings suggest that loss of nuclear Yap during gastrulation (Fig. 5.6a) would correlate with an increase in cell packing of the ectoderm; indeed, we observe this (Fig. 5.6f). We can mimic the increase in cell density and cell packing by inflation (Fig. 5.6d, f; 10*). Mechanistically, these results are consistent with the view that loss of competence is due to cytoplasmic retention of Yap, mediated by an increase in hydrostatic pressure of the blastocoel cavity leading to an increase in cell packing in *Xenopus*. To test the generality of this hypothesis, we differentiated induced pluripotent stem cells (iPSCs) into induced neural crest cells (iNCC) at different densities (Fig. 5.7a) and assessed expression levels of neural crest markers (*Sox10* and *Sox9*). We found an inhibition of iNCC markers at higher densities and higher cell packing (Fig. 5.7a-c). Similarly to our *in vivo* observations, we noted cytoplasmic retention of Yap at higher densities (Fig. 5.7e, d). These observations are consistent with our model that proposes that an **increase in hydrostatic leads to a higher cell packing, inhibiting Yap and neural crest competence during gastrulation.**

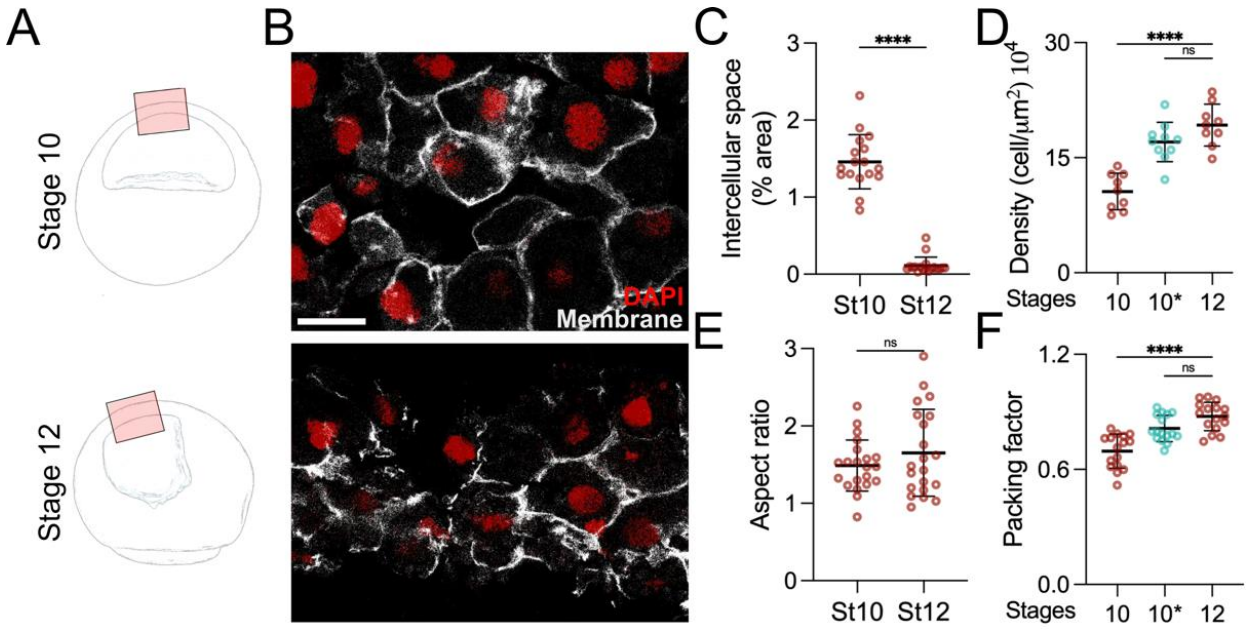

Fig. 5.6 | Yap activity is dependent on cell packing controlled by hydrostatic pressure.

a, Illustration of embryos showing the regions of interest (red square) of ectoderm for analysis. **b**, Immunofluorescence analysis of the ectoderm stained against membrane GFP (gray) and DAPI nuclear staining (red) **c-f**, Quantification indicating the percentage of intercellular space (n_{st10}, n_{st12} = 20 embryos), density (n_{st10} = 9, n_{st10*} = 10, n_{st12} = 9 embryos), aspect ratio (n_{st10} = 17, n_{st12} = 18 embryos), and cell packing index (n_{st10}, n_{st10*}, n_{st12} = 16 embryos) of the ectoderm. 10* are inflated embryos (cyan) compared to control (red) embryos at indicated stages. Scale bar 20 µm (**b**). Data represent mean, and error bars are s.d. Statistical analysis was performed using a two-tailed student *t*-test; NS, $P>0.05$, ****$P \leq 0.001$.

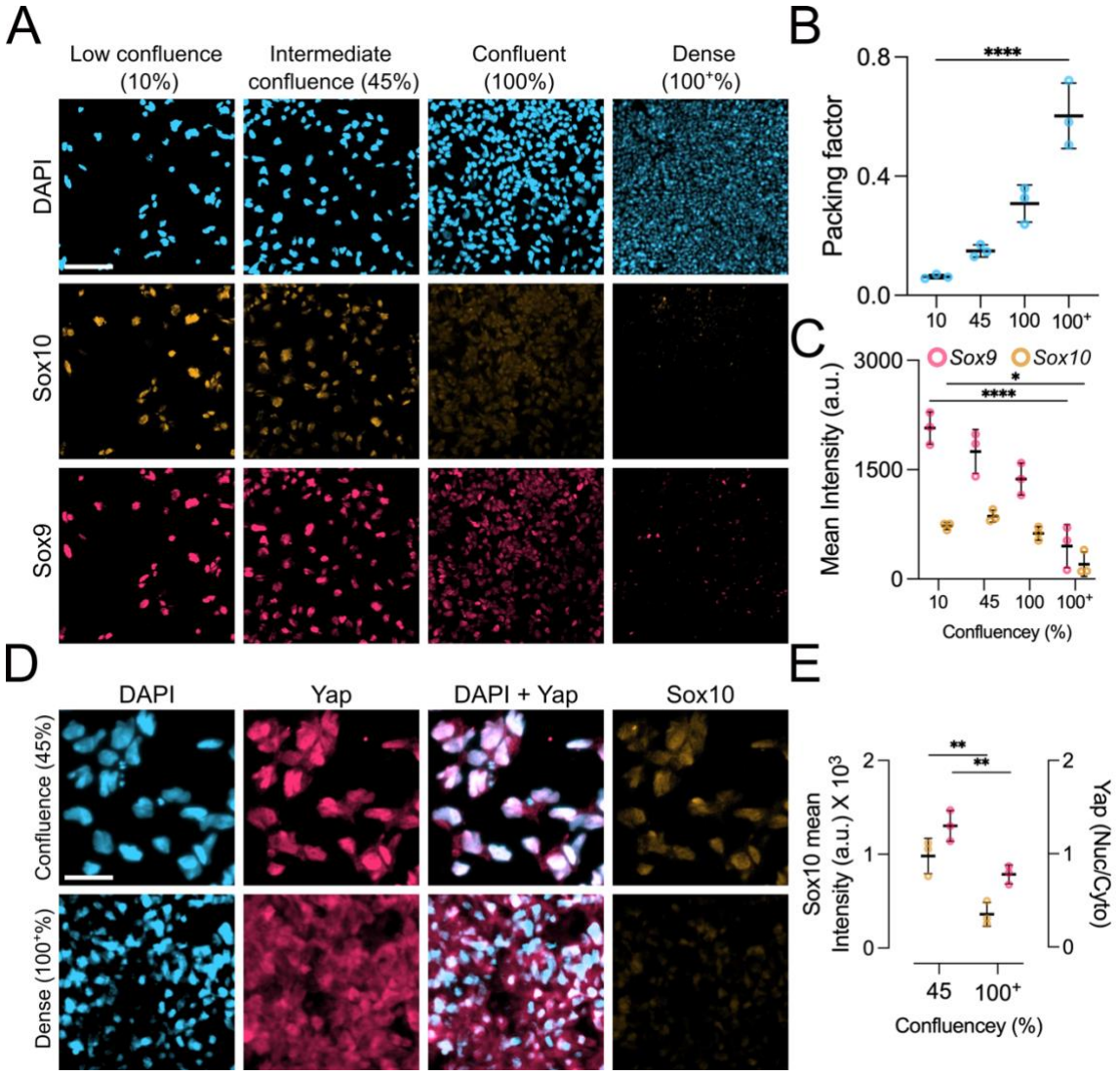

Fig. 5.7 | Higher confluency inhibits differentiation of iNCC.

a, Immunofluorescence of iPSCs differentiated into iNCCs with different confluences expressing *Sox9* (pink) and *Sox10* (orange). **b**, Quantification of cell packing at indicated confluences. **c**, Quantification of mean fluorescence intensity of indicated neural crest markers at different densities. **d**, Immunofluorescence of Yap localization (pink) and *Sox10* (orange) expression at various confluences of iNCCs. **e**, Quantification of mean fluorescence intensity of *Sox10* and Yap at different densities. Scale bar 100 µm (**a**), 65 µm (**d**). Data represent mean, and error bars are s.d. Statistical analysis was performed using a two-tailed student *t*-test (**e**) and Dunnett's test; $*P \leq 0.1$, $**P \leq 0.01$, $****P \leq 0.001$.

5.2.6 Neural crest induction requires an active form of YAP

We demonstrate that Yap is required for neural crest induction. In addition, it is well established that Yap activity depends on its subcellular localization (Aragona et al. 2013; Azzolin et al. 2014b; Piccolo et al. 2022). However, we note that competent ectoderm to induce neural crest show a nuclear form of Yap (Fig 5.5). To directly test the role of nuclear Yap on neural crest competence, we used a mutant that is constitutively active and localized in the nucleus even in the absence of a mechanical stimulus (YapS127A, (Komuro et al. 2003)). This mutation will prevent the phosphorylation of Yap at site 127, subsequently preventing cytoplasmic retention and promoting activation of target genes, as previously shown (Kemppainen et al. 2016; Komuro et al. 2003; Nardone et al. 2017; Panciera et al. 2017; Phelps et al. 2022). Expression of YapS127A in Yap-depleted embryos can rescue neural crest induction and leads to neural crest expansion in control embryos (Fig. 5.8a, b), indicating that ectodermal cells require nuclear Yap to induce neural crest cells.

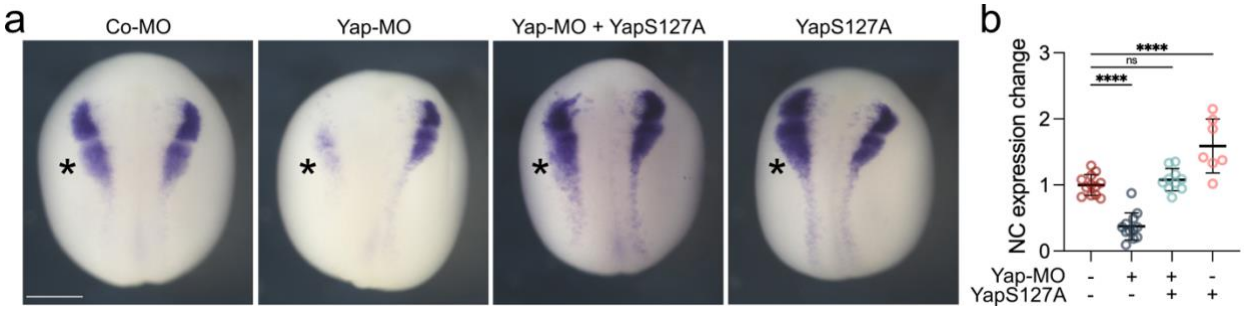

Fig. 5.8 | Neural crest induction requires nuclear YAP.

a, Embryos analyzed via *In situ* hybridization at stage 18 showing *snai2* marker after the indicated treatments, asterisks indicate injected side. **b**, Spread of normalized quantification of *snai2* expression. Scale bar 400 µm (**a**). Data represent mean, and error bars are s.d. Statistical analysis was performed using unpaired *t*-test and unpaired Dunnett's tests; NS, $P>0.05$, ****$P \leq 0.0001$. n = $13_{control}$, $10_{Yap\text{-}MO}$, $12_{Yap\text{-}MO + YapS127A}$, $7_{YapS127A}$ embryos (**b**).

5.2.7 An increase in hydrostatic regulates neural crest induction in a Yap-dependent manner

To further support the idea that mechanical cues regulating the competence of the ectoderm to induce neural crest is mediated by Yap, we inflated (increased hydrostatic pressure) and injected mutant active YapS127A. We theorized that nuclear Yap should rescue the inhibitory phenotype of inflation, as Yap is downstream of hydrostatic pressure in our mechanotransduction model. Indeed, we noted that inhibition of neural crest mediated by increasing hydrostatic pressure could be rescued by expressing YapS127A (Fig. 5.9a, b). These results further support the idea competent ectodermal cells require an active form of Yap to induce neural crest cells.

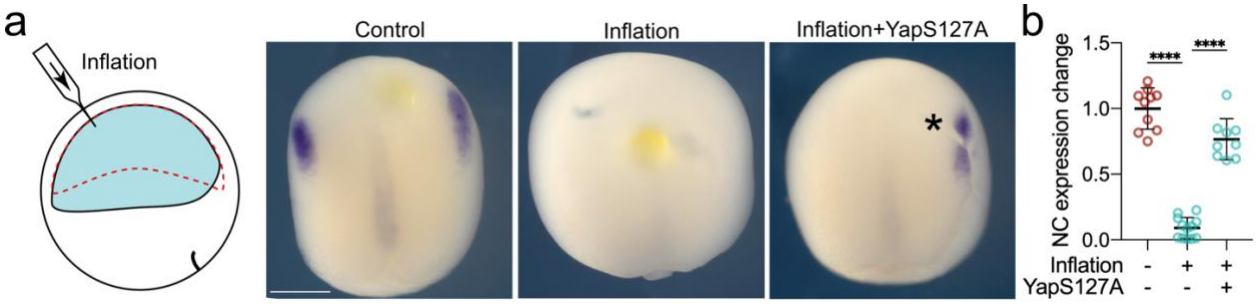

Fig. 5.9 | Hydrostatic pressure regulates fate via active Yap.

a, Illustration of inflation assay and *in situ* hybridization analysis of embryos showing *snai2* marker at stage 14. **b**, Data points indicating normalized expression level of *snai2*. Scale bar 400 µm (**a**). Data represent mean, and error bars are s.d. Statistical analysis was performed using unpaired t-test and unpaired Dunnett's tests; ****P ≤ 0.0001. *n* = $10_{control}$, $12_{inflation}$, $9_{inflation + YapS127A}$ embryos.

5.2.8 Competent ectoderm to induce neural crest requires an active form of Yap

Finally, to test the hypothesis that neural crest competence to DLMZ inductive signals requires nuclear Yap, we performed the DLMZ grafts in non-competent stage 12 embryos previously injected with YapS127A mutant. We noted that neural crest competence is restored at stage 12 by nuclear Yap (Fig. 5.10h, i). Taken together, these data place Yap as a mechanotransduction element

mediated by the hydrostatic pressure of the blastocoel cavity and demonstrate that its nuclear activity confers neural crest competence (Fig. 5.5-5.10).

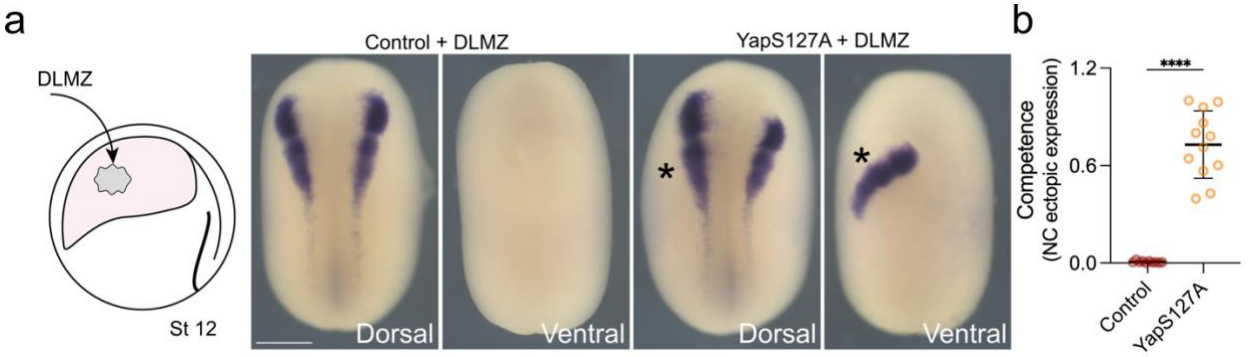

Fig. 5.10 | Ectoderm competence to induce neural crest cell depends on nuclear Yap.

a, Illustration of neural crest competence graft assay at stage 12. Experimental embryos were injected with YapS127A mutant at the 8-cell stage and then grafted with DLMZ, whereas control embryos were only grafted with DLMZ. And *in situ* hybridization analysis of *snai2* marker at stage 18. Asterisks indicate injected side. **b**, Spread of data points indicating neural crest competence normalized to control. Scale bar 400 µm (**a**). Data represent mean, and error bars are s.d. Statistical analysis was performed using unpaired student *t*-test; ****$P \leq 0.0001$. $n = 11_{control}$, $12_{YapS127A}$ embryos (**b**).

5.3 Discussion

In this chapter, we aimed to investigate the mechanotransduction mechanism of how hydrostatic pressure of the blastocoel cavity controls the competence of neural crest induction. Since the ectoderm is in direct contact with the blastocoel cavity, we hypothesized that this mechanical cue regulates Wnt activity, explaining the regional regulation of competence. We confirmed our hypothesis by measuring Wnt activity in control and experimental conditions. In addition, we investigated how these cells via Yap are sensing the change in hydrostatic pressure and controlling Wnt activity. Finally, show that the loss of nuclear activity of Yap during gastrulation leads to loss of neural crest competence.

Chapter 6: Discussion

Gurdon defined embryonic induction as "an interaction between one inducing and another responding tissue, as result of which the responding tissue undergoes a change in its direction or differentiation" (Gurdon 1987). Holtzer classified embryonic induction based on several findings (Browne 1909; Lewis 1904, 1907; Saxen 1977; Spemann 1901; Spemann and Mangold 1924) as either permissive induction (the outcome is mainly governed by induced tissue) or instructive induction (the outcome is mainly governed by inducing tissue) (Holtzer 1968). Indeed, the interaction of an uncommitted (responding) tissue to a specific signal (from inducing tissue) that will dictate the differentiation outcome of the responding tissue is known as instructive embryonic induction; an example of which are mesoderm, neural plate, lens, placode, and neural crest induction.

Furthermore, the capacity of tissues to respond to inductive signals was defined as competence (WADDINGTON 1934), which has been a longstanding topic of intense research, as past investigations have focused only on the role of biochemical signals without yielding a unifying mechanism that explains this phenomenon (Christian et al. 1992; Esmaeili et al. 2020b; Gillespie et al. 1989b; Henig et al. 1998; Lim et al. 2013; Steinbach et al. 1997; Streit et al. 1997). Here we asked whether biomechanics might regulate neural crest competence to the DLMZ. We addressed this idea in neural crest induction as this process is well-characterized (Aybar and Mayor 2002a; Mancilla and Mayor 1996; Mayor et al. 1995; Mayor and Theveneau 2014). In addition, we chose *Xenopus* embryos as a model since they are emendable to mechanical assays.

Our findings demonstrate that the loss of neural crest competence, as noted during gastrulation, results from increased hydrostatic pressure in the blastocoel cavity of *Xenopus* embryos. This increased hydrostatic pressure leads to cytoplasmic retention of Yap, which modulates Wnt activity in the responding ectoderm, a critical signaling pathway for neural crest induction (Curchoe et al.

2010; García-Castro et al. 2002; LaBonne and Bronner-Fraser 1998b; Steventon et al. 2009a).

The role of hydrostatic pressure in development and cell differentiation is a topic of growing interest, as it has been shown to play an essential role in lumen formation in zebrafish gut (Bagnat et al. 2007) and ear (Mosaliganti et al. 2019), in mammalian lungs (Palmer and Nelson 2020) and the blastocyst of mice (Chan and Hiiragi 2020a), in *Drosophila* oogenesis (Imran Alsous et al. 2021), as well as many others (Bagnat, Daga, and di Talia 2022). In *Xenopus,* blastocoel formation is dependent on the activity of the Na+/K+ ATPase (Slack and Warner 1973b), and it starts at the early segmentation stages and continues gradually until gastrulation (Keller 1975a). The blastocoel expands with a continuous fluid influx after the first division (2-cell stage). As in many systems, a change in osmotic pressure is proposed as the mechanism that leads to cell specifications. We demonstrate that the process of neural crest induction can be affected by modifying hydrostatic pressure independently from a change in osmolarity, stipulating that hydrostatic pressure is the main factor in regulating neural crest competence. Furthermore, we show that an increase in mechanical pressure inhibits neural crest induction supporting the notion that the cells sense changes in pressure rather than osmolarity.

Importantly, we observe that this change in hydrostatic pressure during morphogenesis and artificial mechanical assays does not affect the inducer tissue, the mesoderm, nor its ability to produce the key inductive signals to induce neural crest cell *Wnt8*. In addition, we show other processes during gastrulation, such as blastopore closure, are not affected. These observations suggest the specificity effect that hydrostatic pressure elicits during gastrulation on neural crest competence.

The explicit mechanisms by which hydrostatic pressure controls the differentiation outcome by remodeling tissues and regulating biochemical signals remain

elusive. Indeed we show that a change in hydrostatic pressure remodels the ectoderm in *Xenopus* embryos. Our findings *in vivo* and *in vitro* are consistent with previous observations that have shown that a change in cell packing, or cell density, can lead to a change in the activity of the Hippo pathway mediated by translocation of its mechanosensitive protein, Yap. Mechanistically, these previous observations show higher cell packing or cell density leads to cytoplasmic localization of Yap in cell cultures, whereas lower confluency and lower cell packing generate cells with nuclear Yap (Aragona et al. 2013; Biswas et al. 2021; Franklin et al. 2020; Gao et al. 2017; Jorge Barbazan et al. 2021; Varelas et al. 2010; Xia et al. 2019; Zhao et al. 2007). This change in mechanical cues leads to a change in the topography of tissues and translation of mechanical into biochemical signals – as well documented in Yap activity (Aragona et al. 2013). Furthermore, we show that the change in hydrostatic pressure during gastrulation regulates Yap activity, giving rise to the notion that Yap modulates the temporal ability of ectodermal cells to induce neural crest.

The interplay between Hippo/Yap and Wnt/β-catenin has previously been investigated in other systems where multiple mechanisms have been identified, however, often with contradictory outcomes (Azzolin et al. 2014b; Barry et al. 2013; Cai et al. 2010, 2015; Camargo et al. 2007; Gregorieff et al. 2015; Jiang et al. 2020). For instance, two independent groups demonstrated that Wnt-mediated intestinal tumorigenesis is abolished by deletion of Yap (Cai et al. 2015; Gregorieff et al. 2015), whereas other groups noted that Yap attenuation has a negligible effect on intestinal tumorigenesis (Azzolin et al. 2014a; Barry et al. 2013). Moreover, it was demonstrated that Yap inhibition (by deletion of *Sav*) and activation (by overexpression) are crucial for intestinal regeneration (Barry et al. 2013; Cai et al. 2010). Furthermore, in Wnt-driven cellular response, some studies found an increase in Yap target genes (Cai et al. 2015; Rosenbluh et al. 2012), whereas some have shown how Yap inhibits Wnt/β-catenin pathway by promoting the activation of β-catenin destruction complex (Azzolin et al. 2014a).

Our results are consistent with the notion that Yap interacts with the Wnt pathway and promotes its activity and this model is consistent with *in vitro* experiments showing that Yap is required for neural crest formation in human neural crest cells induced from pluripotent stem cells (iPSCs)(Hindley et al. 2016; Piccolo et al. 2022). Mechanistically, Hippo/Yap and Wnt/β-catenin interact at different levels (Oudhoff et al. 2016a). For example, Yap has been shown to interact with Dvl and not β-catenin destruction complex to regulate myogenesis (Sun et al. 2017). In addition, Yap interaction with β-catenin in the cytoplasm (Imajo et al. 2012) and the nucleus has been demonstrated, where this interaction activates tissue-specific gene program (Heallen et al. 2011; Rosenbluh et al. 2012). Moreover, Yap has been shown to interact with Disheveled and AXIN1 (Azzolin et al. 2014a; Barry et al. 2013; Varelas et al. 2010). Lastly, it was shown Yap stabilizes β-catenin and translocates it to promote target genes. Although we do not investigate in depth how Yap interacts with β-catenin, we show that Yap activation promotes Wnt activity and interacts with Wnt pathway downstream of β-catenin destruction complex. A possible mechanism how Hippo/Yap interacts with Wnt/β-catenin supported by our findings is either Yap is upstream of β-catenin (cytoplasmic interaction or stabilization into nucleus) or at level of β-catenin (as binding partner) to promote Wnt activity. Further investigation is required to determine how Yap is promoting Wnt target genes. The literature on how Yap interplay and modulate Wnt/β-catenin pathway is conflicting which adds additional layer of complexity in studying cellular response and function. However, this strengthen the notion that this interaction is system specific.

In the light of our finding and after examination of the possible interaction of Hippo/Yap and Wnt/β-catenin, we propose that at the competent stages, the highly loose ectodermal cells become more packed at the non-competent stages by a rise in hydrostatic pressure leading to an increase in cell density, yielding in cytoplasmic retention of Yap. Indeed, we observed a surge in cell packing during the rise in blastocoel hydrostatic pressure, which is consistent with

this idea. Indeed, the notion that an increase in cell packing will prevent the formation of neural crest cells was further supported by our *in vitro* data, where increased cell packing inhibits inducer neural crest cells. Furthermore, analysis of cell aspect ratio argues against cells being stretched during blastocoel expansion; this is likely since the embryo is constrained by the vitelline membrane, which does not allow an increase in embryo volume during blastocoel expansion. The observation that *Xenopus* and human neural crest competence depends on cell packing controlling Yap argues about the generality of this mechanism across species.

Nevertheless, further studies are necessary to fully establish the details of how Yap is mechanically controlled during the loss of neural crest competence, as many other physical inputs have also been described as regulators of Yap activity (Aragona et al. 2013; Biswas et al. 2021; Gao et al. 2017; Panciera et al. 2017; Xia et al. 2019). Indeed, although we show that an increase in hydrostatic pressure in the blastocoel cavity of *Xenopus* embryos leads to loss of neural crest competence, it is possible that in other embryos with different geometries, diverse mechanical cues also play a role in regulating competence. More broadly, we anticipate a general mechanism in which a wide range of mechanical stimuli could control Yap and other signaling pathways, modulating competence across different tissues, organs, and species.

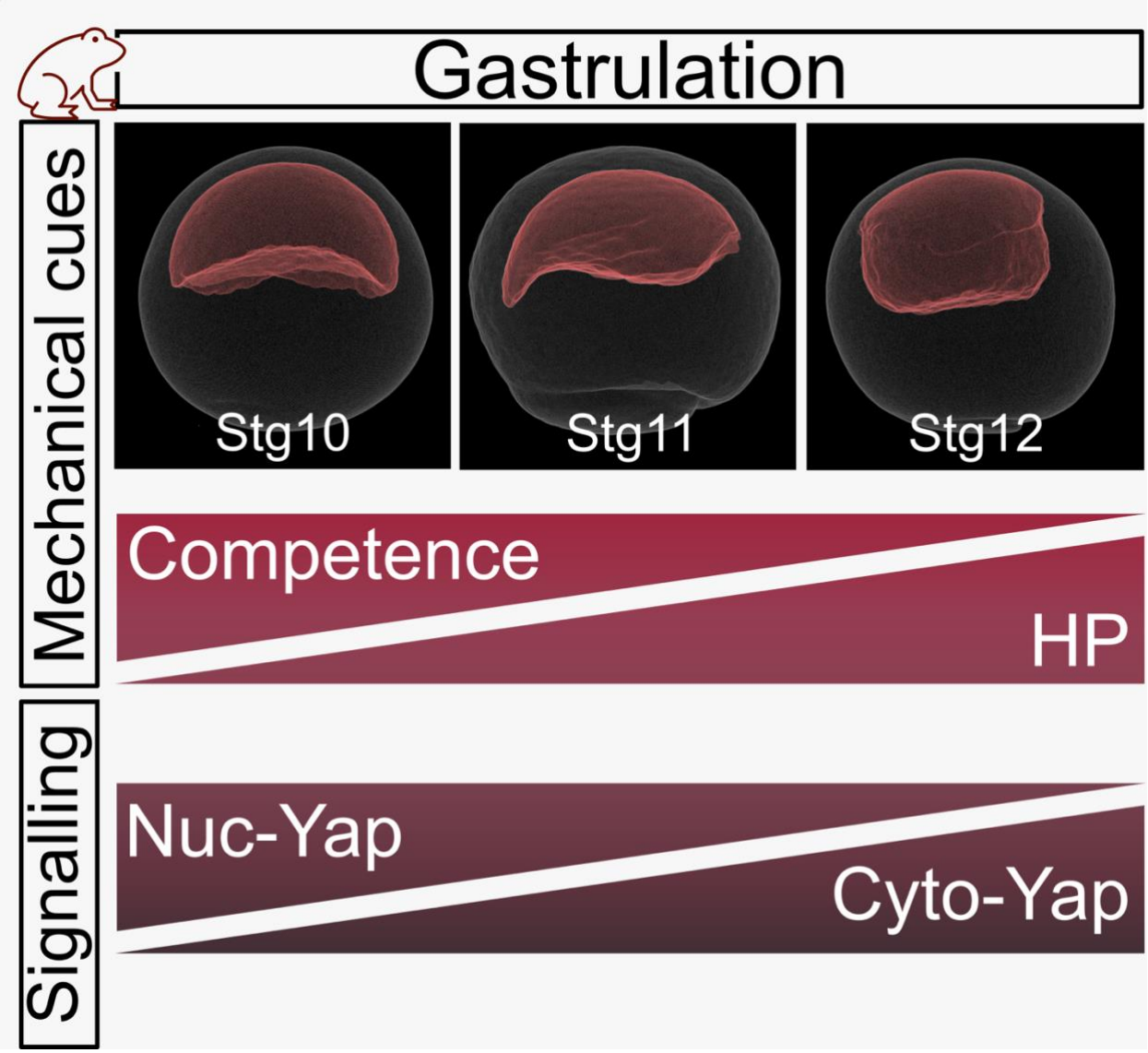

Fig. 6.1 | Graphical conclusion.

During gastrulation of *Xenopus* embryos, the hydrostatic pressure of the blastocoel cavity increases due to the increase of its volume. This increase leads to loss of neural crest induction competence. The mechanism of this loss is mediated by Yap translocation from nuclear to cytoplasm. These findings challenge the current dominant concept that development is genetically controlled and introduce a new model explaining a pivotal phase of embryonic development in which two independent developmental processes, blastocoel morphogenesis and neural crest induction, are linked via tissue mechanics.

Publications

- Delan N Alasaadi[1], Lucas Alvizi, Namid Stillman, Prachiti Moghe, Takashi Hiiragi, Roberto Mayor. Hydrostatic pressure regulates competence for neural crest induction. (in review).

- Elias H Barriga[1], Delan N Alasaadi[1], Chiara Mencarelli, Roberto Mayor, Franck Pichaud. RanBP1 plays an essential role in directed migration of neural crest cells during development. ***Dev Biol***, 2022.

Bibliography

Abu-Elmagd, Muhammad, Carla Garcia-Morales, and Grant N. Wheeler. 2006. 'Frizzled7 Mediates Canonical Wnt Signaling in Neural Crest Induction'. *Developmental Biology* 298(1):285–98. doi: 10.1016/j.ydbio.2006.06.037.

Abuwarda, Hamid, and Medha M. Pathak. 2020. 'Mechanobiology of Neural Development'. *Current Opinion in Cell Biology* 66:104–11. doi: 10.1016/j.ceb.2020.05.012.

Alvarez, Ignacio S., María Araujo, and M. Angela Nieto. 1998. 'Neural Induction in Whole Chick Embryo Cultures by FGF'. *Developmental Biology* 199(1):42–54. doi: 10.1006/dbio.1998.8903.

Amaya, Enrique, Thomas J. Musci, and Marc W. Kirschner. 1991. 'Expression of a Dominant Negative Mutant of the FGF Receptor Disrupts Mesoderm Formation in Xenopus Embryos'. *Cell* 66(2):257–70. doi: 10.1016/0092-8674(91)90616-7.

Anderson, Ryan M., Rolf W. Stottmann, Murim Choi, and John Klingensmith. 2006. 'Endogenous Bone Morphogenetic Protein Antagonists Regulate Mammalian Neural Crest Generation and Survival'. *Developmental Dynamics* 235(9):2507–20. doi: 10.1002/dvdy.20891.

Aragona, Mariaceleste, Tito Panciera, Andrea Manfrin, Stefano Giulitti, Federica Michielin, Nicola Elvassore, Sirio Dupont, and Stefano Piccolo. 2013. 'A Mechanical Checkpoint Controls Multicellular Growth through YAP/TAZ Regulation by Actin-Processing Factors'. *Cell* 154(5):1047–59. doi: 10.1016/j.cell.2013.07.042.

Ariizumi, Takashi, Tatsuo Michiue, and Makoto Asashima. 2017. 'In Vitro Induction of *Xenopus* Embryonic Organs Using Animal Cap Cells'. *Cold Spring Harbor Protocols* 2017(12):pdb.prot097410. doi: 10.1101/pdb.prot097410.

Asashima, M., H. Nakano, H. Uchiyama, M. Davids, S. Plessow, B. Loppnow-Blinde, P. Hoppe, H. Dau, and H. Tiedemann. 1990. 'The Vegetalizing Factor Belongs to a Family of Mesoderm-Inducing Proteins Related to Erythroid

Differentiation Factor'. *Naturwissenschaften* 77(8):389–91. doi: 10.1007/BF01135742.

Asashima, Makoto, and Horst Grunz. 1982. 'Effects of Inducers on Inner and Outer Gastrula Ectoderm Layers of Xenopus Laevis'. *Differentiation* 23(1–3):206–12. doi: 10.1111/j.1432-0436.1982.tb01284.x.

Asashima, Makoto, Hiroshi Nakano, Kazunori Shimada, Kei Kinoshita, Koichi Ishii, Hiroshiro Shibai, and Naoto Ueno. 1990. 'Mesodermal Induction in Early Amphibian Embryos by Activin A (Erythroid Differentiation Factor)'. *Roux's Archives of Developmental Biology* 198(6):330–35. doi: 10.1007/BF00383771.

Aybar, Manuel J., and Roberto Mayor. 2002a. 'Early Induction of Neural Crest Cells: Lessons Learned from Frog, Fish and Chick'. *Current Opinion in Genetics & Development* 12(4):452–58. doi: 10.1016/S0959-437X(02)00325-8.

Aybar, Manuel J., and Roberto Mayor. 2002b. 'Early Induction of Neural Crest Cells: Lessons Learned from Frog, Fish and Chick'. *Current Opinion in Genetics & Development* 12(4):452–58. doi: 10.1016/S0959-437X(02)00325-8.

Azzolin, Luca, Tito Panciera, Sandra Soligo, Elena Enzo, Silvio Bicciato, Sirio Dupont, Silvia Bresolin, Chiara Frasson, Giuseppe Basso, Vincenza Guzzardo, Ambrogio Fassina, Michelangelo Cordenonsi, and Stefano Piccolo. 2014a. 'YAP/TAZ Incorporation in the β-Catenin Destruction Complex Orchestrates the Wnt Response'. *Cell* 158(1):157–70. doi: 10.1016/j.cell.2014.06.013.

Azzolin, Luca, Tito Panciera, Sandra Soligo, Elena Enzo, Silvio Bicciato, Sirio Dupont, Silvia Bresolin, Chiara Frasson, Giuseppe Basso, Vincenza Guzzardo, Ambrogio Fassina, Michelangelo Cordenonsi, and Stefano Piccolo. 2014b. 'YAP/TAZ Incorporation in the β-Catenin Destruction Complex Orchestrates the Wnt Response'. *Cell* 158(1):157–70. doi: 10.1016/j.cell.2014.06.013.

Bae, Chang-Joon, Chang-Soo Hong, and Jean-Pierre Saint-Jeannet. 2018. 'Anosmin-1 Is Essential for Neural Crest and Cranial Placodes Formation in Xenopus'. *Biochemical and Biophysical Research Communications* 495(3):2257–63. doi: 10.1016/j.bbrc.2017.12.127.

Bagnat, Michel, Isla D. Cheung, Keith E. Mostov, and Didier Y. R. Stainier. 2007. 'Genetic Control of Single Lumen Formation in the Zebrafish Gut'. *Nature Cell Biology* 9(8):954–60. doi: 10.1038/ncb1621.

Bagnat, Michel, Bijoy Daga, and Stefano di Talia. 2022. 'Morphogenetic Roles of Hydrostatic Pressure in Animal Development'. *Annual Review of Cell and Developmental Biology* 38(1). doi: 10.1146/annurev-cellbio-120320-033250.

Baker, J. C., R. S. P. Beddington, and R. M. Harland. 1999. 'Wnt Signaling in Xenopus Embryos Inhibits Bmp4 Expression and Activates Neural Development'. *Genes & Development* 13(23):3149–59. doi: 10.1101/gad.13.23.3149.

Banliat, Charles, Coline Mahé, Régis Lavigne, Emmanuelle Com, Charles Pineau, Valérie Labas, Benoit Guyonnet, Pascal Mermillod, and Marie Saint-Dizier. 2022. 'The Proteomic Analysis of Bovine Embryos Developed in Vivo or in Vitro Reveals the Contribution of the Maternal Environment to Early Embryo'. *BMC Genomics* 23(1):839. doi: 10.1186/s12864-022-09076-5.

Barriga, Elias H., Kristian Franze, Guillaume Charras, and Roberto Mayor. 2018. 'Tissue Stiffening Coordinates Morphogenesis by Triggering Collective Cell Migration in Vivo'. *Nature* 554(7693). doi: 10.1038/nature25742.

Barriga, Elias H., Adam Shellard, and Roberto Mayor. 2019. 'In Vivo and In Vitro Quantitative Analysis of Neural Crest Cell Migration'. Pp. 135–52 in.

Barry, Evan R., Teppei Morikawa, Brian L. Butler, Kriti Shrestha, Rosemarie de la Rosa, Kelley S. Yan, Charles S. Fuchs, Scott T. Magness, Ron Smits, Shuji Ogino, Calvin J. Kuo, and Fernando D. Camargo. 2013. 'Restriction of Intestinal Stem Cell Expansion and the Regenerative Response by YAP'. *Nature* 493(7430):106–10. doi: 10.1038/nature11693.

Barth, K. A., Y. Kishimoto, K. B. Rohr, C. Seydler, S. Schulte-Merker, and S. W. Wilson. 1999. 'Bmp Activity Establishes a Gradient of Positional Information throughout the Entire Neural Plate'. *Development* 126(22):4977–87. doi: 10.1242/dev.126.22.4977.

Barua, Debanjan, Serge E. Parent, and Rudolf Winklbauer. 2017. 'Mechanics of Fluid-Filled Interstitial Gaps. II. Gap Characteristics in Xenopus Embryonic Ectoderm'. *Biophysical Journal* 113(4):923–36. doi: 10.1016/j.bpj.2017.06.063.

Basch, Martín L., Marianne Bronner-Fraser, and Martín I. García-Castro. 2006. 'Specification of the Neural Crest Occurs during Gastrulation and Requires Pax7'. *Nature* 441(7090). doi: 10.1038/nature04684.

Beddington, R. S. 1994. 'Induction of a Second Neural Axis by the Mouse Node'. *Development* 120(3):613–20. doi: 10.1242/dev.120.3.613.

Bénazéraf, Bertrand, Mathias Beaupeux, Martin Tchernookov, Allison Wallingford, Tasha Salisbury, Amelia Shirtz, Andrew Shirtz, David Huss, Olivier Pourquié, Paul François, and Rusty Lansford. 2017. 'Multiscale Quantification of Tissue Behavior during Amniote Embryo Axis Elongation'. *Development*. doi: 10.1242/dev.150557.

Betancur, Paola, Marianne Bronner-Fraser, and Tatjana Sauka-Spengler. 2010. 'Genomic Code for *Sox10* Activation Reveals a Key Regulatory Enhancer for Cranial Neural Crest'. *Proceedings of the National Academy of Sciences* 107(8). doi: 10.1073/pnas.0906596107.

Betters, Erin, Ying Liu, Anders Kjaeldgaard, Erik Sundström, and Martín I. García-Castro. 2010. 'Analysis of Early Human Neural Crest Development'. *Developmental Biology* 344(2):578–92. doi: 10.1016/j.ydbio.2010.05.012.

Biswas, Ritusree, Avinanda Banerjee, Sergio Lembo, Zhihai Zhao, Vairavan Lakshmanan, Ryan Lim, Shimin Le, Manando Nakasaki, Vassily Kutyavin, Graham Wright, Dasaradhi Palakodeti, Robert S. Ross, Colin Jamora, Valeri Vasioukhin, Yan Jie, and Srikala Raghavan. 2021. 'Mechanical Instability of Adherens Junctions Overrides Intrinsic Quiescence of Hair Follicle Stem Cells'. *Developmental Cell* 56(6):761-780.e7. doi: 10.1016/j.devcel.2021.02.020.

Borday, Caroline, Karine Parain, Hong Thi Tran, Kris Vleminckx, Muriel Perron, and Anne H. Monsoro-Burq. 2018a. 'An Atlas of Wnt Activity during

Embryogenesis in Xenopus Tropicalis'. *PLOS ONE* 13(4):e0193606. doi: 10.1371/journal.pone.0193606.

Borday, Caroline, Karine Parain, Hong Thi Tran, Kris Vleminckx, Muriel Perron, and Anne H. Monsoro-Burq. 2018b. 'An Atlas of Wnt Activity during Embryogenesis in Xenopus Tropicalis'. *PLOS ONE* 13(4):e0193606. doi: 10.1371/journal.pone.0193606.

Boterenbrood, E. C., and P. D. Nieuwkoop. 1973. 'The Formation of the Mesoderm in Urodelean Amphibians : V. Its Regional Induction by the Endoderm.' *Wilhelm Roux Arch Entwickl Mech Org*.

Browne, E. N. 1909. 'The Production of New Hydranths in Hydra by the Insertion of Small Grafts'. *Journal of Experimental Zoology* 7:1–37.

Buske, Peter, Jens Przybilla, Markus Loeffler, Norman Sachs, Toshiro Sato, Hans Clevers, and Joerg Galle. 2012. 'On the Biomechanics of Stem Cell Niche Formation in the Gut - Modelling Growing Organoids'. *FEBS Journal* 279(18):3475–87. doi: 10.1111/j.1742-4658.2012.08646.x.

Byers, T. J., and P. B. Armstrong. 1986. 'Membrane Protein Redistribution during Xenopus First Cleavage.' *The Journal of Cell Biology* 102(6):2176–84. doi: 10.1083/jcb.102.6.2176.

Cai, Jing, Anirban Maitra, Robert A. Anders, Makoto M. Taketo, and Duojia Pan. 2015. 'β-Catenin Destruction Complex-Independent Regulation of Hippo–YAP Signaling by APC in Intestinal Tumorigenesis'. *Genes & Development* 29(14):1493–1506. doi: 10.1101/gad.264515.115.

Cai, Jing, Nailing Zhang, Yonggang Zheng, Roeland F. de Wilde, Anirban Maitra, and Duojia Pan. 2010. 'The Hippo Signaling Pathway Restricts the Oncogenic Potential of an Intestinal Regeneration Program'. *Genes & Development* 24(21):2383–88. doi: 10.1101/gad.1978810.

Camargo, Fernando D., Sumita Gokhale, Jonathan B. Johnnidis, Dongdong Fu, George W. Bell, Rudolf Jaenisch, and Thijn R. Brummelkamp. 2007. 'YAP1 Increases Organ Size and Expands Undifferentiated Progenitor Cells'. *Current Biology* 17(23):2054–60. doi: 10.1016/j.cub.2007.10.039.

Canales Coutiño, Brenda, and Roberto Mayor. 2021a. 'Mechanosensitive Ion Channels in Cell Migration'. *Cells & Development* 166. doi: 10.1016/j.cdev.2021.203683.

Canales Coutiño, Brenda, and Roberto Mayor. 2021b. 'The Mechanosensitive Channel Piezo1 Cooperates with Semaphorins to Control Neural Crest Migration'. *Development* 148(23). doi: 10.1242/dev.200001.

Cao, Xinwei, Samuel L. Pfaff, and Fred H. Gage. 2008. 'YAP Regulates Neural Progenitor Cell Number via the TEA Domain Transcription Factor'. *Genes & Development* 22(23):3320–34. doi: 10.1101/gad.1726608.

Carmona-Fontaine, Carlos, Gustavo Acuña, Kristina Ellwanger, Christof Niehrs, and Roberto Mayor. 2007. 'Neural Crests Are Actively Precluded from the Anterior Neural Fold by a Novel Inhibitory Mechanism Dependent on Dickkopf1 Secreted by the Prechordal Mesoderm'. *Developmental Biology* 309(2):208–21. doi: 10.1016/j.ydbio.2007.07.006.

Chalmers, Andrew D., Bernhard Strauss, and Nancy Papalopulu. 2003. 'Oriented Cell Divisions Asymmetrically Segregate APKC and Generate Cell Fate Diversity in the Early *Xenopus* Embryo'. *Development* 130(12):2657–68. doi: 10.1242/dev.00490.

Chan, Chii J., and Takashi Hiiragi. 2020a. 'Integration of Luminal Pressure and Signalling in Tissue Self-Organization'. *Development* 147(5). doi: 10.1242/dev.181297.

Chan, Chii J., and Takashi Hiiragi. 2020b. 'Integration of Luminal Pressure and Signalling in Tissue Self-Organization'. *Development* 147(5). doi: 10.1242/dev.181297.

Chan, Chii Jou, Maria Costanzo, Teresa Ruiz-Herrero, Gregor Mönke, Ryan J. Petrie, Martin Bergert, Alba Diz-Muñoz, L. Mahadevan, and Takashi Hiiragi. 2019. 'Hydraulic Control of Mammalian Embryo Size and Cell Fate'. *Nature* 571(7763). doi: 10.1038/s41586-019-1309-x.

Chang, Chenbei, and Ali Hemmati-Brivanlou. 1998. 'Neural Crest Induction by Xwnt7B in Xenopus'. *Developmental Biology* 194(1):129–34. doi: 10.1006/dbio.1997.8820.

Cho, Sangkyun, Manasvita Vashisth, Amal Abbas, Stephanie Majkut, Kenneth Vogel, Yuntao Xia, Irena L. Ivanovska, Jerome Irianto, Manorama Tewari, Kuangzheng Zhu, Elisia D. Tichy, Foteini Mourkioti, Hsin-Yao Tang, Roger A. Greenberg, Benjamin L. Prosser, and Dennis E. Discher. 2019. 'Mechanosensing by the Lamina Protects against Nuclear Rupture, DNA Damage, and Cell-Cycle Arrest'. *Developmental Cell* 49(6):920-935.e5. doi: 10.1016/j.devcel.2019.04.020.

Christian, J. L., J. A. McMahon, A. P. McMahon, and R. T. Moon. 1991. 'Xwnt-8, a Xenopus Wnt-1/Int-1-Related Gene Responsive to Mesoderm-Inducing Growth Factors, May Play a Role in Ventral Mesodermal Patterning during Embryogenesis'. *Development* 111(4):1045–55. doi: 10.1242/dev.111.4.1045.

Christian, J. L., D. J. Olson, and R. T. Moon. 1992. 'Xwnt-8 Modifies the Character of Mesoderm Induced by BFGF in Isolated Xenopus Ectoderm.' *The EMBO Journal* 11(1):33–41. doi: 10.1002/j.1460-2075.1992.tb05024.x.

Conlon, F. L., K. S. Barth, and E. J. Robertson. 1991. 'A Novel Retrovirally Induced Embryonic Lethal Mutation in the Mouse: Assessment of the Developmental Fate of Embryonic Stem Cells Homozygous for the 413.d Proviral Integration'. *Development* 111(4):969–81. doi: 10.1242/dev.111.4.969.

Cox, W. G., and A. Hemmati-Brivanlou. 1995. 'Caudalization of Neural Fate by Tissue Recombination and BFGF'. *Development* 121(12):4349–58. doi: 10.1242/dev.121.12.4349.

Crunz, Horst. 1997. 'Neural Induction in Amphibians'. Pp. 191–228 in.

Cselenyi, Christopher S., Kristin K. Jernigan, Emilios Tahinci, Curtis A. Thorne, Laura A. Lee, and Ethan Lee. 2008. 'LRP6 Transduces a Canonical Wnt Signal Independently of Axin Degradation by Inhibiting GSK3's Phosphorylation of β-Catenin'. *Proceedings of the National Academy of Sciences* 105(23):8032–37. doi: 10.1073/pnas.0803025105.

Curchoe, Carol Lynn, Jochen Maurer, Sonja J. McKeown, Giulio Cattarossi, Flavio Cimadamore, Mats Nilbratt, Evan Y. Snyder, Marianne Bronner-Fraser, and Alexey v. Terskikh. 2010. 'Early Acquisition of Neural Crest Competence During HESCs Neuralization'. *PLoS ONE* 5(11):e13890. doi: 10.1371/journal.pone.0013890.

Dale, L., G. Howes, B. M. Price, and J. C. Smith. 1992. 'Bone Morphogenetic Protein 4: A Ventralizing Factor in Early Xenopus Development'. *Development* 115(2):573–85. doi: 10.1242/dev.115.2.573.

Dale, L., G. Matthews, L. Tabe, and A. Colman. 1989. 'Developmental Expression of the Protein Product of Vg1, a Localized Maternal MRNA in the Frog Xenopus Laevis.' *The EMBO Journal* 8(4):1057–65. doi: 10.1002/j.1460-2075.1989.tb03473.x.

Dale, L., and J. M. Slack. 1987. 'Regional Specification within the Mesoderm of Early Embryos of Xenopus Laevis'. *Development* 100(2):279–95. doi: 10.1242/dev.100.2.279.

Dale, L., J. C. Smith, and J. M. Slack. 1985. 'Mesoderm Induction in Xenopus Laevis: A Quantitative Study Using a Cell Lineage Label and Tissue-Specific Antibodies.' *Journal of Embryology and Experimental Morphology* 89:289–312.

DAN, KATSUMA. 1952. 'CYTO-EMBRYOLOGICAL STUDIES OF SEA URCHINS. II. BLASTULA STAGE'. *The Biological Bulletin* 102(1):74–89. doi: 10.2307/1538625.

De, Antara. 2011. 'Wnt/Ca≪Sup≫2+≪/Sup≫ Signaling Pathway: A Brief Overview'. *Acta Biochimica et Biophysica Sinica* 43(10):745–56. doi: 10.1093/abbs/gmr079.

Deardorff, Matthew A., Change Tan, Jean-Pierre Saint-Jeannet, and Peter S. Klein. 2001. 'A Role for Frizzled 3 in Neural Crest Development'. *Development* 128(19):3655–63. doi: 10.1242/dev.128.19.3655.

Delaune, Emilie, Patrick Lemaire, and Laurent Kodjabachian. 2005. 'Neural Induction in *Xenopus* Requires Early FGF Signalling in Addition to BMP Inhibition'. *Development* 132(2):299–310. doi: 10.1242/dev.01582.

Deng, Yaqi, Lai Man Natalie Wu, Shujun Bai, Chuntao Zhao, Haibo Wang, Jincheng Wang, Lingli Xu, Masahide Sakabe, Wenhao Zhou, Mei Xin, and Q. Richard Lu. 2017. 'A Reciprocal Regulatory Loop between TAZ/YAP and G-Protein Gas Regulates Schwann Cell Proliferation and Myelination'. *Nature Communications* 8(1):15161. doi: 10.1038/ncomms15161.

Dias, Mark S., and Gary C. Schoenwolf. 1990. 'Formation of Ectopic Neurepithelium in Chick Blastoderms: Age-Related Capacities for Induction and Self-Differentiation Following Transplantation of Quail Hensen's Nodes'. *The Anatomical Record* 228(4):437–48. doi: 10.1002/ar.1092280410.

Domingos, Pedro M., Nobue Itasaki, C. Michael Jones, Sara Mercurio, Michael G. Sargent, James C. Smith, and Robb Krumlauf. 2001. 'The Wnt/β-Catenin Pathway Posteriorizes Neural Tissue in Xenopus by an Indirect Mechanism Requiring FGF Signalling'. *Developmental Biology* 239(1):148–60. doi: 10.1006/dbio.2001.0431.

Dumortier, Julien G., Mathieu Le Verge-Serandour, Anna Francesca Tortorelli, Annette Mielke, Ludmilla de Plater, Hervé Turlier, and Jean-Léon Maître. 2019. 'Hydraulic Fracturing and Active Coarsening Position the Lumen of the Mouse Blastocyst'. *Science* 365(6452):465–68. doi: 10.1126/science.aaw7709.

Dupont, Sirio, Leonardo Morsut, Mariaceleste Aragona, Elena Enzo, Stefano Giulitti, Michelangelo Cordenonsi, Francesca Zanconato, Jimmy Le Digabel, Mattia Forcato, Silvio Bicciato, Nicola Elvassore, and Stefano Piccolo. 2011. 'Role of YAP/TAZ in Mechanotransduction'. *Nature* 474(7350):179–83. doi: 10.1038/nature10137.

van den Eijnden-Van Raaij, A. J. M., E. J. J. van Zoelent, K. van Nimmen, C. H. Koster, G. T. Snoek, A. J. Durston, and D. Huylebroeck. 1990. 'Activin-like Factor from a Xenopus Laevis Cell Line Responsible for Mesoderm Induction'. *Nature* 345(6277):732–34. doi: 10.1038/345732a0.

Elkouby, Yaniv M., Sarah Elias, Elena S. Casey, Shelby A. Blythe, Nir Tsabar, Peter S. Klein, Heather Root, Karen J. Liu, and Dale Frank. 2010. 'Mesodermal Wnt

Signaling Organizes the Neural Plate via Meis3'. *Development* 137(9). doi: 10.1242/dev.044750.

Engler, Adam J., Shamik Sen, H. Lee Sweeney, and Dennis E. Discher. 2006. 'Matrix Elasticity Directs Stem Cell Lineage Specification'. *Cell* 126(4):677–89. doi: 10.1016/j.cell.2006.06.044.

Esmaeili, Melody, Shelby A. Blythe, John W. Tobias, Kai Zhang, Jing Yang, and Peter S. Klein. 2020a. 'Chromatin Accessibility and Histone Acetylation in the Regulation of Competence in Early Development'. *Developmental Biology* 462(1):20–35. doi: 10.1016/j.ydbio.2020.02.013.

Esmaeili, Melody, Shelby A. Blythe, John W. Tobias, Kai Zhang, Jing Yang, and Peter S. Klein. 2020b. 'Chromatin Accessibility and Histone Acetylation in the Regulation of Competence in Early Development'. *Developmental Biology* 462(1):20–35. doi: 10.1016/j.ydbio.2020.02.013.

Faure, Sandrine, and Philippe Fort. 2011. 'Atypical RhoV and RhoU GTPases Control Development of the Neural Crest'. *Small GTPases* 2(6):310–13. doi: 10.4161/sgtp.18086.

Fleming, Tom P., Tom Papenbrock, Irina Fesenko, Peter Hausen, and Bhavwanti Sheth. 2000. 'Assembly of Tight Junctions during Early Vertebrate Development'. *Seminars in Cell & Developmental Biology* 11(4):291–99. doi: 10.1006/scdb.2000.0179.

Frankenberg, Stephen. 2018. 'Pre-Gastrula Development of Non-Eutherian Mammals'. Pp. 237–66 in.

Franklin, J. Matthew, Rajarshi P. Ghosh, Quanming Shi, Michael P. Reddick, and Jan T. Liphardt. 2020. 'Concerted Localization-Resets Precede YAP-Dependent Transcription'. *Nature Communications* 11(1):4581. doi: 10.1038/s41467-020-18368-x.

Friesel, R., and I. B. Dawid. 1991. 'CDNA Cloning and Developmental Expression of Fibroblast Growth Factor Receptors from Xenopus Laevis'. *Molecular and Cellular Biology* 11(5):2481–88. doi: 10.1128/mcb.11.5.2481-2488.1991.

Gallera, J. 1977. 'L'expansion Périphérique Du Blastoderme et La Formation de l'aire Vasculaire Chez l'embryon Du Poulet'. *Revue Suisse de Zoologie*. 84:301–8. doi: 10.5962/bhl.part.91388.

Gao, Jing, Lingli He, Yan Shi, Mingjun Cai, Haijiao Xu, Junguang Jiang, Lei Zhang, and Hongda Wang. 2017. 'Cell Contact and Pressure Control of YAP Localization and Clustering Revealed by Super-Resolution Imaging'. *Nanoscale* 9(43):16993–3. doi: 10.1039/C7NR05818G.

García-Castro, Martín I., Christophe Marcelle, and Marianne Bronner-Fraser. 2002. 'Ectodermal Wnt Function as a Neural Crest Inducer'. *Science* 297(5582):848–51. doi: 10.1126/science.1070824.

Gee, Stephen T., Sharon L. Milgram, Kenneth L. Kramer, Frank L. Conlon, and Sally A. Moody. 2011. 'Yes-Associated Protein 65 (YAP) Expands Neural Progenitors and Regulates Pax3 Expression in the Neural Plate Border Zone'. *PLoS ONE* 6(6):e20309. doi: 10.1371/journal.pone.0020309.

Gillespie, L. L., G. D. Paterno, and J. M. Slack. 1989a. 'Analysis of Competence: Receptors for Fibroblast Growth Factor in Early Xenopus Embryos'. *Development* 106(1):203–8. doi: 10.1242/dev.106.1.203.

Gillespie, L. L., G. D. Paterno, and J. M. Slack. 1989b. 'Analysis of Competence: Receptors for Fibroblast Growth Factor in Early Xenopus Embryos'. *Development* 106(1):203–8. doi: 10.1242/dev.106.1.203.

Gimlich, Robert L., and Jonathan Cooke. 1983. 'Cell Lineage and the Induction of Second Nervous Systems in Amphibian Development'. *Nature* 306(5942):471–73. doi: 10.1038/306471a0.

Glavic, Alvaro, Francisca Silva, Manuel J. Aybar, Francisco Bastidas, and Roberto Mayor. 2004. 'Interplay between Notch Signaling and the Homeoprotein *Xiro1* Is Required for Neural Crest Induction in *Xenopus* Embryos'. *Development* 131(2). doi: 10.1242/dev.00945.

Godsave, S. F., and A. J. Durston. 1997. 'Neural Induction and Patterning in Embryos Deficient in FGF Signaling.' *The International Journal of Developmental Biology* 41(1):57–65.

Godsave, Susan F., and Robert A. Shiurba. 1992. 'Xenopus Blastulae Show Regional Differences in Competence for Mesoderm Induction: Correlation with Endogenous Basic Fibroblast Growth Factor Levels'. *Developmental Biology* 151(2):506–15. doi: 10.1016/0012-1606(92)90189-N.

Graff, Jonathan M., R. Scott Thies, Jeffrey J. Song, Anthony J. Celeste, and Douglas A. Melton. 1994. 'Studies with a Xenopus BMP Receptor Suggest That Ventral Mesoderm-Inducing Signals Override Dorsal Signals in Vivo'. *Cell* 79(1):169–79. doi: 10.1016/0092-8674(94)90409-X.

Green, Jeremy. 1999. 'The Animal Cap Assay'. Pp. 1–14 in *Molecular Methods in Developmental Biology*. Vol. 127. New Jersey: Humana Press.

Green, Jeremy B. A., and J. C. Smith. 1990. 'Graded Changes in Dose of a Xenopus Activin A Homologue Elicit Stepwise Transitions in Embryonic Cell Fate'. *Nature* 347(6291):391–94. doi: 10.1038/347391a0.

Gregorieff, Alex, Yu Liu, Mohammad R. Inanlou, Yuliya Khomchuk, and Jeffrey L. Wrana. 2015. 'Yap-Dependent Reprogramming of Lgr5+ Stem Cells Drives Intestinal Regeneration and Cancer'. *Nature* 526(7575):715–18. doi: 10.1038/nature15382.

Groves, Andrew K., and Carole LaBonne. 2014. 'Setting Appropriate Boundaries: Fate, Patterning and Competence at the Neural Plate Border'. *Developmental Biology* 389(1):2–12. doi: 10.1016/j.ydbio.2013.11.027.

Grunz H. 1970. 'Abhangigkeit Der Kompetenz Des Amphibien-Ektoderms von Der Proteinsynthese.' *Wilhelm Roux' Arch. EntwMech. Org.* 165:91–102.

Grunz, Horst. 1992. 'Suramin Changes the Fate of Spemann's Organizer and Prevents Neural Induction in Xenopus Laevis'. *Mechanisms of Development* 38(2):133–41. doi: 10.1016/0925-4773(92)90005-5.

Guémar, Linda, Pascal de Santa Barbara, Emmanuel Vignal, Benjamin Maurel, Philippe Fort, and Sandrine Faure. 2007. 'The Small GTPase RhoV Is an Essential Regulator of Neural Crest Induction in Xenopus'. *Developmental Biology* 310(1):113–28. doi: 10.1016/j.ydbio.2007.07.031.

Guillermin, Oriane, Nikolaos Angelis, Clara M. Sidor, Rachel Ridgway, Anna Baulies, Anna Kucharska, Pedro Antas, Melissa R. Rose, Julia Cordero, Owen Sansom, Vivian S. W. Li, and Barry J. Thompson. 2021. 'Wnt and Src Signals Converge on YAP-TEAD to Drive Intestinal Regeneration'. *The EMBO Journal* 40(13). doi: 10.15252/embj.2020105770.

Gurdon, J. B. 1987. 'Embryonic Induction — Molecular Prospects'. *Development* 99(3):285–306. doi: 10.1242/dev.99.3.285.

Halder, Georg, Sirio Dupont, and Stefano Piccolo. 2012. 'Transduction of Mechanical and Cytoskeletal Cues by YAP and TAZ'. *Nature Reviews Molecular Cell Biology* 13(9):591–600. doi: 10.1038/nrm3416.

Hall, Brian K. 2008. 'The Neural Crest and Neural Crest Cells: Discovery and Significance for Theories of Embryonic Organization'. *Journal of Biosciences* 33(5):781–93. doi: 10.1007/s12038-008-0098-4.

Hannezo, Edouard, and Carl-Philipp Heisenberg. 2022. 'Rigidity Transitions in Development and Disease'. *Trends in Cell Biology* 32(5):433–44. doi: 10.1016/j.tcb.2021.12.006.

Heallen, Todd, Min Zhang, Jun Wang, Margarita Bonilla-Claudio, Ela Klysik, Randy L. Johnson, and James F. Martin. 2011. 'Hippo Pathway Inhibits Wnt Signaling to Restrain Cardiomyocyte Proliferation and Heart Size'. *Science* 332(6028):458–61. doi: 10.1126/science.1199010.

Hemmati-Brivanlou, Ali, and Douglas A. Melton. 1994. 'Inhibition of Activin Receptor Signaling Promotes Neuralization in Xenopus'. *Cell* 77(2):273–81. doi: 10.1016/0092-8674(94)90319-0.

Henig, Clara, Sarah Elias, and Dale Frank. 1998. 'A POU Protein Regulates Mesodermal Competence to FGF in Xenopus'. *Mechanisms of Development* 71(1–2):131–42. doi: 10.1016/S0925-4773(98)00006-9.

Hensen, V. 1876. 'Beobachtungen Über Die Befruchtung Und Entwicklung Des Kaninchens Und Meerschweinchens'. *Z. Anat. EntwGesch.* 1:353–423.

Hindley, Christopher J., Alexandra Larisa Condurat, Vishal Menon, Ria Thomas, Luis M. Azmitia, Jason A. Davis, and Jan Pruszak. 2016. 'The Hippo Pathway

Member YAP Enhances Human Neural Crest Cell Fate and Migration'. *Scientific Reports* 6(1):23208. doi: 10.1038/srep23208.

Holowacz, Tamara, and Sergei Sokol. 1999. 'FGF Is Required for Posterior Neural Patterning but Not for Neural Induction'. *Developmental Biology* 205(2):296–308. doi: 10.1006/dbio.1998.9108.

Holtzer, H. 1968. 'Induction of Chondrogenesis: A Concept in Terms of Mechanisms.' *Williams & Wilkins* 152–64.

Hong, Chang-Soo, and Jean-Pierre Saint-Jeannet. 2007. 'The Activity of Pax3 and Zic1 Regulates Three Distinct Cell Fates at the Neural Plate Border'. *Molecular Biology of the Cell* 18(6). doi: 10.1091/mbc.e06-11-1047.

Honoré, Stella M., Manuel J. Aybar, and Roberto Mayor. 2003. 'Sox10 Is Required for the Early Development of the Prospective Neural Crest in Xenopus Embryos'. *Developmental Biology* 260(1). doi: 10.1016/S0012-1606(03)00247-1.

Huang, Jianbin, Shian Wu, Jose Barrera, Krista Matthews, and Duojia Pan. 2005. 'The Hippo Signaling Pathway Coordinately Regulates Cell Proliferation and Apoptosis by Inactivating Yorkie, the Drosophila Homolog of YAP'. *Cell* 122(3):421–34. doi: 10.1016/j.cell.2005.06.007.

Humphries, Ashley Ceinwen, and Marek Mlodzik. 2018. 'From Instruction to Output: Wnt/PCP Signaling in Development and Cancer'. *Current Opinion in Cell Biology* 51:110–16. doi: 10.1016/j.ceb.2017.12.005.

Imajo, Masamichi, Koichi Miyatake, Akira Iimura, Atsumu Miyamoto, and Eisuke Nishida. 2012. 'A Molecular Mechanism That Links Hippo Signalling to the Inhibition of Wnt/β-Catenin Signalling'. *The EMBO Journal* 31(5):1109–22. doi: 10.1038/emboj.2011.487.

Imran Alsous, Jasmin, Nicolas Romeo, Jonathan A. Jackson, Frank M. Mason, Jörn Dunkel, and Adam C. Martin. 2021. 'Dynamics of Hydraulic and Contractile Wave-Mediated Fluid Transport during *Drosophila* Oogenesis'. *Proceedings of the National Academy of Sciences* 118(10). doi: 10.1073/pnas.2019749118.

Isaacs, H. V., D. Tannahill, and J. M. Slack. 1992. 'Expression of a Novel FGF in the Xenopus Embryo. A New Candidate Inducing Factor for Mesoderm Formation and Anteroposterior Specification'. *Development* 114(3):711–20. doi: 10.1242/dev.114.3.711.

Itza, Erin M., and Nancy M. Mozingo. 2005. 'Septate Junctions Mediate the Barrier to Paracellular Permeability in Sea Urchin Embryos'. *Zygote* 13(3):255–64. doi: 10.1017/S096719940500328X.

Jensen, Pernille Linnert, Marie Louise Grøndahl, Hans Christian Beck, Jørgen Petersen, Lotte Stroebech, Søren Tvorup Christensen, and Claus Yding Andersen. 2014. 'Proteomic Analysis of Bovine Blastocoel Fluid and Blastocyst Cells'. *Systems Biology in Reproductive Medicine* 60(3):127–35. doi: 10.3109/19396368.2014.894152.

Ji, Yu, Hongyan Hao, Kurt Reynolds, Moira McMahon, and Chengji J. Zhou. 2019. 'Wnt Signaling in Neural Crest Ontogenesis and Oncogenesis'. *Cells* 8(10). doi: 10.3390/cells8101173.

Jiang, Liya, Juan Li, Chenxing Zhang, Yufeng Shang, and Jun Lin. 2020. 'YAP-mediated Crosstalk between the Wnt and Hippo Signaling Pathways (Review'. *Molecular Medicine Reports*. doi: 10.3892/mmr.2020.11529.

Jonas, E., T. D. Sargent, and I. B. Dawid. 1985. 'Epidermal Keratin Gene Expressed in Embryos of Xenopus Laevis.' *Proceedings of the National Academy of Sciences* 82(16):5413–17. doi: 10.1073/pnas.82.16.5413.

Jorge Barbazan, Carlos Pérez-González, Manuel Gómez-González, Mathieu Dedenon, Sophie Richon, Ernest Latorre, Marco Serra, Pascale Mariani, Stéphanie Descroix, Pierre Sens, Xavier Trepat, and Danijela Matic Vignjevic. 2021. 'Cancer-Associated Fibroblasts Actively Compress Cancer Cells and Modulate Mechanotransduction'. *BioRxiv*.

Joshi, Pradeep M., and Joel H. Rothman. 2005. 'Nematode Gastrulation: Having a BLASTocoel!' *Current Biology* 15(13):R495–98. doi: 10.1016/j.cub.2005.06.030.

Kalt, Marvin R. 1971a. 'The Relationship between Cleavage and Blastocoel Formation in Xenopus Laevis I'. *Development* 26(1):51–66. doi: 10.1242/dev.26.1.51.

Kalt, Marvin R. 1971b. 'The Relationship between Cleavage and Blastocoel Formation in Xenopus Laevis II'. *Development* 26(1):51–66. doi: 10.1242/dev.26.1.51.

Keller, Raymond E. 1975a. 'Vital Dye Mapping of the Gastrula and Neurula of Xenopus Laevis'. *Developmental Biology* 42(2):222–41. doi: 10.1016/0012-1606(75)90331-0.

Keller, Raymond E. 1975b. 'Vital Dye Mapping of the Gastrula and Neurula of Xenopus Laevis'. *Developmental Biology* 42(2):222–41. doi: 10.1016/0012-1606(75)90331-0.

Kelsh, Robert N., Kirsten Dutton, Joanne Medlin, and Judith S. Eisen. 2000. 'Expression of Zebrafish Fkd6 in Neural Crest-Derived Glia'. *Mechanisms of Development* 93(1–2):161–64. doi: 10.1016/S0925-4773(00)00250-1.

Kemppainen, Kati, Nina Wentus, Taru Lassila, Asta Laiho, and Kid Törnquist. 2016. 'Sphingosylphosphorylcholine Regulates the Hippo Signaling Pathway in a Dual Manner'. *Cellular Signalling* 28(12):1894–1903. doi: 10.1016/j.cellsig.2016.09.004.

Kengaku, M., and H. Okamoto. 1993. 'Basic Fibroblast Growth Factor Induces Differentiation of Neural Tube and Neural Crest Lineages of Cultured Ectoderm Cells from Xenopus Gastrula'. *Development* 119(4):1067–78. doi: 10.1242/dev.119.4.1067.

Kessler, D. S., and D. A. Melton. 1995. 'Induction of Dorsal Mesoderm by Soluble, Mature Vg1 Protein'. *Development* 121(7):2155–64. doi: 10.1242/dev.121.7.2155.

Khokha, Mustafa K., Joanna Yeh, Timothy C. Grammer, and Richard M. Harland. 2005. 'Depletion of Three BMP Antagonists from Spemann's Organizer Leads to a Catastrophic Loss of Dorsal Structures'. *Developmental Cell* 8(3):401–11. doi: 10.1016/j.devcel.2005.01.013.

Khudyakov, Jane, and Marianne Bronner-Fraser. 2009. 'Comprehensive Spatiotemporal Analysis of Early Chick Neural Crest Network Genes'. *Developmental Dynamics* 238(3). doi: 10.1002/dvdy.21881.

Kikuchi, Akira, Hideki Yamamoto, and Akira Sato. 2009. 'Selective Activation Mechanisms of Wnt Signaling Pathways'. *Trends in Cell Biology* 19(3):119–29. doi: 10.1016/j.tcb.2009.01.003.

Kim, Kyeongmi, Olga Ossipova, and Sergei Y. Sokol. 2015. 'Neural Crest Specification by Inhibition of the ROCK/Myosin II Pathway'. *Stem Cells* 33(3):674–85. doi: 10.1002/stem.1877.

Kimelman, David, Judith A. Abraham, Tapio Haaparanta, Thomas M. Palisi, and Marc W. Kirschner. 1988. 'The Presence of Fibroblast Growth Factor in the Frog Egg: Its Role as a Natural Mesoderm Inducer'. *Science* 242(4881):1053–56. doi: 10.1126/science.3194757.

Kishi, M., K. Mizuseki, N. Sasai, H. Yamazaki, K. Shiota, S. Nakanishi, and Y. Sasai. 2000. 'Requirement of Sox2-Mediated Signaling for Differentiation of Early Xenopus Neuroectoderm'. *Development* 127(4):791–800. doi: 10.1242/dev.127.4.791.

Knecht, Anne K., and Marianne Bronner-Fraser. 2002. 'Induction of the Neural Crest: A Multigene Process'. *Nature Reviews Genetics* 3(6):453–61. doi: 10.1038/nrg819.

Komuro, Akihiko, Makoto Nagai, Nicholas E. Navin, and Marius Sudol. 2003. 'WW Domain-Containing Protein YAP Associates with ErbB-4 and Acts as a Co-Transcriptional Activator for the Carboxyl-Terminal Fragment of ErbB-4 That Translocates to the Nucleus'. *Journal of Biological Chemistry* 278(35):33334–41. doi: 10.1074/jbc.M305597200.

Kondo, Mariko, Kosuke Tashiro, Gen Fujii, Misaki Asano, Ryutaro Miyoshi, Ryutaro Yamada, Masami Muramatsu, and Koichiro Shiokawa. 1991. 'Activin Receptor MRNA Is Expressed Early in Xenopus Embryogenesis and the Level of the Expression Affects the Body Axis Formation'. *Biochemical and*

Biophysical Research Communications 181(2):684–90. doi: 10.1016/0006-291X(91)91245-8.

Köster, Manfred, Sigrun Plessow, Joachim H. Clement, Andreas Lorenz, Hildegard Tiedemann, and Walter Knöchel. 1991. 'Bone Morphogenetic Protein 4 (BMP-4), a Member of the TGF-β Family, in Early Embryos of Xenopus Laevis: Analysis of Mesoderm Inducing Activity'. *Mechanisms of Development* 33(3):191–99. doi: 10.1016/0925-4773(91)90027-4.

Kroll, K. L., and E. Amaya. 1996. 'Transgenic Xenopus Embryos from Sperm Nuclear Transplantations Reveal FGF Signaling Requirements during Gastrulation'. *Development* 122(10):3173–83. doi: 10.1242/dev.122.10.3173.

Kühl, Michael, Laird C. Sheldahl, Craig C. Malbon, and Randall T. Moon. 2000. 'Ca2+/Calmodulin-Dependent Protein Kinase II Is Stimulated by Wnt and Frizzled Homologs and Promotes Ventral Cell Fates in Xenopus'. *Journal of Biological Chemistry* 275(17):12701–11. doi: 10.1074/jbc.275.17.12701.

LaBonne, C., and M. Bronner-Fraser. 1998a. 'Neural Crest Induction in Xenopus: Evidence for a Two-Signal Model'. *Development* 125(13):2403–14. doi: 10.1242/dev.125.13.2403.

LaBonne, C., and M. Bronner-Fraser. 1998b. 'Neural Crest Induction in Xenopus: Evidence for a Two-Signal Model'. *Development* 125(13):2403–14. doi: 10.1242/dev.125.13.2403.

LaBonne, C., and M. Whitman. 1994. 'Mesoderm Induction by Activin Requires FGF-Mediated Intracellular Signals'. *Development* 120(2):463–72. doi: 10.1242/dev.120.2.463.

Lamb, T. M., and R. M. Harland. 1995. 'Fibroblast Growth Factor Is a Direct Neural Inducer, Which Combined with Noggin Generates Anterior-Posterior Neural Pattern'. *Development* 121(11):3627–36. doi: 10.1242/dev.121.11.3627.

Latinkic, Brancko v., Muriel Umbhauer, Kathy A. Neal, Walter Lerchner, James C. Smith, and Vincent Cunliffe. 1997. 'The *Xenopus Brachyury* Promoter Is Activated by FGF and Low Concentrations Ofactivinandsuppressed by High

Concentrationsof Activin and by Paired-Type Homeodomain Proteins'. *Genes & Development* 11(23):3265–76. doi: 10.1101/gad.11.23.3265.

Launay, C., V. Fromentoux, D. L. Shi, and J. C. Boucaut. 1996. 'A Truncated FGF Receptor Blocks Neural Induction by Endogenous Xenopus Inducers'. *Development* 122(3):869–80. doi: 10.1242/dev.122.3.869.

Lavado, Alfonso, Yu He, Joshua Paré, Geoffrey Neale, Eric N. Olson, Marco Giovannini, and Xinwei Cao. 2013. 'Tumor Suppressor Nf2 Limits Expansion of the Neural Progenitor Pool by Inhibiting Yap/Taz Transcriptional Coactivators'. *Development* 140(16):3323–34. doi: 10.1242/dev.096537.

Lei, Qun-Ying, Heng Zhang, Bin Zhao, Zheng-Yu Zha, Feng Bai, Xin-Hai Pei, Shimin Zhao, Yue Xiong, and Kun-Liang Guan. 2008. 'TAZ Promotes Cell Proliferation and Epithelial-Mesenchymal Transition and Is Inhibited by the Hippo Pathway'. *Molecular and Cellular Biology* 28(7):2426–36. doi: 10.1128/MCB.01874-07.

Leung, Alan W., Barbara Murdoch, Ahmed F. Salem, Maneeshi S. Prasad, Gustavo A. Gomez, and Martín I. García-Castro. 2016a. 'WNT/β-Catenin Signaling Mediates Human Neural Crest Induction via a Pre-Neural Border Intermediate'. *Development* 143(3):398–410. doi: 10.1242/dev.130849.

Leung, Alan W., Barbara Murdoch, Ahmed F. Salem, Maneeshi S. Prasad, Gustavo A. Gomez, and Martín I. García-Castro. 2016b. 'WNT/β-Catenin Signaling Mediates Human Neural Crest Induction via a Pre-Neural Border Intermediate'. *Development* 143(3):398–410. doi: 10.1242/dev.130849.

Lewis, W. H. 1904. 'Experimental Studies on the Development of the Eye in Amphibia. I. On the Origin of the Lens. Rana Palustris'. *Amer* 505–36.

Lewis, W. H. 1907. 'Transplantation of the Lips of the Blastopore in Rana Palustris'. *Am. J. Anat.* 7:137–43.

Li, Bo, Sei Kuriyama, Mauricio Moreno, and Roberto Mayor. 2009a. 'The Posteriorizing Gene *Gbx2* Is a Direct Target of Wnt Signalling and the Earliest Factor in Neural Crest Induction'. *Development* 136(19). doi: 10.1242/dev.036954.

Li, Bo, Sei Kuriyama, Mauricio Moreno, and Roberto Mayor. 2009b. 'The Posteriorizing Gene *Gbx2* Is a Direct Target of Wnt Signalling and the Earliest Factor in Neural Crest Induction'. *Development* 136(19):3267–78. doi: 10.1242/dev.036954.

LI, Chao-Bo, Li-Li HU, Zhen-Dong WANG, Shu-Qi ZHONG, and Lei LEI. 2009. 'Regulation of Compaction Initiation in Mouse Embryo'. *Hereditas (Beijing)* 31(12). doi: 10.3724/SP.J.1005.2009.01177.

Li, Vivian S. W., Ser Sue Ng, Paul J. Boersema, Teck Y. Low, Wouter R. Karthaus, Jan P. Gerlach, Shabaz Mohammed, Albert J. R. Heck, Madelon M. Maurice, Tokameh Mahmoudi, and Hans Clevers. 2012. 'Wnt Signaling through Inhibition of β-Catenin Degradation in an Intact Axin1 Complex'. *Cell* 149(6):1245–56. doi: 10.1016/j.cell.2012.05.002.

Li, Xian, Julia S. Chu, Li Yang, and Song Li. 2012. 'Anisotropic Effects of Mechanical Strain on Neural Crest Stem Cells'. *Annals of Biomedical Engineering* 40(3). doi: 10.1007/s10439-011-0403-5.

Li, Xian, Rong Xu, Xiaolin Tu, Randall Raphael R. Janairo, George Kwong, Dong Wang, Yiqian Zhu, and Song Li. 2020. 'Differentiation of Neural Crest Stem Cells in Response to Matrix Stiffness and TGF-B1 in Vascular Regeneration'. *Stem Cells and Development* 29(4). doi: 10.1089/scd.2019.0161.

Lilienbaum, Alain, and Alain Israël. 2003. 'From Calcium to NF-KB Signaling Pathways in Neurons'. *Molecular and Cellular Biology* 23(8):2680–98. doi: 10.1128/MCB.23.8.2680-2698.2003.

Lim, Chin Yan, Bruno Reversade, Barbara B. Knowles, and Davor Solter. 2013. 'Optimal Histone H3 to Linker Histone H1 Chromatin Ratio Is Vital for Mesodermal Competence in *Xenopus*'. *Development* 140(4):853–60. doi: 10.1242/dev.086611.

Linker, Claudia, Irene de Almeida, Costis Papanayotou, Matthew Stower, Virginie Sabado, Ehsan Ghorani, Andrea Streit, Roberto Mayor, and Claudio D. Stern. 2009. 'Cell Communication with the Neural Plate Is Required for Induction of Neural Markers by BMP Inhibition: Evidence for Homeogenetic

Induction and Implications for Xenopus Animal Cap and Chick Explant Assays'. *Developmental Biology* 327(2):478–86. doi: 10.1016/j.ydbio.2008.12.034.

Lohr, Jamie L., Maria C. Danos, Travis W. Groth, and H. Joseph Yost. 1998. 'Maintenance of Asymmetricnodal Expression InXenopus Laevis'. *Developmental Genetics* 23(3):194–202. doi: 10.1002/(SICI)1520-6408(1998)23:3<194::AID-DVG5>3.0.CO;2-0.

Maître, Jean-Léon. 2017. 'Mechanics of Blastocyst Morphogenesis'. *Biology of the Cell* 109(9):323–38. doi: 10.1111/boc.201700029.

Maître, Jean-Léon, Ritsuya Niwayama, Hervé Turlier, François Nédélec, and Takashi Hiiragi. 2015a. 'Pulsatile Cell-Autonomous Contractility Drives Compaction in the Mouse Embryo'. *Nature Cell Biology* 17(7):849–55. doi: 10.1038/ncb3185.

Maître, Jean-Léon, Ritsuya Niwayama, Hervé Turlier, François Nédélec, and Takashi Hiiragi. 2015b. 'Pulsatile Cell-Autonomous Contractility Drives Compaction in the Mouse Embryo'. *Nature Cell Biology* 17(7). doi: 10.1038/ncb3185.

Maître, Jean-Léon, Hervé Turlier, Rukshala Illukkumbura, Björn Eismann, Ritsuya Niwayama, François Nédélec, and Takashi Hiiragi. 2016. 'Asymmetric Division of Contractile Domains Couples Cell Positioning and Fate Specification'. *Nature* 536(7616):344–48. doi: 10.1038/nature18958.

Maj, Ewa, Lutz Künneke, Elisabeth Loresch, Anita Grund, Juliane Melchert, Tomas Pieler, Timo Aspelmeier, and Annette Borchers. 2016. 'Controlled Levels of Canonical Wnt Signaling Are Required for Neural Crest Migration'. *Developmental Biology* 417(1):77–90. doi: 10.1016/j.ydbio.2016.06.022.

Mancilla, Alejandra, and Roberto Mayor. 1996. 'Neural Crest Formation in Xenopus Laevis: Mechanisms of Xslug Induction'. *Developmental Biology* 177(2):580–89. doi: 10.1006/dbio.1996.0187.

Marchal, Leslie, Guillaume Luxardi, Virginie Thomé, and Laurent Kodjabachian. 2009. 'BMP Inhibition Initiates Neural Induction via FGF Signaling and Zic

Genes'. *Proceedings of the National Academy of Sciences* 106(41):17437–42. doi: 10.1073/pnas.0906352106.

Marchant, L., C. Linker, P. Ruiz, N. Guerrero, and R. Mayor. 1998. 'The Inductive Properties of Mesoderm Suggest That the Neural Crest Cells Are Specified by a BMP Gradient'. *Developmental Biology* 198(2). doi: 10.1016/S0012-1606(98)80008-0.

Marshall, Abigail R., Gabriel L. Galea, Andrew J. Copp, and Nicholas D. E. Greene. 2023. 'The Surface Ectoderm Exhibits Spatially Heterogenous Tension That Correlates with YAP Localisation during Spinal Neural Tube Closure in Mouse Embryos'. *Cells & Development* 174:203840. doi: 10.1016/j.cdev.2023.203840.

Martinez Arias, Alfonso, and Ben Steventon. 2018. 'On the Nature and Function of Organizers'. *Development* 145(5). doi: 10.1242/dev.159525.

Mason, Devon E., Joseph M. Collins, James H. Dawahare, Trung Dung Nguyen, Yang Lin, Sherry L. Voytik-Harbin, Pinar Zorlutuna, Mervin C. Yoder, and Joel D. Boerckel. 2019. 'YAP and TAZ Limit Cytoskeletal and Focal Adhesion Maturation to Enable Persistent Cell Motility'. *Journal of Cell Biology* 218(4):1369–89. doi: 10.1083/jcb.201806065.

Mayor, R., R. Morgan, and M. G. Sargent. 1995. 'Induction of the Prospective Neural Crest of Xenopus'. *Development* 121(3):767–77. doi: 10.1242/dev.121.3.767.

Mayor, Roberto, and Eric Theveneau. 2014. 'The Role of the Non-Canonical Wnt–Planar Cell Polarity Pathway in Neural Crest Migration'. *Biochemical Journal* 457(1):19–26. doi: 10.1042/BJ20131182.

McBeath, Rowena, Dana M. Pirone, Celeste M. Nelson, Kiran Bhadriraju, and Christopher S. Chen. 2004. 'Cell Shape, Cytoskeletal Tension, and RhoA Regulate Stem Cell Lineage Commitment'. *Developmental Cell* 6(4):483–95. doi: 10.1016/S1534-5807(04)00075-9.

Meier, S. H. 1975. 'Stimulation of Corneal Differentiation by Interaction between Cell Surface and Extracellular Matrix. I. Morphometric Analysis of Transfilter "induction'. *Cell Biol* 66:275–91.

Melton, D. A. 1987. 'Translocation of a Localized Maternal MRNA to the Vegetal Pole of Xenopus Oocytes'. *Nature* 328(6125):80–82. doi: 10.1038/328080a0.

Metscher, Brian D. 2009. 'MicroCT for Comparative Morphology: Simple Staining Methods Allow High-Contrast 3D Imaging of Diverse Non-Mineralized Animal Tissues'. *BMC Physiology* 9(1):11. doi: 10.1186/1472-6793-9-11.

Mikawa, Takashi, Alisa M. Poh, Kristine A. Kelly, Yasuo Ishii, and David E. Reese. 2004. 'Induction and Patterning of the Primitive Streak, an Organizing Center of Gastrulation in the Amniote'. *Developmental Dynamics* 229(3):422–32. doi: 10.1002/dvdy.10458.

Milewski, Rita C., Neil C. Chi, Jun Li, Christopher Brown, Min Min Lu, and Jonathan A. Epstein. 2004. 'Identification of Minimal Enhancer Elements Sufficient for Pax3 Expression in Neural Crest and Implication of Tead2 as a Regulator of Pax3'. *Development* 131(4):829–37. doi: 10.1242/dev.00975.

Mizuseki, Kenji, Tatsunori Sakamoto, Kiichi Watanabe, Keiko Muguruma, Makoto Ikeya, Ayaka Nishiyama, Akiko Arakawa, Hirofumi Suemori, Norio Nakatsuji, Hiroshi Kawasaki, Fujio Murakami, and Yoshiki Sasai. 2003. 'Generation of Neural Crest-Derived Peripheral Neurons and Floor Plate Cells from Mouse and Primate Embryonic Stem Cells'. *Proceedings of the National Academy of Sciences* 100(10):5828–33. doi: 10.1073/pnas.1037282100.

Mongera, Alessandro, Payam Rowghanian, Hannah J. Gustafson, Elijah Shelton, David A. Kealhofer, Emmet K. Carn, Friedhelm Serwane, Adam A. Lucio, James Giammona, and Otger Campàs. 2018. 'A Fluid-to-Solid Jamming Transition Underlies Vertebrate Body Axis Elongation'. *Nature* 561(7723). doi: 10.1038/s41586-018-0479-2.

Monsoro-Burq, Anne-Hélène, Estee Wang, and Richard Harland. 2005. 'Msx1 and Pax3 Cooperate to Mediate FGF8 and WNT Signals during Xenopus Neural Crest Induction'. *Developmental Cell* 8(2). doi: 10.1016/j.devcel.2004.12.017.

Montague, Tessa G., and Alexander F. Schier. 2017. 'Vg1-Nodal Heterodimers Are the Endogenous Inducers of Mesendoderm'. *ELife* 6. doi: 10.7554/eLife.28183.

Moriwaki, Kazumasa, Shoichiro Tsukita, and Mikio Furuse. 2007. 'Tight Junctions Containing Claudin 4 and 6 Are Essential for Blastocyst Formation in Preimplantation Mouse Embryos'. *Developmental Biology* 312(2):509–22. doi: 10.1016/j.ydbio.2007.09.049.

Mosaliganti, Kishore R., Ian A. Swinburne, Chon U. Chan, Nikolaus D. Obholzer, Amelia A. Green, Shreyas Tanksale, L. Mahadevan, and Sean G. Megason. 2019. 'Size Control of the Inner Ear via Hydraulic Feedback'. *ELife* 8. doi: 10.7554/eLife.39596.

Mowry, Kimberly L., and Douglas A. Melton. 1992. 'Vegetal Messenger RNA Localization Directed by a 340-Nt RNA Sequence Element in *Xenopus* Oocytes'. *Science* 255(5047):991–94. doi: 10.1126/science.1546297.

Müller, H. Arno J., and Peter Hausen. 1995. 'Epithelial Cell Polarity in Early Xenopus Development'. *Developmental Dynamics* 202(4):405–20. doi: 10.1002/aja.1002020410.

Muñoz-Sanjuán, Ignacio, and Ali H. Brivanlou. 2002a. 'Neural Induction, the Default Model and Embryonic Stem Cells'. *Nature Reviews Neuroscience* 3(4):271–80. doi: 10.1038/nrn786.

Muñoz-Sanjuán, Ignacio, and Ali H. Brivanlou. 2002b. 'Neural Induction, the Default Model and Embryonic Stem Cells'. *Nature Reviews Neuroscience* 3(4):271–80. doi: 10.1038/nrn786.

Musci, T. J., E. Amaya, and M. W. Kirschner. 1990. 'Regulation of the Fibroblast Growth Factor Receptor in Early Xenopus Embryos.' *Proceedings of the National Academy of Sciences* 87(21):8365–69. doi: 10.1073/pnas.87.21.8365.

Nardone, Giorgia, Jorge Oliver-De La Cruz, Jan Vrbsky, Cecilia Martini, Jan Pribyl, Petr Skládal, Martin Pešl, Guido Caluori, Stefania Pagliari, Fabiana Martino, Zuzana Maceckova, Marian Hajduch, Andres Sanz-Garcia, Nicola Maria

Pugno, Gorazd Bernard Stokin, and Giancarlo Forte. 2017. 'YAP Regulates Cell Mechanics by Controlling Focal Adhesion Assembly'. *Nature Communications* 8(1):15321. doi: 10.1038/ncomms15321.

Nelson, Celeste M. 2022. 'Mechanical Control of Cell Differentiation: Insights from the Early Embryo'. *Annual Review of Biomedical Engineering* 24(1):307–22. doi: 10.1146/annurev-bioeng-060418-052527.

Nieuwkoop, P. D. 1969. 'The Formation of the Mesoderm in Urodelean Amphibians : I. Induction by the Endoderm.' *Wilhelm Roux Arch Entwickl Mech Org* 162:341–73.

Nieuwkoop, P. D. and Faber, J. 1967. 'Normal Table of Xenopus Laevis (Daudin)'. *North Holland*.

Nusse, Roel, and Hans Clevers. 2017a. 'Wnt/β-Catenin Signaling, Disease, and Emerging Therapeutic Modalities'. *Cell* 169(6):985–99. doi: 10.1016/j.cell.2017.05.016.

Nusse, Roel, and Hans Clevers. 2017b. 'Wnt/β-Catenin Signaling, Disease, and Emerging Therapeutic Modalities'. *Cell* 169(6):985–99. doi: 10.1016/j.cell.2017.05.016.

Oppenheimer, J. M. 1991. 'Curt Herbst's Contributions to the Concept of Embryonic Induction'. *Dev Bio* 63–89.

Otto, Anthony, Corina Schmidt, and Ketan Patel. 2006. 'Pax3 and Pax7 Expression and Regulation in the Avian Embryo'. *Anatomy and Embryology* 211(4). doi: 10.1007/s00429-006-0083-3.

Oudhoff, Menno J., Mitchell J. S. Braam, Spencer A. Freeman, Denise Wong, David G. Rattray, Jia Wang, Frann Antignano, Kimberly Snyder, Ido Refaeli, Michael R. Hughes, Kelly M. McNagny, Michael R. Gold, Cheryl H. Arrowsmith, Toshiro Sato, Fabio M. V. Rossi, John H. Tatlock, Dafydd R. Owen, Peter J. Brown, and Colby Zaph. 2016a. 'SETD7 Controls Intestinal Regeneration and Tumorigenesis by Regulating Wnt/β-Catenin and Hippo/YAP Signaling'. *Developmental Cell* 37(1):47–57. doi: 10.1016/j.devcel.2016.03.002.

Oudhoff, Menno J., Mitchell J. S. Braam, Spencer A. Freeman, Denise Wong, David G. Rattray, Jia Wang, Frann Antignano, Kimberly Snyder, Ido Refaeli, Michael R. Hughes, Kelly M. McNagny, Michael R. Gold, Cheryl H. Arrowsmith, Toshiro Sato, Fabio M. V. Rossi, John H. Tatlock, Dafydd R. Owen, Peter J. Brown, and Colby Zaph. 2016b. 'SETD7 Controls Intestinal Regeneration and Tumorigenesis by Regulating Wnt/β-Catenin and Hippo/YAP Signaling'. *Developmental Cell* 37(1):47–57. doi: 10.1016/j.devcel.2016.03.002.

Palmer, Michael A., and Celeste M. Nelson. 2020. 'Fusion of Airways during Avian Lung Development Constitutes a Novel Mechanism for the Formation of Continuous Lumena in Multicellular Epithelia'. *Developmental Dynamics* 249(11):1318–33. doi: 10.1002/dvdy.215.

Pan, Jin-Xiu, Lei Xiong, Kai Zhao, Peng Zeng, Bo Wang, Fu-Lei Tang, Dong Sun, Hao-han Guo, Xiao Yang, Shun Cui, Wen-Fang Xia, Lin Mei, and Wen-Cheng Xiong. 2018. 'YAP Promotes Osteogenesis and Suppresses Adipogenic Differentiation by Regulating β-Catenin Signaling'. *Bone Research* 6(1):18. doi: 10.1038/s41413-018-0018-7.

Panciera, Tito, Luca Azzolin, Michelangelo Cordenonsi, and Stefano Piccolo. 2017. 'Mechanobiology of YAP and TAZ in Physiology and Disease'. *Nature Reviews Molecular Cell Biology* 18(12):758–70. doi: 10.1038/nrm.2017.87.

Park, Hyun Woo, Young Chul Kim, Bo Yu, Toshiro Moroishi, Jung-Soon Mo, Steven W. Plouffe, Zhipeng Meng, Kimberly C. Lin, Fa-Xing Yu, Caroline M. Alexander, Cun-Yu Wang, and Kun-Liang Guan. 2015. 'Alternative Wnt Signaling Activates YAP/TAZ'. *Cell* 162(4):780–94. doi: 10.1016/j.cell.2015.07.013.

Pera, Edgar M., Atsushi Ikeda, Edward Eivers, and Eddy M. de Robertis. 2003. 'Integration of IGF, FGF, and Anti-BMP Signals via Smad1 Phosphorylation in Neural Induction'. *Genes & Development* 17(24):3023–28. doi: 10.1101/gad.1153603.

Perea-Gomez, Aitana, Francis D. J. Vella, William Shawlot, Mustapha Oulad-Abdelghani, Claire Chazaud, Chikara Meno, Veronique Pfister, Lan Chen, Elizabeth Robertson, Hiroshi Hamada, Richard R. Behringer, and Siew-Lan Ang. 2002. 'Nodal Antagonists in the Anterior Visceral Endoderm Prevent the Formation of Multiple Primitive Streaks'. *Developmental Cell* 3(5):745–56. doi: 10.1016/S1534-5807(02)00321-0.

Petrie, Ryan J., Hyun Koo, and Kenneth M. Yamada. 2014. 'Generation of Compartmentalized Pressure by a Nuclear Piston Governs Cell Motility in a 3D Matrix'. *Science* 345(6200):1062–65. doi: 10.1126/science.1256965.

Phelps, Grace B., Adam Amsterdam, Hannah R. Hagen, Nicole Zambrana García, and Jacqueline A. Lees. 2022. 'MITF Deficiency and Oncogenic GNAQ Each Promote Proliferation Programs in Zebrafish Melanocyte Lineage Cells'. *Pigment Cell & Melanoma Research* 35(5):539–47. doi: 10.1111/pcmr.13057.

Piacentino, Michael L., and Marianne E. Bronner. 2018. 'Intracellular Attenuation of BMP Signaling via CKIP-1/Smurf1 Is Essential during Neural Crest Induction'. *PLOS Biology* 16(6):e2004425. doi: 10.1371/journal.pbio.2004425.

Piccolo, Francesco M., Nathaniel R. Kastan, Tomomi Haremaki, Qingyun Tian, Tiago L. Laundos, Riccardo De Santis, Andrew J. Beaudoin, Thomas S. Carroll, Ji-Dung Luo, Ksenia Gnedeva, Fred Etoc, AJ Hudspeth, and Ali H. Brivanlou. 2022. 'Role of YAP in Early Ectodermal Specification and a Huntington's Disease Model of Human Neurulation'. *ELife* 11. doi: 10.7554/eLife.73075.

Piccolo, Stefano, Yoshiki Sasai, Bin Lu, and Eddy M. de Robertis. 1996. 'Dorsoventral Patterning in Xenopus: Inhibition of Ventral Signals by Direct Binding of Chordin to BMP-4'. *Cell* 86(4):589–98. doi: 10.1016/S0092-8674(00)80132-4.

Pieper, Mareike, Katja Ahrens, Elke Rink, Annette Peter, and Gerhard Schlosser. 2012. 'Differential Distribution of Competence for Panplacodal and Neural

Crest Induction to Non-Neural and Neural Ectoderm'. *Development* 139(6):1175–87. doi: 10.1242/dev.074468.

Pierre, Anaëlle, Jérémy Sallé, Martin Wühr, and Nicolas Minc. 2016. 'Generic Theoretical Models to Predict Division Patterns of Cleaving Embryos'. *Developmental Cell* 39(6):667–82. doi: 10.1016/j.devcel.2016.11.018.

Plusa, Berenika, and Anna-Katerina Hadjantonakis. 2016. 'Mechanics Drives Cell Differentiation'. *Nature* 536(7616):281–82. doi: 10.1038/nature18920.

Pownall, M. E., Bryan E. Welm, Kevin W. Freeman, David M. Spencer, Jeffrey M. Rosen, and Harry v Isaacs. 2003. 'An Inducible System for the Study of FGF Signalling in Early Amphibian Development'. *Developmental Biology* 256(1):90–100. doi: 10.1016/S0012-1606(02)00120-3.

Pyke, Magnus. 1956. 'PRINCIPLES OF EMBRYOLOGY. By C. H. Waddington. London: George Allen & Unwin, Ltd. 1956. Pp. 510. £2, 5s'. *Quarterly Journal of Experimental Physiology and Cognate Medical Sciences* 41(4):475–77. doi: 10.1113/expphysiol.1956.sp001218.

Quinlan, Robyn, Manuela Graf, Ivor Mason, Andrew Lumsden, and Clemens Kiecker. 2009. 'Complex and Dynamic Patterns of Wnt Pathway Gene Expression in the Developing Chick Forebrain'. *Neural Development* 4(1):35. doi: 10.1186/1749-8104-4-35.

Quinn, Hazel M., Regina Vogel, Oliver Popp, Philipp Mertins, Linxiang Lan, Clemens Messerschmidt, Alexandro Landshammer, Kamil Lisek, Sophie Château-Joubert, Elisabetta Marangoni, Elle Koren, Yaron Fuchs, and Walter Birchmeier. 2021. 'YAP and β-Catenin Cooperate to Drive Oncogenesis in Basal Breast Cancer'. *Cancer Research* 81(8):2116–27. doi: 10.1158/0008-5472.CAN-20-2801.

Ragland, Jared W., and David W. Raible. 2004. 'Signals Derived from the Underlying Mesoderm Are Dispensable for Zebrafish Neural Crest Induction'. *Developmental Biology* 276(1). doi: 10.1016/j.ydbio.2004.08.017.

Rawles, M. E. 1963. 'Tissue Interactions in Scale and Feather Development as Studied in Dermal-Epidermal Recombinations'. *J Embryol Exp Morphol* 11:765–89.

Rebagliati, M. R., D. L. Weeks, R. P. Harvey, and D. A. Melton. 1985. 'Identification and Cloning of Localized Maternal RNAs from Xenopus Eggs'. *Cell* 42(3):769–77. doi: 10.1016/0092-8674(85)90273-9.

Rebecca F. Spokony, Yoichiro Aoki, Natasha Saint-Germain, Emily Magner-Fink, and Saint-Jeannet JP. 2002. 'The Transcription Factor Sox9 Is Required for Cranial Neural Crest Development in Xenopus'. *Development* 421–32.

Ribisi, Stephen, Francesca v. Mariani, Emil Aamar, Teresa M. Lamb, Dale Frank, and Richard M. Harland. 2000. 'Ras-Mediated FGF Signaling Is Required for the Formation of Posterior but Not Anterior Neural Tissue in Xenopus Laevis'. *Developmental Biology* 227(1):183–96. doi: 10.1006/dbio.2000.9889.

Rogers, C. D. F., T. A. Dijkstra, and I. J. Smalley. 1994. 'Particle Packing from an Earth Science Viewpoint'. *Earth-Science Reviews* 36(1–2):59–82. doi: 10.1016/0012-8252(94)90008-6.

Rosenbluh, Joseph, Deepak Nijhawan, Andrew G. Cox, Xingnan Li, James T. Neal, Eric J. Schafer, Travis I. Zack, Xiaoxing Wang, Aviad Tsherniak, Anna C. Schinzel, Diane D. Shao, Steven E. Schumacher, Barbara A. Weir, Francisca Vazquez, Glenn S. Cowley, David E. Root, Jill P. Mesirov, Rameen Beroukhim, Calvin J. Kuo, Wolfram Goessling, and William C. Hahn. 2012. 'β-Catenin-Driven Cancers Require a YAP1 Transcriptional Complex for Survival and Tumorigenesis'. *Cell* 151(7):1457–73. doi: 10.1016/j.cell.2012.11.026.

Rossant, Janet. 2016. 'Making the Mouse Blastocyst'. Pp. 275–88 in.

Ruiz i Altaba, A., and T. M. Jessell. 1991. 'Retinoic Acid Modifies the Pattern of Cell Differentiation in the Central Nervous System of Neurula Stage Xenopus Embryos'. *Development* 112(4):945–58. doi: 10.1242/dev.112.4.945.

Rutter, W. J., N. K. Wessells, and C. Grobstein. 1964. 'Control of Specific Synthesis in the Developing Pancreas'. *Natl Cancer Inst Monogr* 13:51–65.

Saint-Jeannet, Jean-Pierre, Xi He, Harold E. Varmus, and Igor B. Dawid. 1997. 'Regulation of Dorsal Fate in the Neuraxis by Wnt-1 and Wnt-3a'. *Proceedings of the National Academy of Sciences* 94(25):13713–18. doi: 10.1073/pnas.94.25.13713.

Sasai, Noriaki, Rieko Yakura, Daisuke Kamiya, Yoko Nakazawa, and Yoshiki Sasai. 2008. 'Ectodermal Factor Restricts Mesoderm Differentiation by Inhibiting P53'. *Cell* 133(5):878–90. doi: 10.1016/j.cell.2008.03.035.

SASAI, Y. 1994. 'Xenopus Chordin: A Novel Dorsalizing Factor Activated by Organizer-Specific Homeobox Genes'. *Cell* 79(5):779–90. doi: 10.1016/0092-8674(94)90068-X.

Sasai, Y., B. Lu, S. Piccolo, and E. M. de Robertis. 1996. 'Endoderm Induction by the Organizer-Secreted Factors Chordin and Noggin in Xenopus Animal Caps.' *The EMBO Journal* 15(17):4547–55.

Sasai, Yoshiki, Bin Lu, Herbert Steinbeisser, and Eddy M. de Robertis. 1995. 'Regulation of Neural Induction by the Chd and Bmp-4 Antagonistic Patterning Signals in Xenopus'. *Nature* 376(6538):333–36. doi: 10.1038/376333a0.

Sauka-Spengler, Tatjana, and Marianne Bronner-Fraser. 2008. 'A Gene Regulatory Network Orchestrates Neural Crest Formation'. *Nature Reviews Molecular Cell Biology* 9(7):557–68.

Saxen, L. 1977. 'Directive versus Permissive Induction: A Working Hypothesis'. *Physiol Ser* 32:1–9.

Schulte-Merker, S., J. C. Smith, and L. Dale. 1994. 'Effects of Truncated Activin and FGF Receptors and of Follistatin on the Inducing Activities of BVg1 and Activin: Does Activin Play a Role in Mesoderm Induction?' *The EMBO Journal* 13(15):3533–41. doi: 10.1002/j.1460-2075.1994.tb06660.x.

Schulze, Jens, and Einhard Schierenberg. 2011. 'Evolution of Embryonic Development in Nematodes'. *EvoDevo* 2(1):18. doi: 10.1186/2041-9139-2-18.

Sengel, P. 1976. 'Morphogenesis of Skin'. *Cambridge Univ. Press*.

Servetnick, M., and R. M. Grainger. 1991. 'Changes in Neural and Lens Competence in Xenopus Ectoderm: Evidence for an Autonomous Developmental Timer'. *Development* 112(1):177–88. doi: 10.1242/dev.112.1.177.

Sheldahl, Laird C., Maiyon Park, Craig C. Malbon, and Randall T. Moon. 1999. 'Protein Kinase C Is Differentially Stimulated by Wnt and Frizzled Homologs in AG-Protein-Dependent Manner'. *Current Biology* 9(13):695-S1. doi: 10.1016/S0960-9822(99)80310-8.

Shellard, Adam, and Roberto Mayor. 2021. 'Collective Durotaxis along a Self-Generated Stiffness Gradient in Vivo'. *Nature* 600(7890):690–94. doi: 10.1038/s41586-021-04210-x.

Simões-Costa, Marcos, and Marianne E. Bronner. 2015. 'Establishing Neural Crest Identity: A Gene Regulatory Recipe'. *Development* 142(2):242–57. doi: 10.1242/dev.105445.

Simões-Costa, Marcos, Michael Stone, and Marianne E. Bronner. 2015. 'Axud1 Integrates Wnt Signaling and Transcriptional Inputs to Drive Neural Crest Formation'. *Developmental Cell* 34(5):544–54. doi: 10.1016/j.devcel.2015.06.024.

Slack, Christine, and Anne E. Warner. 1973a. 'Intracellular and Intercellular Potentials in the Early Amphibian Embryo'. *The Journal of Physiology* 232(2):313–30. doi: 10.1113/jphysiol.1973.sp010272.

Slack, Christine, and Anne E. Warner. 1973b. 'Intracellular and Intercellular Potentials in the Early Amphibian Embryo'. *The Journal of Physiology* 232(2):313–30. doi: 10.1113/jphysiol.1973.sp010272.

Slack, J. M., L. Dale, and J. C. Smith. 1984. 'Analysis of Embryonic Induction by Using Cell Lineage Markers'. *Philos Trans R Soc Lond B Biol Sci*.

Slack, J. M. W., B. G. Darlington, J. K. Heath, and S. F. Godsave. 1987. 'Mesoderm Induction in Early Xenopus Embryos by Heparin-Binding Growth Factors'. *Nature* 326(6109):197–200. doi: 10.1038/326197a0.

Smith, J. C. 1987. 'A Mesoderm-Inducing Factor Is Produced by a Xenopus Cell Line'. *Development* 99(1):3–14. doi: 10.1242/dev.99.1.3.

Smith, J. C., B. M. J. Price, K. van Nimmen, and D. Huylebroeck. 1990. 'Identification of a Potent Xenopus Mesoderm-Inducing Factor as a Homologue of Activin A'. *Nature* 345(6277):729–31. doi: 10.1038/345729a0.

Smith, William C., and Richard M. Harland. 1991. 'Injected Xwnt-8 RNA Acts Early in Xenopus Embryos to Promote Formation of a Vegetal Dorsalizing Center'. *Cell* 67(4):753–65. doi: 10.1016/0092-8674(91)90070-F.

Sokol, S., and D. A. Melton. 1991. 'Pre-Existent Pattern in Xenopus Animal Pole Cells Revealed by Induction with Activin'. *Nature* 351(6325):409–11. doi: 10.1038/351409a0.

Sokol, S., G. G. Wong, and D. A. Melton. 1990. 'A Mouse Macrophage Factor Induces Head Structures and Organizes a Body Axis in *Xenopus*'. *Science* 249(4968):561–64. doi: 10.1126/science.2382134.

Spemann, Hans. 1901. 'Uber Korrelationen in Der Entwicklung Des Auges'. *Verh Anat Ges* 15:61–79.

Spemann, Hans. 1921. 'Die Erzeugung Tierischer Chimären Durch Heteroplastische Embryonale Transplantation Zwischen Triton Cristatus Und Taeniatus.' *Archiv Für Entwicklungsmechanik Der Organismen* 48(4):533–70.

Spemann, Hans, and Hilde Mangold. 1924. 'Über Induktion von Embryonalanlagen Durch Implantation Artfremder Organisatoren'. *Mikroskopische Anatomie Und Entwicklungsmechanik* 101–458.

Steinbach, Oliver C., Alan P. Wolffe, and Ralph A. W. Rupp. 1997. 'Somatic Linker Histones Cause Loss of Mesodermal Competence in Xenopus'. *Nature* 389(6649):395–99. doi: 10.1038/38755.

Stern, Claudio D. 2005. 'Neural Induction: Old Problem, New Findings, yet More Questions'. *Development* 132(9):2007–21. doi: 10.1242/dev.01794.

Stern, Claudio D., and Karen M. Downs. 2012. 'The Hypoblast (Visceral Endoderm): An Evo-Devo Perspective'. *Development* 139(6):1059–69. doi: 10.1242/dev.070730.

Steventon, Ben, Claudio Araya, Claudia Linker, Sei Kuriyama, and Roberto Mayor. 2009a. 'Differential Requirements of BMP and Wnt Signalling during Gastrulation and Neurulation Define Two Steps in Neural Crest Induction'. *Development* 136(5):771–79. doi: 10.1242/dev.029017.

Steventon, Ben, Claudio Araya, Claudia Linker, Sei Kuriyama, and Roberto Mayor. 2009b. 'Differential Requirements of BMP and Wnt Signalling during Gastrulation and Neurulation Define Two Steps in Neural Crest Induction'. *Development* 136(5). doi: 10.1242/dev.029017.

Steventon, Benjamin, Lara Busby, and Alfonso Martinez Arias. 2021. 'Establishment of the Vertebrate Body Plan: Rethinking Gastrulation through Stem Cell Models of Early Embryogenesis'. *Developmental Cell* 56(17). doi: 10.1016/j.devcel.2021.08.012.

Storey, K. G., J. M. Crossley, E. M. de Robertis, W. E. Norris, and C. D. Stern. 1992a. 'Neural Induction and Regionalisation in the Chick Embryo'. *Development* 114(3):729–41. doi: 10.1242/dev.114.3.729.

Storey, K. G., J. M. Crossley, E. M. de Robertis, W. E. Norris, and C. D. Stern. 1992b. 'Neural Induction and Regionalisation in the Chick Embryo'. *Development* 114(3):729–41. doi: 10.1242/dev.114.3.729.

Storey, K. G., A. Goriely, C. M. Sargent, J. M. Brown, H. D. Burns, H. M. Abud, and J. K. Heath. 1998. 'Early Posterior Neural Tissue Is Induced by FGF in the Chick Embryo'. *Development* 125(3):473–84. doi: 10.1242/dev.125.3.473.

Storey, K. G., M. A. Selleck, and C. D. Stern. 1995. 'Neural Induction and Regionalisation by Different Subpopulations of Cells in Hensen's Node'. *Development* 121(2):417–28. doi: 10.1242/dev.121.2.417.

Streit, A., K. J. Lee, I. Woo, C. Roberts, T. M. Jessell, and C. D. Stern. 1998. 'Chordin Regulates Primitive Streak Development and the Stability of Induced Neural Cells, but Is Not Sufficient for Neural Induction in the Chick Embryo'. *Development* 125(3):507–19. doi: 10.1242/dev.125.3.507.

Streit, A., S. Sockanathan, L. Perez, M. Rex, P. J. Scotting, P. T. Sharpe, R. Lovell-Badge, and C. D. Stern. 1997. 'Preventing the Loss of Competence for

Neural Induction: HGF/SF, L5 and Sox-2'. *Development* 124(6):1191–1202. doi: 10.1242/dev.124.6.1191.

Streit, Andrea, Alyson J. Berliner, Costis Papanayotou, Andrés Sirulnik, and Claudio D. Stern. 2000. 'Initiation of Neural Induction by FGF Signalling before Gastrulation'. *Nature* 406(6791):74–78. doi: 10.1038/35017617.

Sudarwati, S., and P. D. Nieuwkoop. 1971. 'Mesoderm Formation in the AnuranXenopus Laevis (Daudin).' *Wilhelm Roux Arch Entwickl Mech Org* 166:189–204.

Sun, Congshan, Vanessa De Mello, Abdalla Mohamed, Huascar P. Ortuste Quiroga, Amaya Garcia-Munoz, Abdullah Al Bloshi, Annie M. Tremblay, Alexander von Kriegsheim, Elaina Collie-Duguid, Neil Vargesson, David Matallanas, Henning Wackerhage, and Peter S. Zammit. 2017. 'Common and Distinctive Functions of the Hippo Effectors Taz and Yap in Skeletal Muscle Stem Cell Function'. *Stem Cells* 35(8):1958–72. doi: 10.1002/stem.2652.

Sun, Zhiqi, Shengzhen S. Guo, and Reinhard Fässler. 2016. 'Integrin-Mediated Mechanotransduction'. *Journal of Cell Biology* 215(4):445–56. doi: 10.1083/jcb.201609037.

Suzuki, A., R. S. Thies, N. Yamaji, J. J. Song, J. M. Wozney, K. Murakami, and N. Ueno. 1994a. 'A Truncated Bone Morphogenetic Protein Receptor Affects Dorsal-Ventral Patterning in the Early Xenopus Embryo.' *Proceedings of the National Academy of Sciences* 91(22):10255–59. doi: 10.1073/pnas.91.22.10255.

Suzuki, A., R. S. Thies, N. Yamaji, J. J. Song, J. M. Wozney, K. Murakami, and N. Ueno. 1994b. 'A Truncated Bone Morphogenetic Protein Receptor Affects Dorsal-Ventral Patterning in the Early Xenopus Embryo.' *Proceedings of the National Academy of Sciences* 91(22):10255–59. doi: 10.1073/pnas.91.22.10255.

Swift, Joe, and Dennis E. Discher. 2014. 'The Nuclear Lamina Is Mechano-Responsive to ECM Elasticity in Mature Tissue'. *Journal of Cell Science*. doi: 10.1242/jcs.149203.

Szabó, András, and Roberto Mayor. 2018. 'Mechanisms of Neural Crest Migration'. *Annual Review of Genetics* 52(1):43–63. doi: 10.1146/annurev-genet-120417-031559.

Tamai, Keiko, Mikhail Semenov, Yoichi Kato, Rebecca Spokony, Chunming Liu, Yu Katsuyama, Fred Hess, Jean-Pierre Saint-Jeannet, and Xi He. 2000. 'LDL-Receptor-Related Proteins in Wnt Signal Transduction'. *Nature* 407(6803):530–35. doi: 10.1038/35035117.

Thomsen, G., T. Woolf, M. Whitman, S. Sokol, J. Vaughan, W. Vale, and D. A. Melton. 1990. 'Activins Are Expressed Early in Xenopus Embryogenesis and Can Induce Axial Mesoderm and Anterior Structures'. *Cell* 63(3):485–93. doi: 10.1016/0092-8674(90)90445-K.

Tran, Hong Thi, and Kris Vleminckx. 2014. 'Design and Use of Transgenic Reporter Strains for Detecting Activity of Signaling Pathways in Xenopus'. *Methods* 66(3):422–32. doi: 10.1016/j.ymeth.2013.06.028.

Tríbulo, Celeste, Manuel J. Aybar, Vu H. Nguyen, Mary C. Mullins, and Roberto Mayor. 2003. 'Regulation of Msx Genes by a Bmp Gradient Is Essential for Neural Crest Specification'. *Development* 130(26). doi: 10.1242/dev.00878.

Tschumperlin, Daniel J. 2011. 'Mechanotransduction'. in *Comprehensive Physiology*. Wiley.

Tsutsumi, Ryouhei, Mohammad Masoudi, Atsushi Takahashi, Yumiko Fujii, Takeru Hayashi, Ippei Kikuchi, Yumeko Satou, Masanori Taira, and Masanori Hatakeyama. 2013. 'YAP and TAZ, Hippo Signaling Targets, Act as a Rheostat for Nuclear SHP2 Function'. *Developmental Cell* 26(6):658–65. doi: 10.1016/j.devcel.2013.08.013.

Varelas, Xaralabos, Payman Samavarchi-Tehrani, Masahiro Narimatsu, Alexander Weiss, Katie Cockburn, Brett G. Larsen, Janet Rossant, and Jeffrey L. Wrana. 2010. 'The Crumbs Complex Couples Cell Density Sensing to

Hippo-Dependent Control of the TGF-β-SMAD Pathway'. *Developmental Cell* 19(6):831–44. doi: 10.1016/j.devcel.2010.11.012.

Veeman, Michael T., Diane C. Slusarski, Ajamete Kaykas, Sarah Hallagan Louie, and Randall T. Moon. 2003. 'Zebrafish Prickle, a Modulator of Noncanonical Wnt/Fz Signaling, Regulates Gastrulation Movements'. *Current Biology* 13(8):680–85. doi: 10.1016/S0960-9822(03)00240-9.

Villanueva, Sandra, Alvaro Glavic, Pablo Ruiz, and Roberto Mayor. 2002. 'Posteriorization by FGF, Wnt, and Retinoic Acid Is Required for Neural Crest Induction'. *Developmental Biology* 241(2):289–301. doi: 10.1006/dbio.2001.0485.

Vleminckx, Kris, Rolf Kemler, and Andreas Hecht. 1999. 'The C-Terminal Transactivation Domain of β-Catenin Is Necessary and Sufficient for Signaling by the LEF-1/β-Catenin Complex in Xenopus Laevis'. *Mechanisms of Development* 81(1–2):65–74. doi: 10.1016/S0925-4773(98)00225-1.

Waddington, C. H. 1932. 'III. Experiments on the Development of Chick and Duck Embryos, Cultivated *in Vitro*'. *Philosophical Transactions of the Royal Society of London. Series B, Containing Papers of a Biological Character* 221(474–482):179–230. doi: 10.1098/rstb.1932.0003.

Waddington, C. H. 1933. 'Induction by the Primitive Streak and Its Derivatives in the Chick. Journal of Experimental Biology'. *Journal of Experimental Biology* 10(b):38-u4.

WADDINGTON, C. H. 1934. 'Experiments on Embryonic Induction'. *Journal of Experimental Biology* 11(3):218–23. doi: 10.1242/jeb.11.3.218.

Waddington, C. H. 1936. 'Organizers in Mammalian Development.' *Nature* (a):138–125.

Waddington, C. H. 1937. 'Experiments on Determination in the Rabbit Embryo.' *Arch Biol* 48:273–90.

Watanabe, Tomoko, Yuna Kanai, Shinya Matsukawa, and Tatsuo Michiue. 2015. 'Specific Induction of Cranial Placode Cells from *Xenopus* Ectoderm by

Modulating the Levels of BMP, Wnt, and FGF Signaling'. *Genesis* 53(10):652–59. doi: 10.1002/dvg.22881.

Watson, A. J., D. R. Natale, and L. C. Barcroft. 2004. 'Molecular Regulation of Blastocyst Formation'. *Animal Reproduction Science* 82–83:583–92. doi: 10.1016/j.anireprosci.2004.04.004.

Wawersik, Stefan, Christina Evola, and Malcolm Whitman. 2005. 'Conditional BMP Inhibition in Xenopus Reveals Stage-Specific Roles for BMPs in Neural and Neural Crest Induction'. *Developmental Biology* 277(2):425–42. doi: 10.1016/j.ydbio.2004.10.002.

Weeks, D. L., and D. A. Melton. 1987. 'A Maternal MRNA Localized to the Animal Pole of Xenopus Eggs Encodes a Subunit of Mitochondrial ATPase.' *Proceedings of the National Academy of Sciences* 84(9):2798–2802. doi: 10.1073/pnas.84.9.2798.

Weisz Hubsman, Monika, Natalia Volinsky, Edward Manser, Deborah Yablonski, and Ami Aronheim. 2007. 'Autophosphorylation-Dependent Degradation of Pak1, Triggered by the Rho-Family GTPase, Chp'. *Biochemical Journal* 404(3):487–97. doi: 10.1042/BJ20061696.

Wessells, N. K., and J. H. Cohen. 1967. 'Early Pancreas Organogenesis: Morphogenesis, Tissue Interactions, and Mass Effects'. *Dev Biol* 15:237–70.

Wilson, Sara I., Enrique Graziano, Richard Harland, Thomas M. Jessell, and Thomas Edlund. 2000. 'An Early Requirement for FGF Signalling in the Acquisition of Neural Cell Fate in the Chick Embryo'. *Current Biology* 10(8):421–29. doi: 10.1016/S0960-9822(00)00431-0.

Winklbauer, Rudolf. 2009. 'Chapter 5 Cell Adhesion in Amphibian Gastrulation'. Pp. 215–75 in.

Winklbauer, Rudolf. 2020. 'Mesoderm and Endoderm Internalization in the Xenopus Gastrula'. Pp. 243–70 in.

Wodarz, Andreas, and Roel Nusse. 1998. 'MECHANISMS OF WNT SIGNALING IN DEVELOPMENT'. *Annual Review of Cell and Developmental Biology* 14(1):59–88. doi: 10.1146/annurev.cellbio.14.1.59.

Wolpert, L., and T. Gustafson. 1961. 'Studies on the Cellular Basis of Morphogenesis of the Sea Urchin Embryo'. *Experimental Cell Research* 25(2):374–82. doi: 10.1016/0014-4827(61)90287-7.

Wolpert, L., and E. H. Mercer. 1963. 'An Electron Microscope Study of the Development of the Blastula of the Sea Urchin Embryo and Its Radial Polarity'. *Experimental Cell Research* 30(2):280–300. doi: 10.1016/0014-4827(63)90300-8.

Wu, Jinling, Jing Yang, and Peter S. Klein. 2005. 'Neural Crest Induction by the Canonical Wnt Pathway Can Be Dissociated from Anterior–Posterior Neural Patterning in Xenopus'. *Developmental Biology* 279(1):220–32. doi: 10.1016/j.ydbio.2004.12.016.

Xia, Peng, Daniel Gütl, Vanessa Zheden, and Carl-Philipp Heisenberg. 2019. 'Lateral Inhibition in Cell Specification Mediated by Mechanical Signals Modulating TAZ Activity'. *Cell* 176(6):1379-1392.e14. doi: 10.1016/j.cell.2019.01.019.

Yang, Beining, Hualing Sun, Fangfang Song, Miao Yu, Yanru Wu, and Jiawei Wang. 2017. 'YAP1 Negatively Regulates Chondrocyte Differentiation Partly by Activating the β-Catenin Signaling Pathway'. *The International Journal of Biochemistry & Cell Biology* 87:104–13. doi: 10.1016/j.biocel.2017.04.007.

Yang, Zhibo, Suresh Rayala, Diep Nguyen, Ratna K. Vadlamudi, Shiuan Chen, and Rakesh Kumar. 2005. 'Pak1 Phosphorylation of Snail, a Master Regulator of Epithelial-to-Mesenchyme Transition, Modulates Snail's Subcellular Localization and Functions'. *Cancer Research* 65(8):3179–84. doi: 10.1158/0008-5472.CAN-04-3480.

Yu, Bo, Anuoluwapo Egbejimi, Rachayata Dharmat, Pei Xu, Zhenyang Zhao, Bo Long, Hongyu Miao, Rui Chen, Theodore G. Wensel, Jiyang Cai, and Yan Chen. 2018. 'Phagocytosed Photoreceptor Outer Segments Activate MTORC1 in the Retinal Pigment Epithelium'. *Science Signaling* 11(532). doi: 10.1126/scisignal.aag3315.

Zhao, Bin, Xiaomu Wei, Weiquan Li, Ryan S. Udan, Qian Yang, Joungmok Kim, Joe Xie, Tsuneo Ikenoue, Jindan Yu, Li Li, Pan Zheng, Keqiang Ye, Arul Chinnaiyan, Georg Halder, Zhi-Chun Lai, and Kun-Liang Guan. 2007. 'Inactivation of YAP Oncoprotein by the Hippo Pathway Is Involved in Cell Contact Inhibition and Tissue Growth Control'. *Genes & Development* 21(21):2747–61. doi: 10.1101/gad.1602907.

Ziomek, C. 1980. 'Cell Surface Interaction Induces Polarization of Mouse 8-Cell Blastomeres at Compaction'. *Cell* 21(3):935–42. doi: 10.1016/0092-8674(80)90457-2.